Characterization of telomere protein complexes in *Trypanosoma brucei*

Dissertation zur Erlangung des
naturwissenschaftlichen Doktorgrades
der Julius-Maximilians-Universität Würzburg

vorgelegt von

Helena Reis

aus Pawlodar (Kasachstan)

Würzburg, 2017

Eingereicht am:

Mitglieder der Promotionskommission:

Vorsitzender:
Erstgutachter: Prof. Dr. Christian Janzen
Zweitgutachter: Prof. Dr. Nicolai Siegel

Tag des Promotionskolloquiums:

Doktorurkunde ausgehändigt am:

Erklärungen nach §4 Abs. 3 Satz 3, 5, 8 der Promotionsordnung der Fakultät für Biologie

Affidavit

I hereby declare that my thesis entitled: „*Characterization of telomere protein complexes in Trypanosoma brucei*" is the result of my own work.

I did not receive any help or support from commercial consultants. All sources and/or materials applied are listed and specified in the thesis.

Furthermore, I verify that the thesis has not been submitted as part of another examination process neither in identical nor in similar form.

Eidesstattliche Erklärung

Hiermit erkläre ich an Eides statt, die Dissertation: „*Characterization of telomere protein complexes in Trypanosoma brucei*", eigenständig, d. h. insbesondere selbständig und ohne Hilfe eines kommerziellen Promotionsberaters, angefertigt und keine anderen, als die von mir angegebenen Quellen und Hilfsmittel verwendet zu haben.

Ich erkläre außerdem, dass die Dissertation weder in gleicher noch in ähnlicher Form bereits in einem anderen Prüfungsverfahren vorgelegen hat.

Würzburg, den 22.6.2017

_____

Helena Reis

Parts of this thesis have been submitted to a scientific journal for publication:

Reis H, Schwebs M, Dietz S, Janzen CJ snd Butter F (2017). TelBP1 links stage-specific telomere complexes with developmental expression site silencing in African trypanosomes. Submitted to ***Nature Communications***.

Parts of this thesis have been presented at international conferences:

2016 A novel telomere-binding protein, TelBP1, modulates VSG expression site silencing kinetics in *Trypanosoma brucei*. (oral presentation)
Helena Reis (presenting author), Mario Dejung, Elisabeth Kremmer, Falk Butter, Christian J. Janzen
BSP Trypanosomiasis & Leishmaniasis Seminar,
September 4-7, 2016, Budweis, Czech Republic.

A new piece of the trypanosomal shelterin puzzle. (poster)
Helena Reis (presenting author), Mario Dejung, Elisabeth Kremmer, Falk Butter, Christian J. Janzen
Chromatin Dynamics Symposium,
March 10-12, 2016, München, Germany.

2015 Characterization of a novel telomere-binding protein in *Trypanosoma brucei*. (poster)
Helena Reis (presenting author), Mario Dejung, Elisabeth Kremmer, Falk Butter, Christian J. Janzen
Kinetoplastid Molecular Cell Biology Meeting,
April 25-29, 2015, Woods Hole, USA.

TABLE OF CONTENTS

ACKNOWLEDGMENTS

Firstly, I would like to express my deepest gratitude to my supervisor Christian Janzen for introducing me to the exciting world of telomere research and parasitology, for the continuous support of my Ph.D. study, for his motivation, and immense knowledge. His guidance helped me in all the time of research and writing of this thesis.
I am also very grateful to Nicolai Siegel for kindly agreeing to be the second reviewer of this thesis and for the great input he provided in our meetings.
A very special gratitude goes out to Falk Butter from the IMIB in Mainz for our successful collaboration and the mass spectrometry expertise.
I would like to thank Elisabeth Kremmer from the Helmholtz Center in Munich for providing antibodies.
Special thanks also to Ulrike Kämmerer from the university hospital in Würzburg who was a great mentor for me in the context of the career advancement program of the 'Frauenbüro' of the University of Würzburg. Thank you for your warm encouragement and mental support.
I also thank all former and present lab members of the Siegel group: Juan Jose Vasquez, Amelie Kraus, Carolin Wedel, Laura Müller and Raúl Cosentino. Thank you for our great lab meetings. I would particularly like to thank Laura for our conversations and for proofreading some parts of this thesis.
Many thanks should also be addressed to the whole department for Cell- and Developmental Biology. Thank you for your support and help whenever I needed it. I especially thank Brooke Morriswood for proofreading our manuscript and many helpful comments on it. Thanks to Susanne Kramer for sharing your knowledge regarding RNA extraction and working with radioactivity. I also thank Henriette Zimmermann for several conversations and helpful advice she gave me. Thank you for being such a good colleague and friend!
I am also very grateful to all former and present lab members of the Janzen lab. Thank you for a great atmosphere and the fun in and outside the lab. Elisabeth Meyer-Natus, I appreciate your help throughout my years in the lab and thank you for your skillful support with luciferase assays. I would like to express special thanks to Nicole Eisenhuth and Zdenka Cicova for being amazing colleagues and friends. You supported me greatly and were always willing to help me. I am also grateful to my very talented bachelor students, Klara Thein and Lena Pfaller. I thank Klara for initial studies on luciferase reporters and Lena for successful characterization of a further telomere-binding protein. I also appreciate the work of my great master students, Susanne Bury and Marie Schwebs. I thank Susi for her support with the investigation of TelBP1 isoforms and Marie for amazing continuation of Lena's project and for the conduction of TbTRF Co-IPs.
I must express my very profound gratitude to my parents and to my brother and sister for providing me with unfailing support and continuous encouragement throughout my years of study and through the process of researching and writing this thesis. Thank you.
At the end, my heartfelt appreciation goes to my beloved husband Joschua who was and is always a great support for me. I thank you for your patience, continuous encouragement, and all your love.

ZUSAMMENFASSUNG

Afrikanische Trypanosomiasis ist eine Krankheit, die in Afrika südlich der Sahara endemisch vorkommt und sowohl Menschen als auch Wild- und Haustiere betrifft. Die menschliche Form der Krankheit ist als Schlafkrankheit und die Tierform als Nagana bekannt. Ohne Behandlung verläuft die Krankheit in der Regel tödlich. Der einzellige Parasit *Trypanosoma brucei* ist die Ursache dieser Krankheit. Während seines Lebenszyklus bewegt sich der Parasit zwischen einem Säugetierwirt und einem Insektenvektor, der Tsetsefliege. Im Säugetierwirt vermehrt sich der Parasit als Blutstromform (BSF) extrazellulär im Blutkreislauf und im Lymphsystem. Das Fortbestehen der BSF-Parasiten im Wirt beruht auf einer Immunausweichstrategie durch antigene Variation der Oberflächenproteine. Diese Abwehrstrategie ist erforderlich, da der Parasit durch seinen extrazellulären Lebensstil direkt der Immunantwort ausgesetzt ist. Zu jedem Zeitpunkt wird nur ein variables Oberflächenprotein (VSG) auf der Zelloberfläche aus einem großen Repertoire exprimiert. Dabei wird das aktive VSG von einer von 15 spezialisierten telomerproximalen Transkriptionseinheiten transkribiert, den sogenannten Blutstromform *Expression Sites* (BESs). Die restlichen 14 BESs sind inaktiv. Diese monoallelische Expression und das periodische Wechseln des exprimierten VSG ermöglichen dem Parasiten der Immunantwort zu entgehen und eine persistente Infektion im Säugetierwirt zu etablieren. Während der Differenzierung von BSF zur Insektenvektor-residenten prozyklischen Form (PCF) wird die aktive BES transkriptionell herunter reguliert um die VSG-Transkription zu stoppen. Somit sind alle 15 BESs in PCF-Zellen inaktiv, da die Expression von Oberflächenproteinen stadienspezifisch reguliert ist.

Frühere Veröffentlichungen haben gezeigt, dass die Proteine TbTRF, TbRAP1 und TbTIF2 des Telomerkomplexes an der Transkriptionsregulation von VSG-Genen beteiligt sind. Es ist jedoch unklar, wie genau sie zur Regulation beitragen. Darüber hinaus gibt es keine Informationen über die Rolle von Telomeren bei der Initiation und Regulation der BES-Inaktivierung während der Differenzierung. Um Einblicke in die regulatorischen Mechanismen von Telomeren auf die VSG-Transkription und differenzierungsbedingte Repression der aktiven BES zu gewinnen, ist es daher notwendig, die vollständige Zusammensetzung der Telomerkomplexe in Trypanosomen zu identifizieren.

Zu diesem Zweck wurden zwei komplementäre biochemische Ansätze und quantitative Massenspektrometrie genutzt um die Zusammensetzung von Telomerproteinkomplexen in *T. brucei* zu bestimmen. Zunächst wurden mittels einer Affinitätschromatographie mit TTAGGG-Oligonukleotiden 17 potentielle telomerbindende Proteine gefunden. Darunter waren auch die bereits bekannten telomerbindenden Proteine TbTRF und TbTIF2. Zweitens wurde mit Hilfe eines Co-Immunpräzipitationsexperiments um die Interaktionen von TbTRF aufzuklären, fünf Proteine aufgereinigt. Alle diese fünf Proteine wurden auch mit telomerischer DNA in der Affinitätschromatographie angereichert.

Um diese Daten zu validieren, wurde eines der in beiden Experimenten gefundenen Proteine (TelBP1) charakterisiert. In BSF-Zellen co-lokalisiert TelBP1 mit TbTRF und interagiert mit bereits beschriebenen telomerbindenden Proteinen wie TbTRF, TbTIF2 und TbRAP1. Dies deutet darauf, dass TelBP1 eine weitere Komponente des Telomerkomplexes in Trypanosomen ist. Interessanterweise deuteten Proteininteraktionsstudien in PCF-Zellen auf eine andere Zusammensetzung des Telomerkomplexes im Vergleich zu BSF-Zellen.

Im Gegensatz zu den bekannten Mitgliedern des Telomerkomplexes ist TelBP1 für das Zellwachstum nicht essentiell. Damit könnte die Funktion von TelBP1 von den bekannten telomerbindenden Proteinen entkoppelt sein. Die Überexpression von TelBP1 zeigte auch keinen Einfluss auf das

Zellwachstum, führte aber zur Entdeckung von zwei weiteren kürzeren Isoformen von TelBP1. Ihr Ursprung und Funktion blieben jedoch ungeklärt.
Obwohl TelBP1 für das Zellwachstum entbehrlich ist, zeigten Westernblot-Analysen eine 4-fache Hochregulierung von TelBP1 in BSF-Zellen im Vergleich zu PCF-Zellen. Die stadienspezifische Regulation von TelBP1 unterstützt damit das Konzept von einer dynamischen Zusammensetzung der Telomerkomplexe. Zudem wurde beobachtet, dass TelBP1 die Kinetik der Inaktivierung der aktiven BES während der Differenzierung von der BSF zur PCF beeinflusst. Die Deletion von TelBP1 führte zu einem schnelleren Abschalten der BES im Vergleich zu Wildtyp-Parasiten.
Zusammengefasst zeigt die Funktion von TelBP1, dass das Abschalten der aktiven BES während der Differenzierung ein fein abgestimmter Prozess ist, der stadienspezifische Veränderungen der Telomerkomplexe beinhaltet.

SUMMARY

African trypanosomiasis is a disease endemic to sub-Saharan Africa. It affects humans as well as wild and domestic animals. The human form of the disease is known as sleeping sickness and the animal form as nagana, which are usually fatal if left untreated. The cause of African trypanosomiasis is the unicellular parasite *Trypanosoma brucei*. During its life cycle, *Trypanosoma brucei* shuttles between a mammalian host and the tsetse fly vector. In the mammalian host the parasite multiplies as bloodstream form (BSF) extracellularly in the bloodstream or the lymphatic system. Survival of BSF parasites relies on immune evasion by antigenic variation of surface proteins because its extracellular lifestyle leads to direct exposure to immune responses. At any given time each BSF cell expresses a single type of variant surface glycoprotein (VSG) on its surface from a large repertoire. The active VSG is transcribed from one of 15 specialized subtelomeric domains, termed bloodstream expression sites (BESs). The remaining 14 BESs are silenced. This monoallelic expression and periodic switching of the expressed VSG enables to escape the immune response and to establish a persistent infection in the mammalian host. During developmental differentiation from BSF to the insect vector-resident procyclic form (PCF), the active BES is transcriptionally silenced to stop VSG transcription. Thus, all 15 BESs are inactive in the PCF cells as surface protein expression is developmentally regulated.

Previous reports have shown that the telomere complex components TbTRF, TbRAP1 and TbTIF2 are involved in VSG transcriptional regulation. However, the precise nature of their contribution remains unclear. In addition, no information is available about the role of telomeres in the initiation and regulation of developmental BES silencing. To gain insights into the regulatory mechanisms of telomeres on VSG transcription and developmental repression it is therefore essential to identify the complete composition of the trypanosome telomere complex.

To this end, we used two complementary biochemical approaches and quantitative label-free interactomics to determine the composition of telomere protein complexes in *T. brucei*. Firstly, using a telomeric pull-down assay we found 17 potential telomere-binding proteins including the known telomere-binding proteins TbTRF and TbTIF2. Secondly, by performing a co-immunoprecipitation experiment to elucidate TbTRF interactions we co-purified five proteins. All of these five proteins were also enriched with telomeric DNA in the pull-down assay.

To validate these data, I characterized one of the proteins found in both experiments (TelBP1). In BSF cells, TelBP1 co-localizes with TbTRF and interacts with already described telomere-binding proteins such as TbTRF, TbTIF2 and TbRAP1 indicating that TelBP1 is a novel component of the telomere complex in trypanosomes. Interestingly, protein interaction studies in PCF cells suggested a different telomere complex composition compared to BSF cells. In contrast to known members of the telomere complex, TelBP1 is dispensable for cell viability indicating that its function might be uncoupled from the known telomere-binding proteins. Overexpression of TelBP1 had also no effect on cell viability, but led to the discovery of two additional shorter isoforms of TelBP1. However, their source and function remained elusive.

Although TelBP1 is not essential for cell viability, western blot analysis revealed a 4-fold upregulation of TelBP1 in the BSF stage compared to the PCF stage supporting the concept of a dynamic telomere complex composition. We observed that TelBP1 influences the kinetics of transcriptional BES silencing during developmental transition from BSF to PCF. Deletion of TelBP1 caused faster BES silencing compared to wild-type parasites.

Taken together, TelBP1 function illustrates that developmental BES silencing is a fine-tuned process, which involves stage-specific changes in telomere complex formation.

ABBREVIATIONS

2T1	VSG221 expressing, Tagged, clone1
3'UTR	3' untranslated region
5'UTR	5' untranslated region
aa	Amino acid
AAT	Animal African trypanosomiasis
ALD	Aldolase
ALT	Alternative Lengthening of Telomeres
Amp	Ampicillin
ASF1A	Anti-silencing factor 1A
AT	African trypanosomiasis
ATP	Adenosine triphosphate
BARP	Brucei alanine-rich protein
Base J	β-D-glucopyranosyloxymethyluracil
BDF	Bromodomain factor
BES	Bloodstream expression site
Blas	Blasticidin
BLE	Phleomycin resistance gene
bp	Base pair(s)
BSA	Covine serum albumin
BSD	Blasticidin resistance gene
BSF	Bloodstream form
C	Cytokinesis
CAF-1b	Chromatin assembly factor-1b
cAMP	Cyclic adenosine monophosphate
CDC13	Cell division control protein 13
cDNA	Complementary DNA
ChIP	Chromatin immunoprecipitation
ClTFA	Class I transcription factor A
Clr4	Cryptic loci regulator 4
Co-IP	Co-Immunoprecipitation
CST complex	CTC1, STN1, TEN1 complex
CTC1	Conserved telomere capping protein 1
Ct	C-terminal
C-terminal	Carboxy-terminal
dH_2O	Distilled water
DMSO	Dimethyl sulfoxide
DNA	Deoxyribonucleic acid
DNase	Deoxyribonuclease
dNTP	Deoxynucleotide
DOT1B	Disruptor of telomeric silencing 1B
DSB	Double-strand break
DTM	Differentiating trypanosome medium

DTT	Dithiothreitol
E. coli	*Escherichia coli*
EDTA	Ethylendiaminetetraacetic acid
EMSA	Electromobility shift assay
ES	Expression site
ESAG	Expression site associated gene
ESB	Expression site body
EtBr	Ethidium bromide
FACT	Facilitates chromatin transcription
FAIRE	Formaledehye-assisted isolation of regulatory elements
FCS	Fetal calf serum
Fluc	Firefly luciferase
fw	Forward
FYRP	Phenylalanine/ tyrosine rich protein
G1	Gap1 phase
G2	Gap2 phase
G418	Neomycin
GCV	Ganciclovir
gDNA	Genomic DNA
Gent	Gentamicin
GPI	Glycosylphosphatidylinositol
H3K9	Histone 3 lysine 9
H3K76	Histone 3 lysine 76
H3.V	Histone 3 variant
HAT (disease)	Human African trypanosomiasis
HAT (protein)	Histone acetyltransferase
HDAC	Histone deacetylase
HisMBP	Histidin-Maltose binding protein
HMGB	High mobility group box
HOT1	Homeobox telomere-binding protein 1
HP1	Heterochromatin protein 1
HR	Homologous recombination
hr	Hours
HSV-TK	Herpes simplex virus thymidine kinase
HYG	Hygromycin phosphotransferase gene
Hygro	Hygromycin
IFA	Immunofluorescence analysis
IN	Input
IP	Immunoprecipitation
ISWI	Imitation of switch
JBP	J-binding protein
kbp	Kilobase pair
kDa	Kilodalton
LB	Luria Bertani medium
LS	Long slender
M (cell-cycle)	Mitosis

M (concentration)	Molar
mM	Millimolar
Mbp	Mega base pairs
MES	Metacyclic expression site
MCM-BP	Minichromosome maintenance-binding protein
MITat	Molteno institute trypanozoon antigen type
µg	Microgram
µl	Microliter
µm	Micometer
ml	Mililiter
MRE11	Meiotic recombination 11
mRNA	Messenger RNA
MS	Mass spectrometry
mVSG	Metacyclic VSG
NAD	Nicotinamide Adenine Dinucleotide
NEO	Aminoglycoside phosphotransferase gene
NLP	Nucleoplasmin-like protein
NLS	Nuclear localization signal
nt	Nucleotide
Nt	N-terminal
N-terminal	Amino-terminal
NUP-1	Nuclear periphery protein-1
OE	Overexpression
ORC1	Origin recognition complex 1
ORF	Open reading frame
P	Pellet
PAC	Puromycin N-acetyltransferase gene
PAD1	Protein associated with differentiation 1
PAGE	Polyacrylamide gel electrophoresis
PBS	Phosphate-buffered saline
PCF	Procyclic form
PCR	Polymerase chain reaction
PDT	Population doubling time
PFR	Paraflagellar rod
P. falciparum	*Plasmodium falciparum*
PfEMP1	*Plasmodium falciparum* erythrocyte membrane protein 1
PfHda2	*Plasmodium falciparum* histone deacetylase 2
PfSET2	*Plasmodium falciparum* Suv(var)3-9, Enhancer-of-zeste, Trithorax 2
Phleo	Phleomycin
PICh	Proteomics of isolated chromatin segments
PIP1	POT1-interacting protein
PIP5K	Phosphatidylinositol 5-kinase
PIP5Pase	Phosphatidylinositol 5-phosphatase
Pol	Polymerase
POT1	Protection of telomeres 1

pro	Promoter
PTOP	TIN2-organizing protein
PTU	Polycistronic transcription unit
Puro	Puromycin
PVDF	Polyvinylidene fluoride
RAP1	Repressor activator protein 1
RCCP	Regulator of chromosome condensation 1-like protein
rDNA	Ribosomal DNA
Rif	Rap1-interacting protein
RIPA	Radio immunoprecipitation assay buffer
RIT-Seq	RNA interference target sequencing
RNA	Ribonucleic acid
RNAi	RNA interference
Rluc	Renilla luciferase
RT	Room temperature
rv	Reverse
S	Synthesis phase
SAS	Splice acceptor site
S. cerevisiae	*Saccharomyces cerevisiae*
S. pombe	*Schizosaccharomyces pombe*
SD	Standard deviation
SDS	Sodium dodecyl sulfate
Sir	Silent information regulator
SIR2rp1	Silent information regulator 2 related protein 1
SIF	Stumpy induction factor
SL	Spliced leader
SLT	Spliced leader trapping
SM	Single marker
SN	Supernatant
SS	Short stumpy
SSC	Saline sodium citrate buffer
ST-1	Subtelomere- and telomere-binding 1
ST-2	Subtelomere- and telomere-binding 2
STN1	Suppressor of cdc thirteen 1
SUMO	Small ubiquitin-like modifier
SUN1	SUN domain-containing protein 1
Swi6	Switch 6, an HP1 homolog
SWI/SNF	Switch/ sucrose non-fermentable
T7RNAP	T7 RNA polymerase
Taz1	Telomere length regulator
T. brucei	*Trypanosoma brucei*
TDP1	Trypanosome DNA binding protein 1
tel	Telomere
TelBP1	Telomere-binding protein 1
TEN1	Telomere length regulation protein

TERRA	Telomeric repeat-containing RNA
Tet	Tetracycline
TETR	Tetracycline repressor
Ti	Tetracycline inducible
TIN2	TRF-interacting nuclear protein 2
TINT1	TIN2-interacting protein 1
TK	Thymidine kinase
T-loop	Telomeric loop
TPE	Telomere position effect
TPP1	TINT1, PTOP, PIP1
TRF	TTAGGG repeat factor
TSS	Transcription start site
TTS	Transcription termination site
TUB	Tubulin
UTR	Untranslated region
VEX1	VSG exclusion 1
VSG	Variant surface glycoprotein
W	Wash
WC	Whole cell lysate
WHO	World Health Organization
WT	Wild-type
w/v	Weight per volume
v/v	Volume per volume
Δ	Deletion

FIGURES AND TABLES INDEX

Figures

Tables

1 INTRODUCTION

1.1 Telomere biology

1.1.1 Major milestones in telomere research

Telomeres are defined as nucleoprotein complexes at the end of linear chromosomes (Blackburn, 1991), consisting of repetitive DNA sequence and its associated proteins (reviewed in Linger and Price, 2009). The main function of telomeres is to maintain genome stability and integrity (reviewed in de Lange, 2005).

Nowadays, telomere research is of growing importance in many disciplines like chemistry, structural biology, cell biology, developmental biology, aging and cancer biology, but also parasitology. Telomeres are studied to answer questions like: How are telomeres involved in tumorigenesis and aging? What are the underlying mechanisms and participating molecular players? How are telomeres involved in microbial virulence and pathogenicity? Hence, investigation of telomeres provides opportunities for developing novel cancer therapeutics and also influences our understanding of cell biology and parasitology.

Scientific research in the field of telomere began in the year 1938 when telomeres were discovered and named by Hermann J. Muller (Muller, 1938). During his work on *Drosophila melanogaster* he found that the chromosome ends behaved like a cap structure, which protected the chromosome tips against mutagenic X-rays, deletions or inversions. Later, Barbara McClintock demonstrated an important role for telomeres in chromosomal integrity in 1941 as she observed broken chromosome ends tending to fuse end-to-end (McClintock, 1941). Investigations on how cellular lifespan was controlled by telomeres were the beginning of the research field 'telomeres and aging'. In 1961, Leonard Hayflick and colleagues observed that cultured human fetal cells have a limited replicative capacity which was termed the Hayflick limit (Hayflick and Moorhead, 1961). However, the source of the replication clock remained unknown. In 1972, James Watson recognized the 'end replication problem' in which the DNA polymerase machinery cannot completely replicate the 3' ends of a linear duplex DNA (Watson, 1972). Around the same time, the 'end replication problem' was also pointed out by Alexey Olovnikov. Suggesting that progressive telomere shortening would lead to cellular aging, he was able to functionally connect the 'end replication problem' with the Hayflick limit (Olovnikov, 1973). Both Watson and Olovnikov presumed the existence of a molecular machinery necessary for maintenance of telomere length and integrity.

It was in 1978 that Elizabeth Blackburn and Joseph Gall started to experimentally address the end replication problem. They found that the chromosome ends from the ciliated protozoan *Tetrahymena thermophila* contain a repetitive TTGGGG sequence motif (Blackburn and Gall, 1978). The repetitiveness of these sequences was later shown to be evolutionarily conserved across diverse organisms: In 1981, Blackburn demonstrated in collaboration with Jack Szostak that telomeric sequence can be transferred from one organism (*Tetrahymena*) to another (*Saccharomyces cerevisiae*) and that this foreign sequence is capable of fulfilling telomere function in the recipient cell (Szostak and Blackburn, 1982). Using *Tetrahymena* as a model organism was the key decision for the breakthrough of telomere research as it comprises thousands of chromosomes and thus, provides a high amount of telomeric material to study (Blackburn, 2009).

Shortly after, understanding of telomere maintenance was further advanced when Carol Greider described the telomerase, a ribonucleoprotein that uses its RNA component as a template for

elongation and *de novo* synthesis of telomeric repeats at chromosomal ends (Greider and Blackburn, 1985, Greider and Blackburn, 1987, Greider and Blackburn, 1989).
The study of human telomeres was rather challenging because human telomeres are not as abundant as telomeres of *Tetrahymena* and the telomerase is expressed at much lower levels (reviewed in Corey, 2009). In 1988, soon after the discovery of telomeres in *Tetrahymena*, Robert K. Moyzis proved that telomeres in human cells likewise consisted of TTAGGG repeats (Moyzis et al., 1988). In 1989, the human telomerase homolog was found in human cells by Gregg Morin (Morin, 1989). In 1994, further efforts of different groups revealed a connection between telomerase activity and cancer cell proliferation (Counter et al., 1994, Kim et al., 1994). Telomerase activity, for example, was detected in ~90% of human primary cancer cells and cell lines. In contrast, telomerase was undetectable in nonmalignant somatic cells. Today it is widely accepted, that other tumor cells use an alternative mechanism for telomere length extension, termed Alternative Lengthening of Telomeres (ALT), which is based on homologous recombination (reviewed in Conomos et al., 2013). Telomerase activity was also identified in proliferative stem cells (Broccoli et al., 1995) and germ cells (Mantell and Greider, 1994).
To understand the underlying mechanisms of chromosome end maintenance across many cell divisions it was, therefore, essential to comprehend the organization and precise function of telomeres.

1.1.2 Telomere organization and function

Multiple discoveries in the 20th century have contributed to our understanding of telomere organization in the nucleus and its crucial role for genome stability. In the following I am going to review on the proteins that are involved in this process and introduce important differences across different phylae.

Telomere-binding proteins

Telomeres consist of DNA and protein complexes. The telomeric DNA contains a double-stranded DNA-sequence of G-rich, non-coding, tandem repeats, which end in a 3' G-rich single-stranded overhang (Makarov et al., 1997, McElligott and Wellinger, 1997). The sequence of telomeric repeats and the length of the duplex region and the 3' overhang are species-specific (reviewed in Shore, 2001). To prevent that the telomeric DNA is recognized as a double-strand break (DSB) the 3' single-stranded overhang folds back and invades the double-stranded region, forming a telomeric loop (T-loop) (Griffith et al., 1999). The formation of this cap-like structure is stabilized by proteins, which are associated with telomeric DNA. In mammals, the core telomere protein complex is called shelterin, which includes six components (Figure 1).

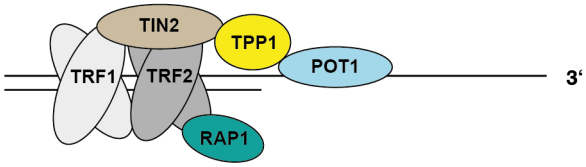

Figure 1. Structure of shelterin.
Shelterin is a multiprotein complex, which binds double-stranded and single-stranded telomeric repeats. Shelterin is composed of the TTAGGG repeat factors TRF1 and TRF2, TIN2 (TRF-interacting nuclear protein 2), RAP1 (Repressor activator protein 1), TPP1 (previously called TINT1, PTOP, PIP1) and POT1 (Protection of telomeres 1).

Three proteins of the shelterin complex directly bind telomeric DNA: TTAGGG repeat factor 1 and 2 (TRF1, TRF2) and Protection of telomeres 1 (POT1). The other three proteins are associated with the

shelterin complex through protein-protein interactions: TRF-interacting nuclear protein 2 (TIN2), TPP1 (previously called TINT1, PTOP, PIP1) and Repressor activator protein 1 (RAP1) (reviewed in de Lange, 2005). TRF1 was the first mammalian telomere-binding protein identified through its interaction with double-stranded telomeric repeats (Zhong et al., 1992, Chong et al., 1995). Few years later, TRF2 was found as a TRF1 paralog by bioinformatic searches (Bilaud et al., 1997, Broccoli et al., 1997). Two-hybrid screens with TRF1 and TRF2 revealed TIN2 and RAP1 as interaction partners, respectively (Kim et al., 1999, Li et al., 2000). Homology searches based on unicellular eukaryotes uncovered POT1 as a single-stranded telomeric DNA-binding protein (Baumann and Cech, 2001). Finally, analysis of TIN2- and POT1-interacting proteins led to the discovery of TPP1 (Houghtaling et al., 2004, Liu et al., 2004, Ye et al., 2004b). In 2004, several mass spectrometry (MS) analyses of shelterin-associated proteins identified no further shelterin components or telomere-binding proteins (Liu et al., 2004, O'Connor et al., 2004, Ye et al., 2004a). However, with the improvement of MS technology, Kappei and colleagues were able to find a novel direct telomere-binding protein, Homeobox telomere-binding protein 1 (HOT1), which promotes telomerase association with telomeric chromatin (Kappei et al., 2013).
In addition, several accessory proteins interact with the shelterin components and either antagonize or support their function at telomeres (reviewed in Galati et al., 2013). Later, a second protein complex was found at telomeres. The trimeric complex CST, which is composed of Conserved telomere capping protein 1 (CTC1), Suppressor of CDC thirteen 1 (STN1) and TEN1, localizes to single-stranded telomeric DNA and contributes to telomere length maintenance (reviewed in Rice and Skordalakes, 2016).

Function of shelterin proteins

The shelterin complex performs crucial and diverse functions to ensure chromosome end shielding and genome stability. For example, shelterin proteins are indispensable for protection of chromosome ends from degradation, inappropriate DNA repair, recombination, and DNA end-to-end fusions by forming a cap that hides the telomeres from being recognized as DSBs (reviewed in Palm and de Lange, 2008). Thus, downregulation of any of the shelterin components (with RAP1 being an exception), protection of chromosome ends is impaired, resulting in DNA damage response, cell cycle arrest and finally in replicative senescence or apoptosis (reviewed in Palm and de Lange, 2008). Interestingly, RAP1 is not necessary for telomere protection and RAP1 null mice display no impairment in viability and fertility (Martinez et al., 2010, Sfeir et al., 2010). The main phenotype of RAP1 loss is a higher tendency of telomeres to undergo homologous recombination (Sfeir et al., 2010).
Furthermore, telomere-binding proteins are important for the recruitment of the telomerase to the chromosome ends in order to maintain the telomere length through each round of DNA replication (reviewed in Pfeiffer and Lingner, 2013). Thereby TPP1 functions as a positive regulator and together with POT1 increases telomerase processivity (Abreu et al., 2010, Latrick and Cech, 2010). On the other hand, shelterin also negatively controls telomerase to achieve telomere length homeostasis. This negative regulation is based on the action of TRF1, TRF2 and POT1 (van Steensel and de Lange, 1997, Smogorzewska et al., 2000, Loayza and De Lange, 2003).
Replication of telomeric DNA is difficult due to its tandem repeats and complexity in structure. Therefore, telomere replication depends on specialized helicases and telomere-binding proteins (reviewed in Sampathi and Chai, 2011). Especially, TRF1, TRF2 and POT1 act synergistically with the replication machinery to promote accurate replication of telomeric DNA. Without their aid, replication forks frequently stall and collapse, thereby causing defects in telomere structure and loss of telomere DNA (reviewed in Martinez and Blasco, 2015).

Telomeres also contribute to nuclear organization, which is important for gene regulation and genome stability (Crabbe et al., 2012). For example, telomere clustering to the nuclear envelope plays a central role for correct pairing and recombination of homologous chromosomes during meiosis (Ding et al., 2007). Moreover, it has been shown that telomeres also localize to the nuclear periphery during nuclear reassembly after mitosis (Crabbe et al., 2012). Telomere tethering to the nuclear matrix requires the function of the nuclear membrane protein SUN domain-containing protein 1 (SUN1). In addition, it has been demonstrated that RAP1 can interact with SUN1. However, telomeres can also be attached to the nuclear envelope by a RAP1-independent pathway (Scherthan et al., 2011).

Moreover, telomeres exert a gene regulatory effect, which relies on the formation of a heterochromatic structure. Thereby, transcription of telomere-proximal genes is reversibly suppressed. This phenomenon of telomeric silencing is known as the telomere position effect (TPE), which is based on epigenetic regulation by chromatin modifications (reviewed in Blasco, 2007, Schoeftner and Blasco, 2009). The TPE was first described in *Drosophila melanogaster* and in *Saccharomyces cerevisiae* (Levis et al., 1985, Gottschling et al., 1990). The TPE in mammals is maintained by the sirtuin-6 (SIRT6) histone deacetylase (Tennen et al., 2011) and involves Heterochromatin protein 1 (HP1) binding to telomeric and subtelomeric domains (Koering et al., 2002). Benetti and colleagues demonstrated that TRF2 influences the epigenetic properties of telomeres (Benetti et al., 2008). They showed that TRF2 overexpression in mice leads to a loss of heterochromatin marks, which impairs telomeric silencing suggesting that shelterin might be involved in the regulation of the epigenetic status of telomeres.

1.1.3 Yeast as a model organism for telomere studies

Establishing yeast as model organism has given many insights in the principal concepts of telomere biology. In the following sections telomere protein complexes and TPE in budding and fission yeast will be briefly revisited.

Telomeres of the budding yeast *Saccharomyces cerevisiae* consist of heterogeneous $C_{1-3}A/TG_{1-3}$ repeats and are protected by two separate protein complexes, namely CST and Rap1/Rif1/Rif2 (Figure 2B). The trimeric complex Cell division control protein 13 (Cdc13)/Stn1/Ten1 (CST) binds the G-strand overhang while the Rap1/ Rap1-interacting factor 1 (Rif1)/ Rap1-interacting factor 2 (Rif2) complex interacts with the duplex part (reviewed in Kupiec, 2014). In contrast to mammal Rap1, the yeast ortholog binds telomeric DNA directly and the homology to the human Rap1 is limited. Orthologs of other shelterin components are missing in budding yeast. Finally, telomere length maintenance in budding yeast is also ensured by the telomerase (Cohn and Blackburn, 1995).

Like in mammals, yeast telomeres appear to be of heterochromatic nature and silence genes adjacent to telomeres through TPE (Figure 3). The TPE in *S. cerevisiae* is established by Rap1 and Silent information regulator (Sir) proteins, which have nicotinamide adenine dinucleotide (NAD)-dependent histone deacetylase activity (Aparicio et al., 1991, Kyrion et al., 1993). To assemble heterochromatin at telomeric regions, Sir proteins are recruited to telomeres by Rap1 and then spread to subtelomeric regions. Transcriptional repression is caused by hypoacetylation of the core histones H3 and H4 by Sir proteins. As HP1 proteins are missing in budding yeast, Sir proteins carry out their function (reviewed in Blasco, 2007).

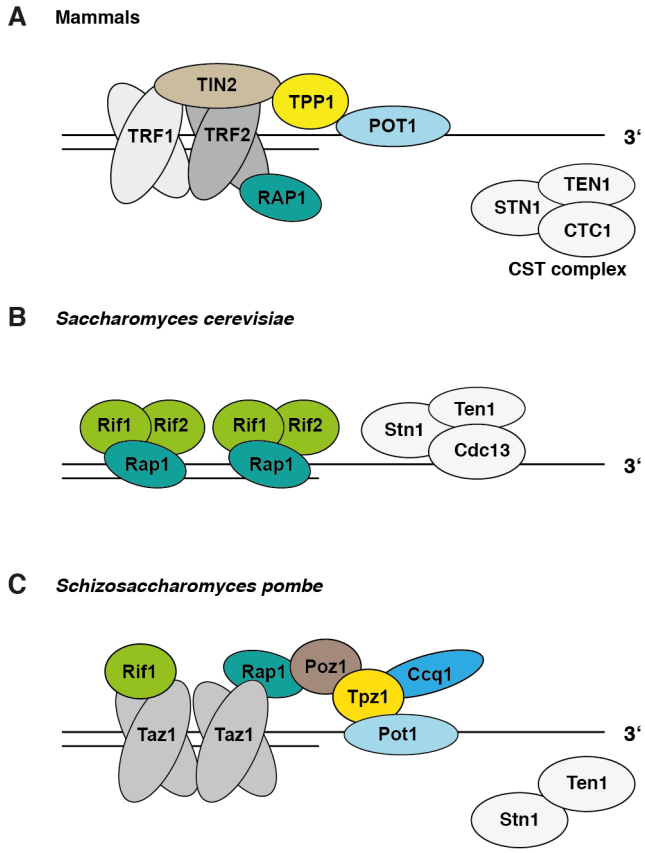

Figure 2. Comparison of yeast and human telomere protein complexes.
(**A**) Illustration of the mammalian telomere protein complex shelterin and of the trimeric CST complex. (**B**) Telomere protein complexes in *S. cerevisiae*. (**C**) Telomere protein complexes in *S. pombe.* Orthologous proteins are shaded in the same color.

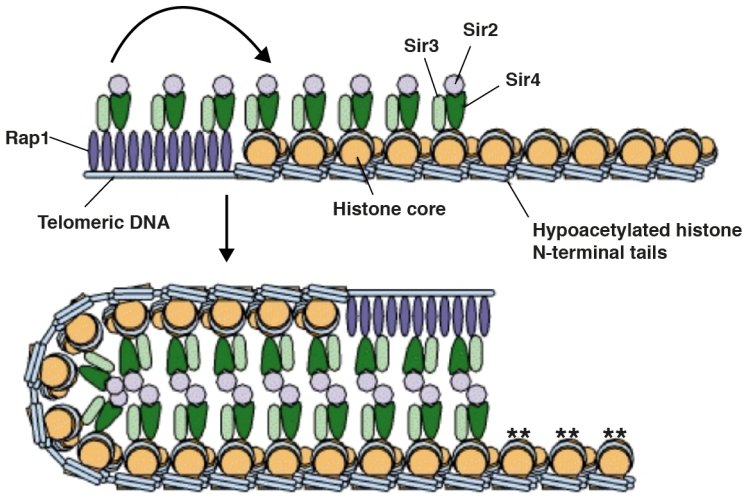

Figure 3. Telomere position effect in *S. cerevisiae*.
Rap1 binds telomeric DNA and recruits the Sir complex to the telomere. The Sir2 histone deacetylase sequentially removes the acetyl residues from N-terminal tails of histones H3 and H4 of nearby nucleosomes. This permits binding of Sir3 and Sir4 to histone tails and thus recruits more Sir3 and Sir4 to telomeres promoting the spreading of silencing along the telomeric and subtelomeric region. Telomeric heterochromatin is stabilized by the folding back of the telomeres facilitating additional Rap1-Sir and Sir-Sir interactions. Asterisks: hyperacetylated histone N-terminal tails. Picture adapted from Lodish H, Berk A, Zipursky et al. Molecular Cell Biology 4th edition, 1999.

In the fission yeast *S. pombe*, the telomere complex is structurally more similar to the shelterin complex of mammalian cells than to the telomere protein complexes of *S. cerevisiae* (reviewed in

Armstrong and Tomita, 2017). Homologs of all six shelterin proteins have been identified in *S. pombe* (Figure 2C). In addition, fission yeast contains orthologs of the CST complex components Stn1 and Ten1, which associate with each other to protect telomeres (Martin et al., 2007). Like in other eukaryotes, a telomerase is expressed in fission yeast (Nakamura et al., 1997).
The telomeric heterochromatin assembly machinery in *S. pombe* is also more closely related to that of mammals than to that of budding yeast. The histone methyltransferase Cryptic loci regulator 4 (Clr4) methylates histone H3 at lysine 9 (H3K9) and offers a binding site for the chromatin-associated protein Switch 6 (Swi6), an ortholog of HP1. Moreover, the siRNA machinery and the telomere-binding protein Taz1, a TRF homolog, contributes to establish telomeric heterochromatin (reviewed in Blasco, 2007).
Taken together, although apparent differences in the protein composition of telomere complexes can be observed, the fundamental mechanisms that regulate telomere organization seem to be conserved.

1.1.4 Pathogens and telomere-dependent regulation of contingency genes

Telomeres of pathogenic microbes have been in the spotlight since the discovery that telomeric regions harbor contingency genes. Contingency genes are subject to pre-emptive mutational events and thereby ensure rapid, clonal switches in phenotype through which the pathogen's persistence in the host is established (reviewed in Barry et al., 2003). The regulation of these genes relies on the support from the telomeric environment. There are many examples of pathogenic microbes containing such genes in the telomeric regions including the protozoan parasites *Plasmodium falciparum* and *Trypanosoma brucei*. Both parasites use clonal antigenic variation to evade the host immune response. The malaria parasite and the parasite *T. brucei* express *var* genes and variant surface glycoprotein (VSG) genes from subtelomeric loci, respectively.

Telomeres of Plasmodium falciparum

The telomeres of the *P. falciparum* are composed of tandem GGGTT(T/C)A repeats and are maintained by telomerase activity with each round of replication (Bottius et al., 1998). In contrast to human and yeast, less is known about telomere-specific proteins in *P. falciparum*. Homology searches for telomere-binding proteins in the *P. falciparum* proteome identified some orthologs of yeast telomere-binding proteins (reviewed in Scherf et al., 2001, Hernandez-Rivas et al., 2013), but only the telomerase was experimentally verified (Figueiredo et al., 2005). Interestingly, a recent study using oligonucleotide pull-downs revealed a telomere complex composed of seven proteins (Sierra-Miranda et al., 2017). However, further investigations are needed to solve their function in telomere biology.
Besides the function in chromosome end maintenance, telomeres of *P. falciparum* are essential for mutually exclusive expression of one out of 60 members of the multigene virulence family *var*, which codes for the surface protein *Plasmodium falciparum* erythrocyte membrane protein 1 (PfEMP1) (Scherf et al., 1998). PfEMP1 is presented at the surface of infected erythrocytes and allows cytoadherence within the microvasculature (reviewed in Pasternak and Dzikowski, 2009). While one *var* gene is active, the others are subject to telomeric heterochromatin-mediated silencing similar to the TPE in yeast and humans. This silencing involves telomere anchoring at the nuclear periphery, enrichment in heterochromatic histone marks and the action of the histone methyltransferase, PfSET2 (*Plasmodium falciparum* Suv(var)3-9, Enhancer-of-zeste, Trithorax 2), the histone deacetylase, PfHda2 (*Plasmodium falciparum* histone deacetylase 2), and the histone code reader, PfHP1 (reviewed in Duraisingh and Horn, 2016). Members of the sirtuin histone deacetylase gene family have also been identified in *P. falciparum*. Especially, PfSir2 was shown to silence *var* genes through

its binding to *var* promoters (Tonkin et al., 2009). In contrast to the situation in yeast, where Rap1 recruits Sir2, it remains elusive how PfSir2 is recruited to telomeres in *P. falciparum*.

Telomeres of Trypanosoma brucei

Like mammalian telomeres, the telomeres of the African trypanosomes contain a TTAGGG-repeated sequence and end in a 3' G-rich single-stranded overhang (reviewed in Dreesen et al., 2007). Telomere length is mainly maintained by the action of telomerase but telomerase-independent mechanisms of chromosome end stabilization seem to exist since telomerase loss does not lead to cell cycle arrest (Glover et al., 2007).

Several attempts to identify telomere-binding proteins in *T. brucei* have been already conducted. For instance, Eid and Sollner-Webb discovered two telomeric proteins in BSF and PCF *T. brucei*, ST-1 and ST-2 (Eid and Sollner-Webb, 1995, Eid and Sollner-Webb, 1997). These proteins were named ST-1 and ST-2 for subtelomere- and telomere-binding activity. Eid and Sollner-Webb showed that each protein is part of two major telomeric complexes but, unfortunately, the protein sequence is still unknown of these candidates. Next, a report by Field and Field indicated the existence of a G-strand-binding protein in nuclear extracts (Field and Field, 1996). This protein-DNA complex was neither purified nor characterized. Further, Cano and colleagues purified three protein complexes (complexes C1-C3) associated with single-stranded telomeric DNA (Cano et al., 2002). However, mass spectrometry analysis to identify the components of these complexes failed due to low protein abundance.

Homology searches for telomere-binding proteins led only to the identification of a TRF2 homolog, TbTRF (Li et al., 2005). Yeast two-hybrid screens with TbTRF revealed an additional telomere-binding protein, TbRAP1 (Yang et al., 2009). Finally, TbTIF2, the trypanosome TIN2 homolog, was found by co-immunoprecipitation experiments to interact with TbTRF as well (Jehi et al., 2014b). Up to now, only these three functional homologs of shelterin members have been described in *T. brucei* (Figure 4).

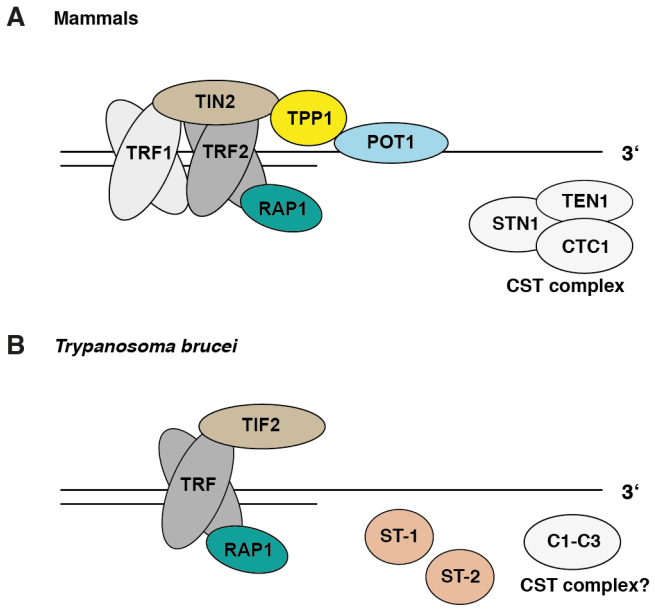

Figure 4. Telomere complex composition in *T. brucei*.
(**A**) Schematic representation of shelterin and CST complex. (**B**) Illustration of known functional homologs of the shelterin complex members and identified telomere-binding proteins in *T. brucei*.

Telomeres of trypanosomes also exert a sirtuin-dependent silencing effect on promoters inserted adjacent to telomeres but not on VSG genes (Alsford et al., 2007). Interestingly, mechanisms distinct from the sirtuin-mediated silencing exist to regulate VSG gene expression (reviewed in Duraisingh and Horn, 2016). Those mechanisms also include the known telomere-binding proteins, but an HP1 homolog has not been found in trypanosomes. How telomeres are involved in the regulation of mutually exclusive VSG expression in trypanosomes is still elusive.
In the following, the current knowledge of antigenic variation in *T. brucei* and the parasite itself will be presented in more detail.

1.2 Trypanosoma brucei

1.2.1 African trypanosomiasis

African trypanosomiasis (AT) is a vector-borne disease caused by an extracellular protozoan parasite belonging to the genus *Trypanosoma*. Depending on the mammalian host two different forms of the disease are distinguished: the animal form of African trypanosomiasis (AAT) (reviewed in Auty et al., 2015), and the human African trypanosomiasis (HAT), known as sleeping sickness (reviewed in Brun et al., 2010). AT primarily affects poor rural populations of countries in sub-Saharan Africa (reviewed in Franco et al., 2014).
The parasites are transmitted to humans and animals by the bite of a tsetse, a fly from the genus *Glossina*. Tsetse flies are present in sub-Saharan Africa only, thus leading to the endemic restriction of the disease to this area (reviewed in Franco et al., 2014).
AAT is specifically caused by *T. congolense*, *T. vivax* and *T. brucei brucei* and affects wild and domestic animals and is usually fatal unless treated. Infections of domestic animals, in particular cattle, cause rapid death and result in a severe burden for African agriculture and economy (reviewed in Auty et al., 2015).
HAT is caused by *T. brucei gambiense*, which is present in western and central Africa and by *T. brucei rhodensiense*, which is found in eastern and southern Africa (reviewed in Franco et al., 2014). The species *T. brucei gambiense* is responsible for 97% of reported cases of HAT and causes a chronic infection (WHO, 2017). The infection can last for month or even years without symptoms. *T. brucei rhodensiense* is responsible for 3% of reported cases and leads to an acute infection (Franco et al., 2017, WHO, 2017). First symptoms appear a few month or weeks after infection.
The disease progression of HAT is characterized by two phases: an early haemo-lymphatic and a late meningo-encephalic stage (reviewed in Franco et al., 2014). In the early stage, the parasite is present in the bloodstream and lymphatic system of the mammalian host causing unspecific symptoms like headache, fever and physical weakness. In the late stage, the parasite crosses the blood-brain barrier and infects the central nervous system. Patients reaching the late stage suffer progressive neurological damage leading to disturbed sleep-wake cycle and neuropsychiatric disorders including behavioral changes, confusion, poor coordination and extreme lethargy. Finally, the late stage leads to coma, severe organ failure, and eventually death. Although the disease symptoms of HAT caused by the two subspecies of *T. brucei* are generally the same, they differ in frequency, severity and kinetic appearance. Current treatments of sleeping sickness are inadequate due to toxicity of drugs and no available vaccine. Due to early infection screening programs as well as increased efforts of vector elimination the number of newly reported cases of HAT has declined since 2001. Therefore, in 2015, the number of new reported cases was 2804 (WHO, 2017).

1.2.2 Life cycle of *T. brucei*

During its life cycle *T. brucei* lives solely extracellularly and shuttles between a mammalian host and an insect vector (Figure 5). To manage the different environments, *T. brucei* has developed a sophisticated life cycle characterized by an alternation of proliferating and non-proliferating stages. These stages are adapted to the changing environmental conditions and therefore, differ in multiple elementary biological processes like morphology, energy metabolism and motility of the parasite (reviewed in Matthews, 2005, Fenn and Matthews, 2007).

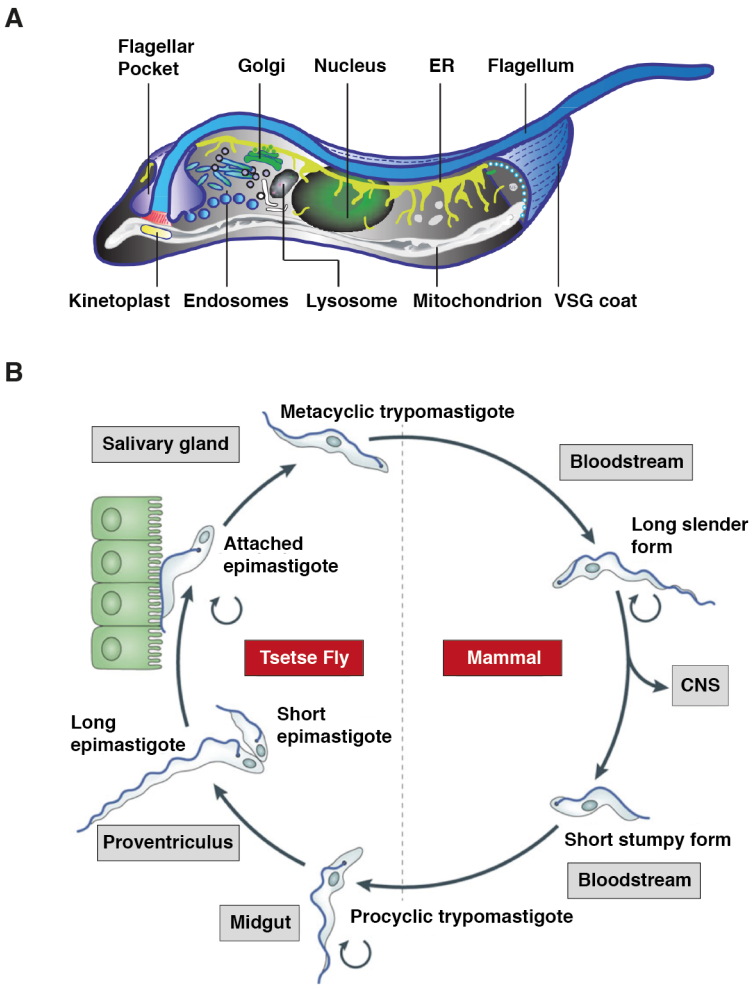

Figure 5. *Trypanosoma brucei* and its life cycle and different developmental forms.
(**A**) Illustration of a *T. brucei* bloodstream form cell showing the morphology and organelles of the parasite. Endoplasmatic Reticulum (ER). Image from (Overath and Engstler, 2004). (**B**) Scheme of the *T. brucei* life cycle. Trypanosomes shuttle between a mammalian host and the tsetse fly vector and have to adapt to different environmental conditions throughout their life cycle. Central nervous system (CNS). Illustration adapted from (Langousis and Hill, 2014)

In mammals, trypanosomes proliferate in the bloodstream and the lymphatic system as morphologically long slender forms (LS). The extracellular life style of trypanosomes leads to direct confrontation of the bloodstream form (BSF) pathogen and the host adaptive immune response. Trypanosomes evade the humoral immune response by antigenic variation which involves periodic expression of immunologically distinct variable surface glycoproteins (VSGs) (reviewed in Horn, 2014). These surface proteins are linked to the surface membrane by a glycosylphosphatidylinositol (GPI) anchor (Ferguson et al., 1985).

As the parasite numbers increase, LS parasites differentiate by a quorum sensing-like mechanism into non-proliferative short stumpy forms (SS) (Reuner et al., 1997). This differentiation event is

induced by a parasite-released signaling molecule, the stumpy induction factor (SIF), via a cAMP-mediated signal transduction pathway (Vassella et al., 1997). Interestingly, a recent study has revealed that LS parasites are also able to use a SIF-independent differentiation pathway (Zimmermann et al., 2017). Differentiation to SS cells is coupled to a morphological transformation, cell cycle arrest in G1/G0 phase, and adaptation of the transcriptome (Jensen et al., 2009) and the proteome (Dejung et al., 2016, Butter et al., 2013). For example, PAD1 (Protein associated with differentiation 1) expression is initiated in SS cells (Dean et al., 2009). PAD1 belongs to the carboxylate surface transporter family and enables SS cells sensing the differentiation signal, which contains citrate/ cis-aconitate (Engstler and Boshart, 2004, Czichos et al., 1986). Upon transmission to the tsetse vector, SS parasites differentiate inside the fly midgut to procyclic form (PCF) trypomastigotes and reenter the cell cycle (Roditi and Lehane, 2008). The temperature decreases and the presence of citrate in the fly midgut trigger this developmental transition (Czichos et al., 1986). As a prerequisite of the host adaptation, the VSG coat is replaced by procyclins like GPEETs and EPs, which are also GPI-anchored (reviewed in Roditi and Liniger, 2002). Another major change that takes place during the differentiation to the PCF is the expansion of the mitochondrion and the activation of the mitochondrion-based oxidative phosphorylation for energy generation, while in BSF parasites energy metabolism relies exclusively on glycolysis in the glycosome (reviewed in Hellemond et al., 2005).

Procyclic trypomastigotes migrate from the tsetse midgut to the proventriculus, where they undergo asymmetric cell division resulting in one long epimastigote and one short epimastigote (Van Den Abbeele et al., 1999). At this stage, epimastigotes change their surface coat and express the surface protein BARP (*brucei* alanine-rich protein) (Urwyler et al., 2007). The short epimastigotes further migrate to the salivary gland, where they attach to epithelial cells and elongate (Van Den Abbeele et al., 1999). Asymmetric division of attached epimastigotes generates growth-arrested metacyclic trypomastigotes, which are freely moving in the salivary gland lumen. The metacyclic form parasites are preadapted to survive in the mammalian host as they acquire a new coat composed of metacyclic VSGs (mVSGs). With the blood-meal of the tsetse fly, metacyclic trypomatigotes are released into the bloodstream of the mammalian host (reviewed in Sharma et al., 2009). There, parasites resume cell division and differentiate to LS parasites.

For BSF and PCF trypanosomes, *in vitro* cultures are well established and the developmental transition from BSF to PCF can be performed *in vitro* as well. Two types of BSF culture strains are distinguished: the pleomorphic and the monomorphic strain. Pleomorphic trypanosomes are able to differentiate from LS into SS under axenic conditions on agarose plates (Reuner et al., 1997, Vassella and Boshart, 1996). Therefore, the differentiation process to PCF cells can be induced synchronously and efficiently. In contrast, the culture-adapted monomorphic BSF strains have a uniform slender morphology and have lost the ability to differentiate to SS parasites due to a defect in the SIF signaling pathway. Nevertheless, using a membrane-permeable cAMP derivative allows slender-to-stumpy development of monomorphic *T. brucei* (Breidbach et al., 2002). Although monomorphic cells lack the competence for slender-to-stumpy transition, *in vitro* differentiation into PCF has been achieved for monomorphic strains as well, but less efficiently and asynchronously compared to pleomorphic cells. Differentiation of both monomorphic and pleomorphic BSFs to PCFs is induced by lowering the temperature from 37°C to 27°C and addition of citrate and/ or cis-aconitate into the culture medium (Brun and Schönenberger, 1981, Czichos et al., 1986, Overath et al., 1986).

In addition, an *in vitro* differentiation approach based on the overexpression of the RNA-binding protein 6 (RBP6) has been described for the developmental transition of procyclics to long and short epimastigotes and finally to metacyclic parasites (Kolev et al., 2012).

1.2.3 Genome organization and gene expression regulation in *T. brucei*

To understand how the complex life cycle of *T. brucei* is regulated, and how the different events are coordinated on a molecular level, knowledge about the genome sequence and organization is essential. The genome of *T. brucei* was completely sequenced in the year 2005 (Berriman et al., 2005) and greatly facilitated a more precise study of gene function, gene expression and cellular mechanisms in trypanosomes. It was the genome of *T. brucei* TREU 927, a strain capable of passing the complete life cycle (van Deursen et al., 2001), that was subjected to sequencing, although most laboratory research at that time and today use the *T. brucei* Lister 427 strain as a model organism.

Chromosome organization

The nuclear genome of *T. brucei* is composed of 11 diploid megabase chromosomes (0.9-5.7 Mbp), 1 to 5 intermediate chromosomes (200-900 kbp), and ~100 minichromosomes (30-150 kbp), of which the latter two chromosome types are probably haploid (Figure 6) (Berriman et al., 2005, reviewed in Ersfeld, 2011).

The megabase chromosomes contain an internal chromosome core of housekeeping genes, transcribed by RNA polymerase II (Pol II) and specialized telomeric transcription units termed VSG expression sites (ESs) from where VSG genes are transcribed by RNA polymerase I (Pol I). The ESs are separated from the core region by 50 bp repeats (Figure 6). Nearly all protein coding genes are found on megabase chromosomes (reviewed in Ersfeld, 2011).

The intermediate chromosomes harbor a core of non-repetitive DNA, stretches of subtelomeric 177 bp repeats and canonical telomeric repeats. A few VSG ESs are located on intermediate chromosomes and can be activated by an *in situ* switch (detailed explanation in section 1.2.4.)

Approximately 55% of the minichromosome sequence is composed of 177 bp repeats. Towards the chromosome ends, 70 bp repeats, VSG genes and canonical telomeric repeats are found (reviewed in Ersfeld, 2011).

The genome sequence of *T. brucei* encompasses ~9000 predicted genes (Berriman et al., 2005), of which ~1500 genes belong to the large VSG repertoire distributed over large subtelomeric VSG arrays found on megabase chromosomes. Single VSG genes are also located in ESs of megabase and intermediate chromosomes and in subtelomeric regions on minichromosomes. This large VSG repertoire increases the capacity of VSG variation.

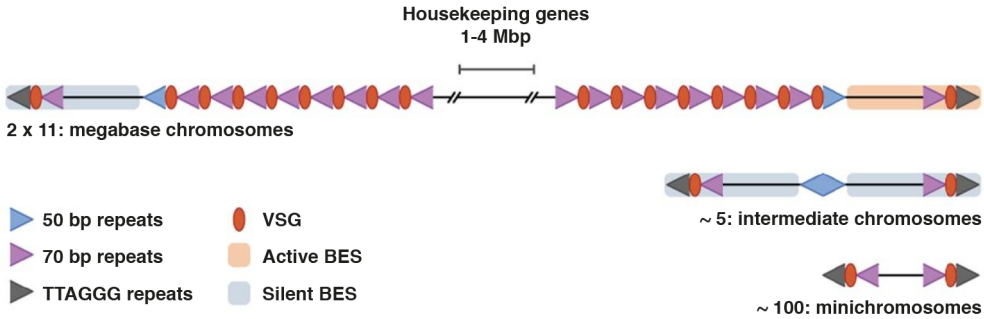

Figure 6. Chromosome organization in *T. brucei*.
The schematic shows the three different classes of *T. brucei* chromosomes and their structure. In addition, it illustrates how the huge VSG repertoire occupies the subtelomeres of all three chromosome classes. Image adapted from (Glover et al., 2013b).

RNA polymerase II transcription of housekeeping genes and mRNA maturation

Protein-coding genes in *T. brucei* are, with some exceptions, intron-free and organized in polycistronic transcription units (PTU) (Imboden et al., 1987), in which genes are generally not functionally related (reviewed in Clayton, 2002). Only two genes have been reported to contain

introns: the Poly(A) Polymerase and an ATP-dependent DEAD/H RNA helicase (Berriman et al., 2005, Mair et al., 2000).
The transcription of housekeeping genes containing PTUs is driven by RNA polymerase II. With one exception, no other promoters for Pol II transcription have been identified in *T. brucei*. Rather, the boundaries of PTUs are associated with epigenetic marks defining transcription start sites (TSS) and transcription termination sites (TTS) (Siegel et al., 2009). Once transcription is initiated, the maturation of polycistronic mRNAs occurs co-transcriptionally which is based on coupled *trans*-splicing and polyadenylation. The *trans*-splicing process involves cleavage of mRNAs from the polycistronic primary transcripts and addition of the 39 nucleotide spliced leader (SL) sequence from a short SL RNA exon. The SL sequence harbors the cap structure which is crucial for translation of the mRNA (Perry et al., 1987). Thus, every individual mRNA contains a SL sequence at its 5' end (Parsons et al., 1984). The SL RNA has to be available in large quantities in the cell. It is encoded in an array of monocistronic tandem repeats, which are also transcribed by Pol II. In contrast to the protein-coding genes, a Pol II promoter has been characterized for the genes coding the SL precursor RNA (Gilinger and Bellofatto, 2001).
An elegant study has used the conserved SL sequence for selective sequencing of the region downstream of the SL acceptor site (Nilsson et al., 2010). This high throughput sequencing approach, named spliced leader trapping (SLT), was applied to LS, SS and PCF cDNA libraries in order to map splice acceptor sites (SASs) and to investigate the developmental regulation of mRNA abundance. Using this approach more than 2500 alternative splicing events were found, many of which turned out to be developmentally regulated (Nilsson et al., 2010). Alternative splicing events can result in gain or loss of N-terminal targeting signals, leading to changed intracellular localization of the arising proteins. Consequently, alternative splicing belongs to the mechanisms contributing to gene expression variability.
Generally, Pol II transcription in *T. brucei* is constitutive and thus regulated very little, if at all (reviewed in Clayton, 2014). Therefore, mRNA abundance is mainly regulated post-transcriptionally on the level of *trans*-splicing, polyadenylation, mRNA stability, mRNA export, translation control, and protein stability (reviewed in Kramer, 2012). Furthermore, mRNA stability and translation can be influenced by the 3' untranslated region (UTR), which contains regulatory sequence elements for RNA-binding proteins (reviewed in Clayton, 2013). Those sequence elements also contribute to developmentally regulated gene expression (reviewed in Kramer, 2012).

RNA polymerase I transcription of surface protein-coding genes

A special feature of African trypanosome species is the Pol I-driven transcription of protein-coding genes. Usually, Pol I only transcribes rRNA genes in other eukaryotes. In *T. brucei*, Pol I transcribes not only rRNA genes (reviewed in Horn, 2001), but also comprises protein-coding genes, namely VSGs and procyclin, the major surface proteins of the BSF and PCF parasites, respectively.
Like the Pol II-transcribed genes, procyclin genes are transcribed from polycistronic transcription units, which are organized internally on megabase chromosome 6 and 10 with other protein-coding genes (reviewed in Daniels et al., 2010). The control of procyclin expression is dependent on transcriptional and post-transcriptional mechanisms (Biebinger et al., 1996). For instance, elements present in the 3' UTR of procyclin mRNAs determine the stage-specific expression as these elements cause instability of procyclin mRNA in the BSF stage but not in the PCF stage (Hotz et al., 1997).
VSG genes are expressed from subtelomeric transcription units, the bloodstream ESs (BESs) in the BSF or the metacyclic ESs (MESs) in the metacyclic form (reviewed in Pays et al., 2001). Both classes of ESs differ in their structure (Figure 7). MESs are characterized by a small size of 1 to 5 kb. They contain a Pol I promoter, highly degenerated 70 bp repeats and a mVSG gene at the telomere

(Ginger et al., 2002). The expression of mVSGs is unusual in two aspects. Firstly, MESs are the only clear examples of monocistronic transcription of protein-coding genes in *T. brucei* (Alarcon et al., 1994, Graham and Barry, 1995). Secondly, the mVSG expression is controlled mainly at the level of transcription initiation (Pedram and Donelson, 1999). It was estimated that a repertoire of 27 or fewer mVSG genes is used by the metacyclic trypanosome population (Turner et al., 1988) resulting in a heterogeneous population. However, this estimation was conducted using *T. brucei rhodensiense*. A recent assembly of Lister 427 VSG repertoire identified six MESs, of which one was atypical (Cross et al., 2014). The vast majority of metacyclic cells express only a single mVSG of the repertoire (Ramey-Butler et al., 2015) and the choice of the mVSG type occurs randomly (Tetley et al., 1987, Barry et al., 1998).

BESs are polycistronic units of 40 to 60 kb in length and are as followed organized: a 50 bp repeat region, a Pol I promoter, expression site associated genes (ESAGs), 70 bp repeats, and a VSG gene proximal to telomeric repeats (Hertz-Fowler et al., 2008). Each BES contains a variable composition and amount of ESAGs. Several of these ESAG genes encode surface molecules, and at least two of them contribute to host adaptation (reviewed in Pays et al., 2001, Pays, 2006). The 70 bp repeats are sequence elements residing upstream of nearly all VSGs in the genome of *T. brucei* (Marcello and Barry, 2007, Cross et al., 2014, Hovel-Miner et al., 2016). This repetitive DNA sequence offers recombinational homology during VSG switching (Hovel-Miner et al., 2016). The described composition of the BES is highly conserved among all present BESs (Hertz-Fowler et al., 2008). There are around 15 functional BESs in the genome of Lister 427 (Hertz-Fowler et al., 2008) of which only one is actively transcribed while the remaining are silenced. This monoallelic transcription of BESs is regulated on multiple levels, which are described below.

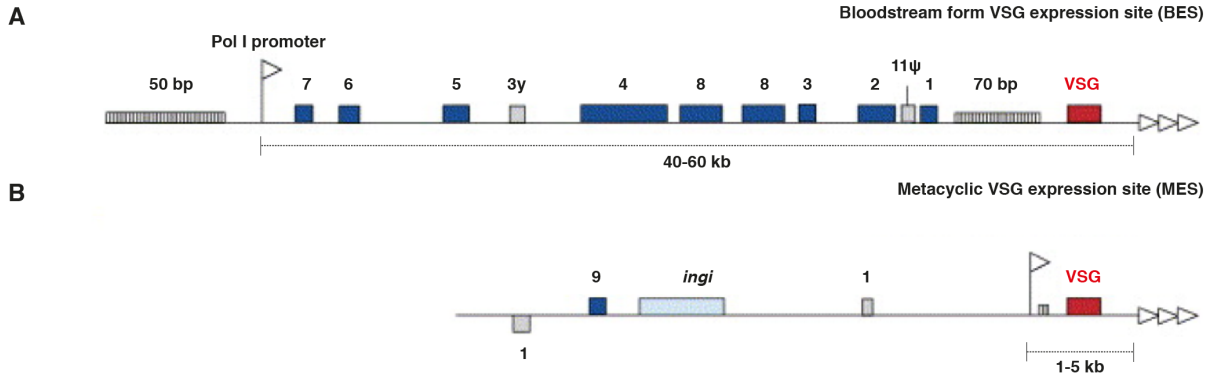

Figure 7. Organization of VSG expression sites.
(**A**) Structure of a bloodstream form expression site (BES). Upstream of the Pol I-driven promoter (white flag) 50 bp repeats are located. Downstream of the promoter the BES is as followed arranged: expression site associated genes (ESAGs, in blue), possible pseudo-ESAGs (in grey), 70 bp repeats, and the VSG gene (in red) at telomeric repeats. (**B**) Structure of a metacyclic expression site (MES). This locus contains a Pol I-driven promoter (white flag), highly degenerated 70 bp repeats and the metacyclic VSG gene nearby the telomeric repeats. Upstream of the Pol-I promoter ESAGs (in blue), pseudo-ESAGs (in grey) or retrotransposons (in light blue) can be located. Image adapted from (Taylor and Rudenko, 2006).

1.2.4 Antigenic variation in bloodstream form trypanosomes

Antigenic variation is a widespread mechanism among pathogens to evade the host's immune attack (Deitsch et al., 2009). BSF trypanosomes utilize this form of immune evasion strategy in order to establish a persistent infection in the mammalian host. Thus, their chance to be taken up by the tsetse fly is increased. Two main characteristics determine the success of antigenic variation in BSF parasites. Firstly, monoallelic expression of the VSG gene ensures that only one type of VSG is present on the cell surface. The cell surface is covered with 10 million identical VSG copies forming a dense protective layer. Secondly, stochastic switching of the VSG genes enables establishing a new

wave of parasitaemia after elimination of the current parasite populations by the host adaptive immune response. Consequently, the host's immune system has to react with a novel antibody response, as novel antigens are present. The next stochastic event of a VSG switch ensures the next immune escape. How antigenic variation is regulated is still not well understood. Several studies have shown that VSG expression regulation occurs on multiple levels, for example it relies on chromatin structure, telomeric location and nuclear organization (reviewed in Glover et al., 2013b).

Chromatin and regulation of monoallelic expression

Monoallelic VSG expression is based on the exclusive activation of one BES and the maintenance of the silent state of the other 14 BESs (Hertz-Fowler et al., 2008). Several different factors have been identified to be responsible for the selective transcriptional status of the different BESs (Figure 8) (reviewed in Glover et al., 2013b).

One of these factors is chromatin structure. In every eukaryotic cell, nucleosomes are the elementary units of chromatin and are composed of 147 bp DNA wrapped around an octamer containing two copies of each core histone: H2A, H2B, H3, H4 (Kornberg, 1974). The N-terminal tails of these histones are subject of post-translational modifications (PTMs) leading to changes in the chromatin structure, but not to changes in the DNA sequence. Such a regulation form is referred to as epigenetic (reviewed in Kouzarides, 2007). Epigenetic processes include also nucleosomal positioning and remodeling and regulate chromatin assembly, DNA replication, recombination and repair, and transcriptional activity (reviewed in Saha et al., 2006, Kouzarides, 2007). Therefore, it is not surprising that distinct chromatin architecture of the BESs plays a role in BES repression and activation. In this way, silent BESs contain a nucleosome-enriched chromatin structure while the active BES possesses an open and nucleosome-depleted chromatin structure (Figueiredo and Cross, 2010). The importance of nucleosome organization within inactive BESs has been demonstrated by depletion of the core histone H3 (Alsford and Horn, 2012) or the linker histone H1 (Pena et al., 2014, Povelones et al., 2012). Both led to removal of repression, referred to as derepression, of silent BES promoters, but not of the telomere-proximal VSG gene.

Multiple chromatin-associated proteins have been described mediating either BES promoter silencing, VSG silencing or complete BES silencing (reviewed in Horn and McCulloch, 2010). As chromatin remodelers influence the access of the transcriptional machinery to the nucleosomal DNA by changing structure, composition and positioning of nucleosomes, the impact of the chromatin remodeler Switch/ sucrose non-fermentable (SWI/SNF2)-like ATPase TbISWI on BES silencing has been investigated (Hughes et al., 2007). Depletion of TbISWI or any of its interacting proteins such as Nucleoplasmin-like protein (NLP), the Regulator of chromosome condensation 1-like protein (RCCP) and Phenylalanine/ tyrosine rich protein (FYRP) resulted in derepression of the BES at the promoter region (Stanne et al., 2011, Stanne et al., 2015). A similar phenotype was observed upon RNAi-mediated knockdown of the Histone deacetylase 3 (HDAC3), indicating that HDAC3 contributes to BES promoter silencing as well (Wang et al., 2010). This is consistent with the observation that ISWI remodelers act at inactive regions lacking acetylation (Corona et al., 2002).

It has been reported that the repression of the BES promoter also depends on the subunits Spt16 and Pob3 of the Facilitates chromatin transcription (FACT) histone chaperone complex, which is highly enriched at silent BES promoters and where it appears to stabilize chromatin compaction (Denninger et al., 2010, Denninger and Rudenko, 2014). The histone chaperones, Chromatin assembly factor-1b (CAF-1b) and the Anti-silencing factor 1A (ASF1A) were demonstrated to be involved in BES promoter silencing as well. Depletion of either CAF-1b or ASF1A caused derepression of a promoter-proximal reporter (Alsford and Horn, 2012).

That chromatin-modifying factors are not only responsible for promoter repression of inactive BESs but also for the complete BES silencing became apparent by the functional analysis of the Disruptor of telomeric silencing 1B (DOT1B) protein. DOT1B is a dispensable methyltransferase responsible for the trimethylation of histone H3 at lysine 76 (H3K76). Deletion of DOT1B led to derepression of silent VSGs and to a delayed transcriptional VSG switch indicating, that trimethylation of H3K76 is important to maintain the repressed status of inactive BESs and to achieve rapid VSG switching (Figueiredo et al., 2008). The acetyl-lysine binding proteins, Bromodomain factor 2 and 3 (BDF2 and BDF3) were shown to contribute to BES silencing as well (Schulz et al., 2015).
Proteins of the replication machinery also contribute to the regulation of monoallelic VSG transcription since depletion of the Origin recognition complex 1 (ORC1) (Benmerzouga et al., 2013) or Minichromosome maintenance-binding protein (MCM-BP) results in derepression of silent BESs (Kim et al., 2013b).
Since all BESs are located adjacent to a telomere, the effect of classical sirtuin-dependent telomeric silencing on monoallelic VSG expression has been investigated in trypanosomes. Although the Silent information regulator 2 related protein 1 (SIR2rp1) and the Histone acetyltransferase 1 (HAT1) have an impact on the expression of reporters inserted at the telomere, these proteins appear not to be responsible for VSG suppression (Alsford et al., 2007, Kawahara et al., 2008).
In summary, many different chromatin-associated proteins have been shown to maintain the silent BES status. In contrast, little is known about how the maintenance of the active BES is mediated. Only few proteins have been identified to be associated with an open and active chromatin status. The high mobility group box (HMGB) protein, Trypanosome DNA binding protein 1 (TDP1) is highly enriched along the active BES compared to silent ones. Depletion of TDP1 leads to chromatin condensation and a decrease in BES transcription suggesting that TDP1 functions in the maintenance of the nucleosome-depleted BES structure (Narayanan and Rudenko, 2013, Aresta-Branco et al., 2016). This decondensed chromatin architecture facilitates the recruitment of transcription activators. Other findings suggest that the histone deacetylase HDAC1 antagonizes SIR2rp1-mediated telomeric silencing in BSF cells indicating that histone modifications might influence the open state of the active BESs (Wang et al., 2010). However, it has not been tested if the anti-silencing effect of HDAC1 also antagonizes VSG silencing in the active BES. Depletion of the transcription regulator NLP elucidates that BES activity and BES silencing are interconnected (Narayanan et al., 2011). Nucleoplasmins function as histone chaperones and consequently regulate the chromatin condensation state (Frehlick et al., 2007). Besides the described derepression phenotype upon NLP knockdown, NLP depletion leads to downregulation of the active BES suggesting that NLP regulates transcription levels of active and silent BESs (Narayanan et al., 2011).
To sum up, various chromatin associated factors and epigenetic control mechanisms are of great importance for VSG expression and repression (Figure 8), but our understanding of the underlying processes remains incomplete. The challenge for the future is to solve the interplay of these epigenetic factors and to identify further players in the process of VSG expression regulation.

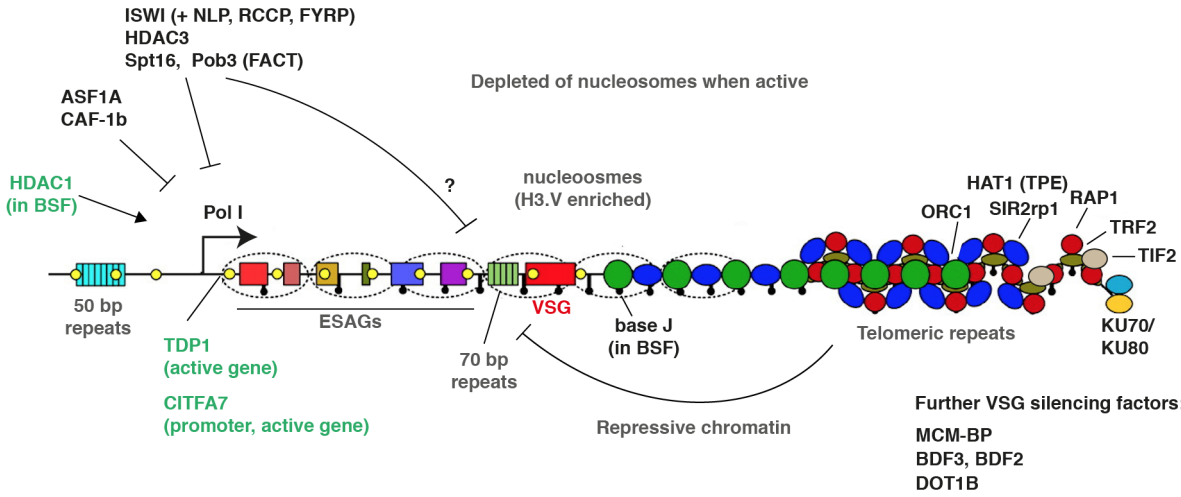

Figure 8. Overview of chromatin factors involved in ES transcriptional regulation.
A repressive chromatin conformation is formed by the telomere-binding proteins TbRAP1, TbTRF and TbTIF2 as well as by TbORC1. TbSIR2rp1 is recruited to telomeres and is responsible for the propagation of basal telomeric silencing along the chromosome end but not for VSG silencing. It is not known how TbSIR2rp1 is tethered to telomeres and if other proteins fulfill the function of yeast Sir3 and Sir4. The histone acetyltransferase TbHAT1 also contributes to basal telomeric silencing in *T. brucei* without influencing VSG silencing. Base J and the histone variant H3.V are highly enriched at silent BESs. In addition, several histone chaperone (TbFACT, TbASF1A, TbCAF-1b), chromatin remodeling (TbISWI and its interactions) and histone modifying factors (TbHDAC3) contribute to BES promoter silencing. Histone modifying enzymes (TbDOT1B), histone modification-binding proteins (TbBDF2, 3) and regulators of DNA replication (TbMCM-BP) are involved in VSG silencing mechanisms. In contrast, the HMG box protein TbTDP1 associates with the active BES and ensures the open chromatin status. Furthermore, TbCITFA7 predominantly localizes to the active BES promoter and is required for effective Pol I transcription initiation. TbHDAC1 is also important for activated expression. Image adapted from (Maree and Patterton, 2014).

Nuclear organization and regulation of monoallelic expression

An additional level of BES regulation is the nuclear organization (Figure 9). Spatial localization is important for the exclusive activity of one single BES as it localizes in a Pol I extranucleolar body termed the ES body (ESB) (Navarro and Gull, 2001). The ESB seems to contain factors critical for transcription elongation since Pol I transcription is initiated at each BES but only elongated at the active BES (Vanhamme et al., 2000). However, no ESB-specific factors have been identified so far. Moreover it is not known how the ESB assembly around the BES is regulated: either the ESB determines randomly which BES is going to be active or the active BES recruits the ESB. Due to the study carried out by Vanhamme and colleagues, the common notion is that BES transcription is regulated rather at the level of transcription elongation than initiation (Vanhamme et al., 2000). However, recent studies on the Class I transcription factor A (CITFA) provided evidence that the BES activity might be regulated via transcription initiation (Nguyen et al., 2014). CITFA is an essential factor for RNA Pol I transcription of the active BES, rRNA genes and the procyclin genes (Brandenburg et al., 2007). Investigation of CITFA revealed that CITFA predominantly localizes to the active BES promoter compared to a silent BES. Depletion of two CITFA proteins, CITF-2 and CITF-7, led to rapid loss of rRNA and active VSG mRNA and subsequently to parasite death (Nguyen et al., 2014). The authors hypothesized that the sequestration of CITFA restricts effective Pol I transcription initiation to the nucleolus and the ESB. Another study showed that the ESB is enriched in SUMOylated proteins, which associate with the active BES promoter (Lopez-Farfan et al., 2014). Small ubiquitin-like modifier (SUMO) is a reversible post-translational modification, which regulates protein function (reviewed in Eifler and Vertegaal, 2015). BES-associated SUMOylated proteins are proposed to be necessary for efficient RNA Pol I recruitment to the BES promoter (Lopez-Farfan et al., 2014).

While the active BES is localized in a nuclear subcompartment (Navarro and Gull, 2001), the inactive ones are thought to occupy the peripheral heterochromatic space within the nucleus. However, direct experimental evidence is still missing. Knockdown of the Nuclear periphery protein-1 (NUP-1), a lamina-like and major structural protein of the nuclear envelope, leads to derepression of silent BESs supporting the view that the silent BESs might be associated with heterochromatin. As NUP-1 co-localizes with telomeres in the nuclear periphery the observed derepression upon NUP-1 depletion suggests that nuclear position of the telomeres is an essential aspect for BES repression (DuBois et al., 2012).

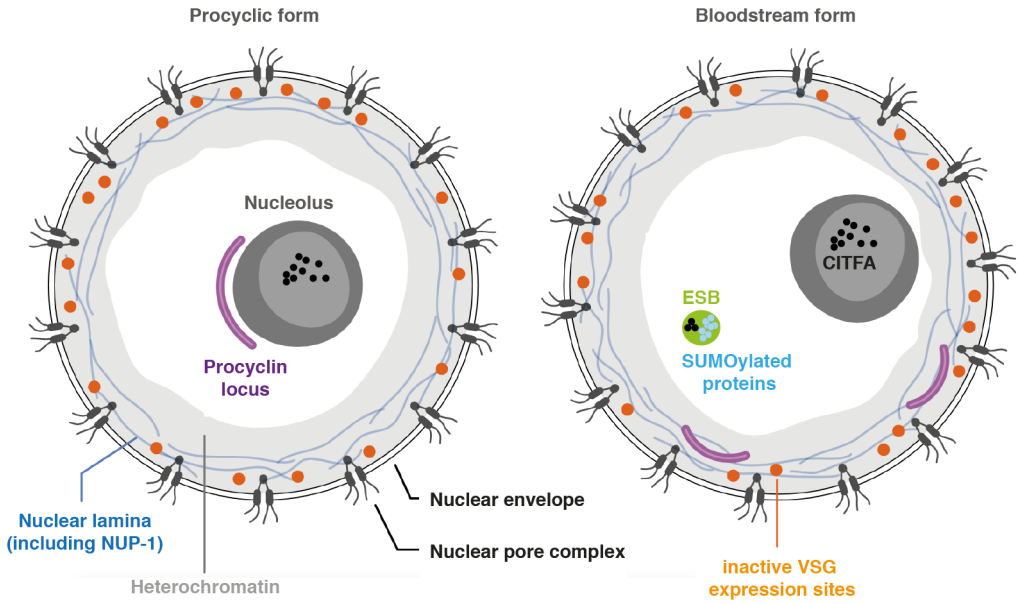

Figure 9. Nucleus organization in procyclic and bloodstream form parasites.
Schematic representation of a procyclic and bloodstream form nucleus. The heterochromatin region is displayed in grey in the nuclear periphery. The nucleolus is illustrated as a dark grey structure and is associated with the procyclin loci (in purple) in the procyclic form. Inactive VSG expression sites (in orange) are tethered to the nuclear periphery in the procyclic form. The silent VSG expression sites in BSF cells are also thought to be located at the nuclear periphery probably tethered by NUP-1. The single active VSG expression site associates with the expression site body, which is enriched in the transcription factor CITFA and SUMOylated proteins. Image adapted from (Glover et al., 2013b).

VSG switching

In the case that the monoallelic VSG expression is impaired, the parasites either derepress silent VSGs or switch to a completely new VSG. Hence, monoallelic VSG expression and switching are interrelated and catalyze antigenic variation 'hand-in-hand'. Periodic switching of the surface coat embodies one of the most important virulence factors for parasite survival in the bloodstream of the mammalian host. The expressed VSG type can be changed either by a transcriptional switch or DNA recombination (Figure 10) (reviewed in Taylor and Rudenko, 2006).

The transcription-based strategy involves simultaneous silencing of the active BES and activation of a silent BES. This type of switching is termed *in situ* switch and is limited by the BES number (Bernards et al., 1984, Michels et al., 1984). Although a wide range of factors have been analyzed that contribute to the regulation of ES transcription, the mechanisms that induce or accomplish an *in situ* switch remain elusive (Batram et al., 2014, Cestari and Stuart, 2015, Figueiredo et al., 2008, Glover et al., 2016, reviewed in Glover et al., 2013b, and Gunzl et al., 2015).

In contrast, the initial processes of VSG switching by DNA recombination are becoming clearer (reviewed in Devlin et al., 2017). During the DNA recombination reaction the active VSG is replaced by a silent VSG gene from anywhere in the VSG repertoire. The recombination switch can rely on different mechanisms: a crossover or a gene conversion event (reviewed in McCulloch et al., 2015).

The crossover occurs within two chromosome ends and leads to telomere exchange (Pays et al., 1985). The gene conversion is based on replacing the VSG in the active BES with a copy of a formerly silent VSG. The VSG gene conversion event can occur in two different scenarios: firstly, duplication of a complete, functional VSG or secondly, generation of a novel mosaic VSG by segmental gene conversion using multiple silent VSGs from the entire VSG archive. Duplicative gene conversion of functional VSGs uses the 70 bp repeats upstream of the VSG gene and highly conserved elements in the VSG 3'UTR as recombination sites (Hovel-Miner et al., 2016, Bernards et al., 1981). Besides, telomeres can also provide homology for recombination (De Lange et al., 1983). For the assembly of mosaic VSGs, the gene conversion occurs within the VSG ORF (Pays et al., 1983b, reviewed in Marcello and Barry, 2007). Several studies have revealed that components of the conserved DNA repair pathway of homologous recombination (HR) act on VSG switching (reviewed in Devlin et al., 2017). As this repair strategy is initiated by DSBs, it becomes apparent that DSB formation in the BES might be one of the major triggers for VSG switching (reviewed in Li, 2015). Inducing a DSB adjacent to 70 bp repeats and immediately upstream of the active VSG leads to an increase in VSG switching rates (Glover et al., 2013a). This effect is locus-specific, as no influence on VSG switching is observed upon DSB induction in other locations along the active BES (Boothroyd et al., 2009). There are different hypotheses on how DSBs are generated in the BES. One possibility is that an endonuclease action causes DSB formations. However, such an endonuclease has not been found in *T. brucei*, yet. A second source of DSBs might be clashes between transcription and replication leading to DNA fragility (reviewed in Bermejo et al., 2012). A third model suggests that telomeres render adjacent loci fragile as BESs contain a higher prevalence for DSBs compared to a chromosome-internal locus (Glover et al., 2013a). Hereby, the telomere length plays an important role since critically short telomeres were shown to initiate breaks in the BES (Hovel-Miner et al., 2012, reviewed in Li, 2015).

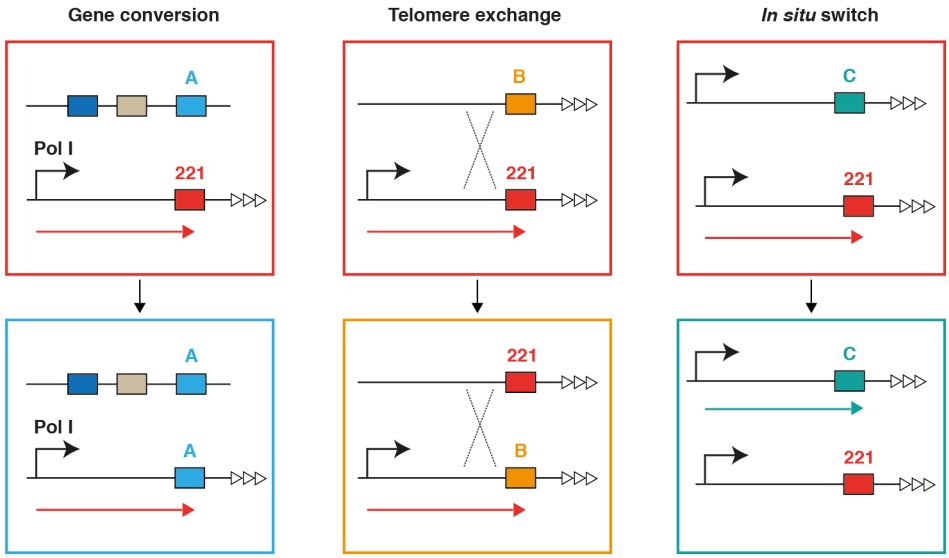

Figure 10. VSG switching mechanisms.
Gene conversion relies on the duplication of a VSG gene from the silent VSG repertoire and the replacing of the VSG in the active BES. A crossover event from an active and a silent BES leads to telomere exchange and thus to the expression of a new VSG gene. An *in situ* switch is based on the transcriptional inactivation of the active BES and the simultaneous activation of a previously repressed BES. Image adapted from (Taylor and Rudenko, 2006).

Telomeres and regulation of antigenic variation

Looking at the regulatory mechanisms of monoallelic transcription and switching of the VSG gene one structure is always involved: the telomere.

Telomeres often form a heterochromatic structure, which exerts a repressive effect on telomere-proximal genes. This phenomenon is known as the TPE. A TPE as epigenetic regulation mechanism of BES silencing was first proposed by Horn and Cross (Horn and Cross, 1995). They discovered that, transcription from promoters was repressed when they were inserted at telomere regions of a silent BES at the BSF stage. This repressive effect was stable and inherited over many generations. In addition, they demonstrated that the observed silencing effect was position-dependent. Transcriptional repression of the promoters was detected either when the promoters were inserted in an inactive BES or at a non-telomeric silent VSG locus (Horn and Cross, 1997). They also presented that the repression was more pronounced at positions closer to the telomere.

However, a series of publications pointed out that BES silencing and telomeric silencing might be mechanistically distinct. Firstly, the deacetylase SIR2rp1 was described to be required for DNA repair and for RNA Pol I repression at telomere-adjacent loci, but not for VSG silencing (Alsford et al., 2007). In yeast, the Sir2 protein is known to interact with the telomere-binding protein Rap1 to establish a heterochromatic telomere environment (Kyrion et al., 1993). It is not clear how exactly SIR2rp1 functions at telomeres in trypanosomes. Moreover, it was shown, that deletion of telomeres disrupted basal telomere-mediated silencing, while the VSG silencing was maintained (Glover et al., 2007). Studies on the nuclear lamina component NUP-1 indicated that only VSG silencing relies on the intact nuclear periphery organization, as only reporters inserted in inactive BESs were derepressed upon NUP-1 depletion, but not reporters integrated upstream of a *de novo* telomere (DuBois et al., 2012). Nonetheless, it remains possible that other components of the nuclear lamina contribute to basal telomeric silencing.

Telomeric chromatin and nuclear environment display some exclusive properties in trypanosomes. For instance, the telomeric TTAGGG repeats of inactive BESs contain a modified DNA nucleotide named base J. Base J is a β-D-glucosyl-hydroxymethyluracil that replaces 13% of thymidines in telomeres of BSF parasites and is absent from the PCF stage. However, the prominence of this modification at silent telomeres seems not to be responsible for transcriptional repression of BESs. When the two J-binding proteins (JBP), JBP1 and JBP2, which are required for J synthesis, were knocked out, the telomeric VSG silencing remained unaffected (reviewed in Borst and Sabatini, 2008).

In addition, the analysis of histone variants in trypanosomes uncovered an enrichment of the histone 3 variant (H3.V) at telomeres (Lowell and Cross, 2004). Histone variants play a crucial role in a wide range of genetic and epigenetic processes such as transcription regulation, DNA repair and chromosome segregation. Nonetheless, the work by Lowell and Cross could not prove that the H3.V association with telomeres had an effect on VSG silencing. However, two recent studies provided evidence for H3.V to be a repressive chromatin mark required for the maintenance of VSG silencing as H3.V loss led to VSG derepression from silent BESs (Reynolds et al., 2016, Schulz et al., 2016). As H3.V co-localizes with base J at telomeres, Reynolds and colleagues investigated the effect of base J loss in a H3.V null background and observed upregulation of some previously derepressed VSGs indicating that base J acts synergistically with H3.V in transcriptional silencing of telomeric regions. To understand how these epigenetic marks of telomeres act in antigenic variation, it is essential to identify which histone chaperones and chromatin remodeling complexes incorporate H3.V at telomeres and hence, permit regulated gene expression. For example, such tasks could be performed either by known or unidentified telomere-binding proteins.

The characterization of telomere-associated and -binding proteins in *T. brucei* has improved our understanding of VSG expression control, however it remains far from being complete. Surprisingly, many telomere-associated proteins have little influence on VSG silencing or switching such as the DNA repair proteins, MRE11 (Meiotic recombination 11) and KU70/KU80. In yeast, MRE11 is

required for chromosomal integrity at telomeres (Nugent et al., 1998). In trypanosomes, it exhibits a function in chromosomal rearrangement and DNA repair, without influencing telomere length or VSG switching (Robinson et al., 2002). The heterodimer KU70/KU80 also does not impact VSG switching or silencing although it is essential for telomere length maintenance (Conway et al., 2002, Janzen et al., 2004).

In contrast, the components of the core telomere protein complex indeed influence monoallelic and switchable VSG transcription. Up to now, only three homologous proteins of the shelterin complex members have been described in trypanosomes: TbTRF, TbTIF2 and TbRAP1 (Figure 4) (Li et al., 2005, Jehi et al., 2014b, Yang et al., 2009). All three telomeric factors are essential for trypanosome viability. While TbTRF and TbTIF2 only play a minor role for VSG silencing, TbRAP1 is critical for BES-linked VSG suppression. Depletion of TbRAP1 leads to derepression of silent BESs with the most prominent effect at telomere-proximal regions. The simultaneous expression of several different VSGs coincides with the assembly of multiple Pol I foci within the nucleus. Interestingly, no dramatic telomere shortening was observed when TbRAP1 expression was downregulated for two days (Yang et al., 2009). A recent study revealed why TbRAP1 is indispensable for parasite viability. In fact, TbRAP1 loss leads to increased read-through into the telomere downstream of the active BES resulting in higher levels of long, non-coding telomeric repeat-containing RNAs (TERRA) and telomeric RNA:DNA hybrids. In addition, more DSBs were detected at telomeres and subtelomeres of active and silent BESs, which increased the VSG switching frequency by initiating VSG gene conversion (Nanavaty et al., 2017).

A component of the inositol phosphate pathway, the Phosphatidylinositol 5-phosphatase (TbPIP5Pase), was lately discovered to associate with TbRAP1 and TbTRF (Cestari and Stuart, 2015). Depletion of TbPIP5-Pase disrupted BES silencing, whereby the effect on silent VSGs was strongest similar to the TbRAP1 derepression phenotype. Downregulation of a further component of the inositol phosphate pathway, the Phosphatidylinositol 5-kinase (TbPIP5K), which localizes to the plasma membrane, resulted in a comparable derepression phenotype (Cestari and Stuart, 2015). In both cases, BES derepression was associated with the formation of additional Pol I foci and altered distribution of TbRAP1 and TbTRF proteins within the nucleus. Hence, inositol phosphate signaling, which is known to be involved in chromatin remodeling and transcription regulation in other eukaryotes (Steger et al., 2003, Yildirim et al., 2013), seems to contribute to antigenic variation control via telomeric silencing.

In contrast to TbPIP5Pase, depletion of the TbRAP-associated factors, TbTRF and TbTIF2, did not influence TbRAP1-mediated VSG silencing. TbTRF and TbTIF2, which are essential for genome stability, were rather shown to suppress VSG switching by inhibiting DNA recombination. Knockdown of either proteins resulted in increased gene conversion-mediated VSG switching events. The underlying mechanisms seems to rely on independent and overlapping mechanisms (Jehi et al., 2016). While TbTIF2 knockdown leads to the accumulation of subtelomeric DSBs, which have the potential to trigger VSG switching, the increased switching frequency upon TbTRF depletion is independent from subtelomeric DSBs. This mechanistic overlap is apparently based on the fact that TbTIF2 stabilizes TbTRF protein level by suppressing its degradation by the 26S proteasome (Jehi et al., 2016). Although TbTRF, TbTIF2 and TbRAP1 are components of the same complex, only TbRAP1 is crucial for telomeric VSG silencing, suggesting that TbTIF2 and TbTRF act independently from TbRAP1. Interaction studies using the yeast two-hybrid system support this idea, as only a weak interaction between TbRAP1 and TbTRF (Yang et al., 2009), and a very strong interaction of TbTRF and TbTIF2 was observed (Jehi et al., 2014b). No direct interaction between TbRAP1 and TbTIF2 was found.

As the active VSG is expressed from a subtelomeric locus, it was long proposed that a telomere-specific factor establishes this differential expression state among all 15 BESs. To find such a factor, Glover and colleagues used a genetic screen for silencing defects at telomere-proximal regions of BESs and thereby identified two candidates, Tb927.6.4330 and VSG exclusion 1 (VEX1) (Glover et al., 2016). Both proteins associate with telomeres. Tb927.6.4330 partially co-localize with TbTRF. VEX1 is concentrated only in a single spot in close vicinity to the ESB, and is sequestered to the active BES in a transcription-dependent manner. While depletion of Tb927.6.4330 was accompanied by a moderate VSG derepression, VEX1 depletion resulted in a more pronounced VSG silencing defect. Given VEX1 sequestration at the active BES, the authors proposed a *trans* silencing effect mediated by VEX1 from the active BES based on homology-dependent interference between BESs sequences (Figure 11). They speculated that this form of silencing could involve RNA-based repression, as found in other eukaryotes (reviewed in Holoch and Moazed, 2015).

Overexpression of VEX1 also resulted in defects in BES silencing suggesting that VEX1 coordinates both BES silencing and activation. How exactly the activation and silencing of BES are regulated by VEX1 is still unclear. Recent work indicates that VEX1 interacts with the CAF-1 chaperone complex (Faria et al., 2017).

To sum up, the characterization of the telomere structure and telomere-associated proteins in trypanosomes has revealed the nuclear positioning of telomeres and the composition of the telomeric environment as crucial for VSG transcription regulation (Figure 11). But if and how the multiple identified components interfere with each other is unclear. The search for yet unidentified telomere-binding proteins might fill the gaps in our understanding of telomere contribution to antigenic variation in *T. brucei*.

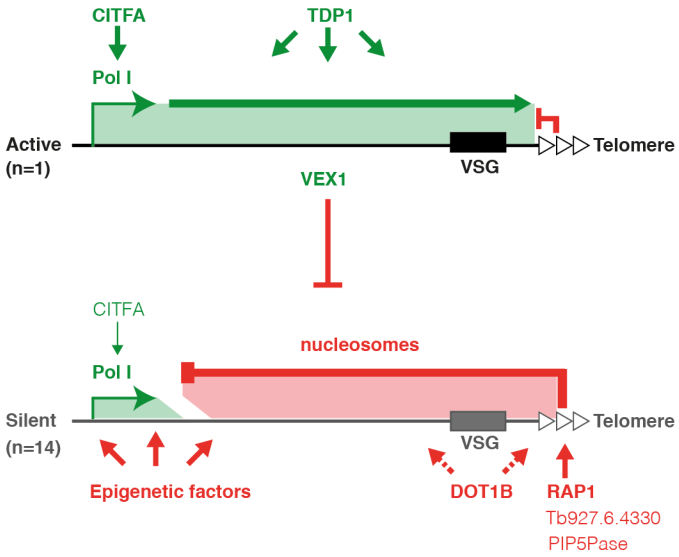

Figure 11. Model of VSG expression site regulation.
The characterization of numerous BES regulation factors leads to the model of two opposing and each other antagonizing forces present at the BES. The active BES is defined by high transcription initiation rates and greatly diminished telomere-mediated epigenetic silencing. Thereby the active state of the BES relies on the presence and enrichment of TbTDP1 and TbCITFA at the active BES and Pol I-driven promoter, respectively. In addition VEX1 is sequestered by the active BES and is thought to mediate a *trans* silencing effect to keep the remaining 14 BESs repressed. The inactive BESs are characterized by a nucleosome-rich structure and low level Pol I transcription initiation. Telomeric silencing spreads from the telomere towards the Pol I promoter. This silencing depends on TbDOT1B and TbRAP1. However, it is unknown how TbDOT1B associates with BESs (dashed line). Factors and products of the inositol phosphate pathway were shown to be involved in RAP1-mediated silencing, too. The telomere-associated protein Tb927.6.4330 also contributes to BES silencing. Epigenetic factors may act together to establish a repressive chromatin conformation at the promoter of inactive BESs. Image modified from (Gunzl et al., 2015)

1.2.5 Developmentally regulated VSG silencing mechanisms

Throughout the parasite's life cycle BES silencing remains important. All 15 BESs are repressed when the parasite enters the insect stage as the surface coat is developmentally regulated. In the tsetse vector stage PCF of the parasite procyclin replaces the VSG coat (Figure 12) (Roditi et al., 1989). Hence, during developmental differentiation from BSF to PCF the active BES is silenced in order to stop VSG transcription (Amiguet-Vercher et al., 2004) and the ESB appears to disintegrate (Navarro and Gull, 2001). During this process developmental BES silencing appears to rely on rapid BES promoter repositioning to the nuclear envelope (Landeira and Navarro, 2007), where it is silenced presumably by chromatin condensation (Navarro et al., 1999).

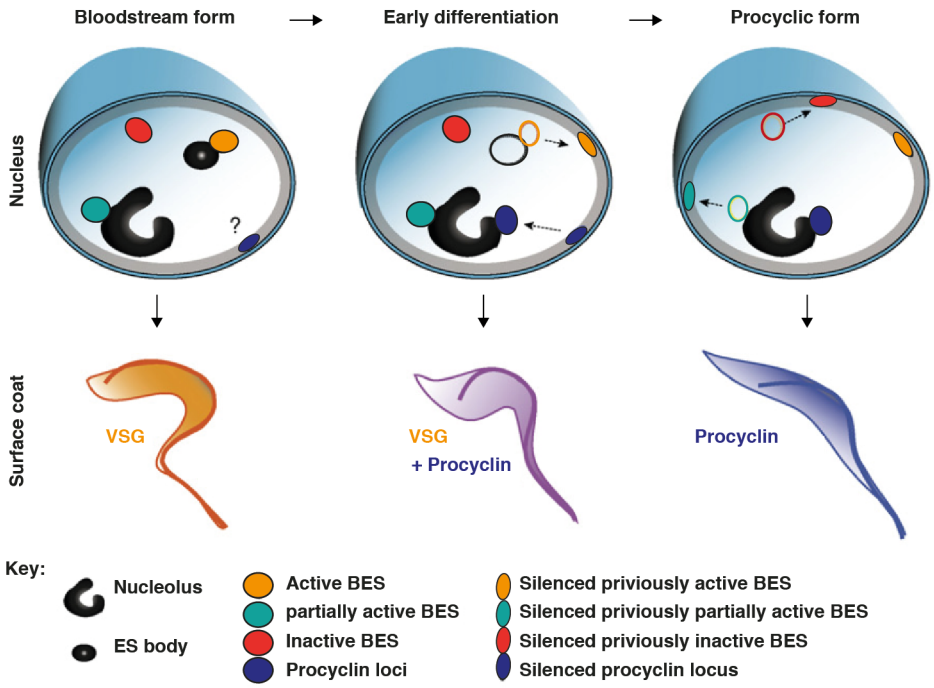

Figure 12. Developmental silencing of VSG genes and nucleus restructuring during differentiation.
In the bloodstream form, the active BES (orange sphere) selectively associates with the expression site body (ESB, black sphere), whereas the repressed BESs (red sphere) are localized somewhere else within the nucleoplasm. They are thought to associate with the nuclear lamina. The procyclin locus (purple sphere) is repressed in BSF cells and is most likely to be positioned near the nuclear envelope. Early during the developmental transition from the BSF to PCF stage both VSG and procyclin mRNAs are detectable leading to mixed surface coats. During this early event the active BES undergoes rapid repositioning to the nuclear periphery where it is silenced presumably by chromatin condensation and the ESB disintegrates. Furthermore, in order to initiate procyclin transcription the procyclin locus is repositioned to a transcriptionally active perinucleolar location. In established procyclics the previously partially active and inactive BESs display a more condensed chromatin structure compared to BSF parasites indicating that these BESs eventually reposition to the nuclear envelope. Image modified from (Navarro et al., 2007).

BES silencing mechanisms in the BSF and during the differentiation process to PCF seem to have distinct as well as overlapping properties (Horn and Cross, 1995, Glover and Horn, 2006). Most of the mentioned chromatin-associated silencing factors have been studied in BSF trypanosomes. Only few data are available concerning their potential role during developmental BES silencing or keeping BESs inactive in PCF parasites. Factors, which are essential for BES silencing in both life cycle stages, indicate overlapping silencing mechanisms in BSF and PCF parasites. This category of silencing factors include for instance the linker histone H1 (Povelones et al., 2012), the FACT component Spt16 (Denninger et al., 2010), the histone deacetylase HDAC3 (Wang et al., 2010), the nuclear lamina protein NUP-1 (DuBois et al., 2012) and the telomere-binding protein TbRAP1 (Yang et al., 2009). Interestingly, the TbRAP1-mediated silencing effect was shown to be stronger in the

PCF than in the BSF indicating that additional chromatin-related processes might contribute to this effect in PCF parasites (Pandya et al., 2013).

On the other hand, factors, which only influence BES silencing in either stages indicate stage-specific regulation. For example, while base J is enriched at BSF telomeres, it is absent from PCF telomeres indicating that different telomere environments might be responsible for BES silencing in either stage (Gommers-Ampt et al., 1991, van Leeuwen et al., 1996). Furthermore, ESB disappearance in the PCF stage coincides with VEX1 redistribution (Glover et al., 2016). If and how VEX1 acts as negative regulator of BES transcription in PCF cells is not known yet. A mechanism distinct from the VEX1-mediated silencing in BSF cells is necessary to silence the BESs in PCF parasites.

The developmental differentiation process is accompanied by chromatin restructuring (Schlimme et al., 1993, Burri et al., 1994, Rout and Field, 2001). A recent study by our laboratory provided evidence that the histone trimethylase DOT1B is essential for these structural changes as cells lacking DOT1B failed to differentiate to the PCF stage. DOT1B is required for VSG silencing propagation along the BES during the developmental transition (Dejung et al., 2016). In addition, the developmental silencing is dependent on NUP1-mediated BES repositioning, further emphasizing the importance of telomere positioning and thus, peripheral chromatin organization during differentiation (DuBois et al., 2012). To study the influence of the telomere silencing protein TbRAP1 during the differentiation process is challenging, as TbRAP1 is essential for cell viability. If and how telomere-binding proteins contribute to the developmental differentiation has not been studied, yet.

In addition, little is known about how BES silencing is initiated, timed and regulated on the DNA level during the differentiation process. It has been demonstrated that BES transcriptional activity and differentiation are mechanistically linked (Batram et al., 2014). Furthermore, it was shown that transcriptional BES attenuation can initiate the differentiation process whereby BES transcription stops before the chromatin condensates (Aresta-Branco et al., 2016). Thereby, TDP1 maintains the open chromatin architecture. Interestingly, bromodomain proteins were described to counteract the developmental transition from BSF to PCF parasites (Schulz et al., 2015). Bromodomain proteins bind acetylated lysines of histones and control gene expression by interacting with the transcriptional machinery (reviewed in Josling et al., 2012).

Life cycle differentiation requires a temporally fine-tuned control of transcription and chromatin organization. To ensure a precisely coordinated BES silencing each event has to be executed with a specific kinetic and it is likely that these regulation mechanisms involve still unidentified regulatory factors.

1.3 Aim of this study

Regulation of VSG genes in the context of monoallelic expression, antigenic variation and developmental silencing appears to be a complex and multi-factorial process. Although many factors influencing antigenic variation have been identified and described, a comprehensive model on how VSG expression is controlled is still missing. Since the VSG genes are expressed from subtelomeric loci, the telomere is an obvious structure to find answers to the open questions. Indeed, there are several reports proving telomeric contribution to VSG expression regulation. For instance, the telomere-binding proteins, TbTRF, TbRAP1 and TbTIF2, were shown to be involved in the regulation of antigenic variation (Yang et al., 2009, Jehi et al., 2014b, Jehi et al., 2016, Nanavaty et al., 2017). So far, no further components of the telomere protein complex in *T. brucei* have been described. However, it is unlikely that all members of the telomere protein complex have been found. To understand how the characterized telomere-binding proteins and other epigenetic regulators participate in VSG silencing, VSG activation and VSG switching, it is essential to identify the complete composition of the telomere protein complexes in *T. brucei*.

Up to now, no systematic screen has been conducted to determine the complete telomere protein complex in *T. brucei*. Thus, the aim of this thesis was to identify novel telomere-binding proteins by quantitative label-free mass spectrometry analyses of telomere DNA interactions and TbTRF interactions. As a proof of principle to validate these interactomics data, one of those candidates should be analyzed regarding its contribution to antigenic variation and developmental silencing of the VSG gene during developmental differentiation from the BSF to the PCF stage.

2 MATERIALS AND METHODS

All standard chemicals used in this study were obtained from Applichem, Invitrogen, Merck, Roth, Sigma, and Sigma-Aldrich, unless stated otherwise.

2.1 Bacterial culture and DNA plasmids

2.1.1 Bacterial strains

Table 1. *Escherichia coli* strains used in this study.

Strain	Genotype	Application
TOP10	F- mcrA Δ(mrr-hsdRMS-mcrBC) ϕ80lacZΔM15 ΔlacX74 nupG recA1 araD139 Δ(ara-leu)7697 galE15 galK16 rpsL(StrR) endA1 λ-	Plasmid propagation, molecular cloning
DB3.1	F- gyrA62 endA1 Δ(sr1-recA) mcrB mrr hsdS20(rB-, mB-) supE44 ara-14 galK2 lacY1 proA2 rpsL20(SmR) xyl-5-λ-leu mtl1	CcdB plasmid propagation
BL21 (DE3) pRare T1	F- ompT hsdSB(rB- mB-) gal dcm λ(DE3) tonA	Recombinant protein expression

2.1.2 Growth of *E. coli*

Bacterial cells were either cultivated as liquid culture in Luria Bertani (LB) medium (0.5% (w/v) yeast extract, 1% (w/v) bacto tryptone, 1% NaCl (w/v), pH 7.5) or on LB agar plates (LB medium containing 1.5% (w/v) agar). The LB medium was autoclaved at 121°C for 20 min and supplemented with appropriate antibiotics (100 µg/ml ampicillin and/or 34 µg/ml chloramphenicol or 25 µg/ml gentamicin).

2.1.3 Transformation of *E. coli*

100 µl of chemically competent *E. coli* TOP10 were thawed on ice, mixed with 10 ng of plasmid DNA or 10 µl of a ligation reaction and incubated for 30 min on ice. Bacterial cells were heat shocked at 42°C for 45 sec and cooled on ice for 2 min. 500 µl of SOC medium (0.5% (w/v) yeast extract, 2% (w/v) tryptone, 10 mM NaCl, 2.5 mM KCl, 10 mM $MgCl_2$, 10 mM $MgSO_4$, 20 mM glucose) was added to cells prior incubation at 37°C for 1 h at 225 rpm on a shaker. Afterwards, cells were plated on selective LB agar plates and incubated overnight at 37°C.

2.1.4 DNA extraction from *E. coli*

Plasmid DNA was isolated from 4 ml or 100 ml *E. coli* TOP10 overnight cultures using NucleoSpin® plasmid miniprep or Nucleobond® PC100 midiprep kit (Macherey-Nagel) according to the manufacturer's instructions. For miniprep, DNA was eluted in 30 µl EB buffer (Macherey-Nagel) and for midiprep in 100 µl dH_2O.

2.1.5 Plasmids used and generated in this study

Table 2. Plasmids used and generated in this study.

Name	Description	Resistance in *E. coli*	Resistance in *T. brucei*	Reference
pDONR207	Intermediate vector used in the Gateway Cloning strategy to generate RNAi constructs. It contains a ccdB-cassette flanked by attachment sequences attB1 and attB2, which are necessary for recombination of the RNAi fragment into the vector.	Gent	---	Invitrogen
pTrypRNAiGate	Modified pLew100 vector for RNAi in *T. brucei*. It contains two copies of the ccdB gene, which are flanked by attachment sequences attR1 and attR2 for recombination of the RNAi fragment from the intermediate vector pDONR207 into the final RNAi vector.	Amp	Phleo	(Kalidas et al., 2011)
pGL2084	Combination of Gateway Cloning and single locus targeting strategy. This vector was designed for 2T1 cells, which contain the puromycin and phleomycin resistance gene (Alsford and Horn, 2008). After correct integration of pGL2084 into the marked rDNA locus cells are phleomycin and hygromycin resistant and puromycin sensitive.	Amp	Hygro	(Jones et al., 2014)
pLew100v5b1d	Used for ectopic overexpression from rDNA locus. Contains a T7 promoter.	Amp	Phleo	G. Cross
pyrFEKO-HYG	Used for gene knockouts in *T. brucei*.	Amp	Hygro	(Kim et al., 2013a)
pyrFEKO-PUR	Used for gene knockouts in *T. brucei*.	Amp	Puro	(Kim et al., 2013a)
pyrFEKO-BLE	Used for gene knockouts in *T. brucei*.	Amp	Phleo	(Kim et al., 2013a)
pLew100Cre-EP1	Tetracycline-inducible expression of Cre recombinase in order to remove loxP flanked sites in the genome. Is transiently transfected.	Amp	Phleo	(Kim et al., 2013a)
pLew82	Used to amplify phleomycin resistance gene.	Amp	Phleo	G. Cross
pMOTag 2T	Plasmid for PCR-based Ty1 C-terminal *in situ* tagging of *T. brucei* genes. All pMOTag vectors are based on the pBluescriptIIKS+ plasmid (Stratagene).	Amp	Puro	(Oberholzer et al., 2006)
pTH5	Was cut with EcoRI to release a 162 bp fragment containing telomeric repeats. This fragment was either used for EMSA or as telomere probe in telomeric southern blot.	Amp	---	(de Lange et al., 1990)
pCJ25A	Used for integration of Firefly luciferase reporter gene in ΨVSG pseudogene in 221 BES, expression is controlled by BES promoter. Linearization with: BstApI	Amp	Blas	(Janzen et al., 2006)
pFG14n	pFG14 (received from L. Figueiredo) encodes a Renilla luciferase reporter gene and contains a hygromycin and neomycin resistance cassette. The neomycin resistance cassette was removed using KT9 and KT10 primers both containing NruI restriction sites. The PCR product was cut with NruI and ligated resulting in pFG14n. Linearization with: KpnI, SacI	Amp	Hygro	K. Thein
pTrypRNAiGate TelBP1	441 bp TelBP1 fragment (187-627) was PCR amplified using F29/F30 primer pair and first recombined into pDONR207 vector and then into the pTrypRNAi Gate.	Amp	Phleo	H. Reis

Name	Description	Resistance in *E. coli*	Resistance in *T. brucei*	Reference
pyrFEKO-HYG-TelBP1	SB1/2 primer pair was used to amplify 300 bp of TelBP1 5'UTR. SB1 and 2 contained PvuII and HindIII restriction sites, respectively. SB3/4 primer pair was used to amplify 300 bp of TelBP1 3'UTR. SB3 was designed with a BamHI restriction site and SB4 with a SdaI restriction site. pyrFEKO plasmid was first cut open with BamHI/SdaI for cloning 3'UTR into the vector. Then, the resulting plasmid was cut open with HindIII/PvuII for cloning 5'UTR into the vector. Linearization with: PvuII/SdaI	Amp	Hygro	S. Bury
pyrFEKO-PUR-TelBP1	Cloned as pyrFEKO-HYG-TelBP1	Amp	Puro	S. Bury
pyrFEKO-BLE-TelBP1	Cloned as pyrFEKO-HYG-TelBP1	Amp	Phleo	H. Reis
pLew100v5b1d_ TelBP1	TelBP1 ORF was amplified with HW74 and HW75 containing HindIII and BamHI restriction sites, respectively and cloned into BamHI/HindIII cut open plasmid. Linearization with: NotI	Amp	Phleo	H. Reis
pLew100v5b1d_ TelBP1-Ty1	TelBP1 ORF was amplified using the primers HW74/SB20 containing HindIII and BamHI sites, respectively and cloned into BamHI/HindIII cut open plasmid. The rv primer introduced the Ty1-tag at the C-terminus. Linearization with: NotI	Amp	Phleo	S. Bury
pLew100v5b1d_ Ty1-TelBP1	HR25/26 primers containing HindIII and BamHI sites, respectively were used to amplify the TelBP1 ORF. The fw primer contained the Ty1 sequence. Linearization with: NotI	Amp	Phleo	H. Reis
pGL2084_TbTRF	TbTRF fragment (530-1143) was amplified using HW91/92 primers and recombined into pGL2084. Linearization with: AscI	Amp	Hygro	H. Reis
pGL2084_Nt-TelBP1	F29/30 TelBP1 fragment (187-627)	Amp	Hygro	H. Reis
pGL2084_Ct-TelBP1	SB9/12 TelBP1 fragment (634-1203)	Amp	Hygro	H. Reis
pLew100v5b1d_ TelBP1_M1L	pLew100v5b1d_TelBP1 was PCR-amplified using the primers HR5/6 to introduce a point mutation at the 1st base of the ORF: 1A>C Linearization with: NotI	Amp	Phleo	H. Reis
pLew100v5b1d_ TelBP1_M212L	pLew100v5b1d_TelBP1 was PCR-amplified using the primers HW93/94 to introduce a point mutation at base 634 of the ORF: 634A>C Linearization with: NotI	Amp	Phleo	H. Reis
pLew100v5b1d_ TelBP1_M1L_M212L	pLew100v5b1d_TelBP1_M212L was PCR-amplified using the primers HR5/6 to introduce a point mutation at base 1 of the ORF: 1A>C. Sequencing revealed an additional point mutation at base 589 resulting in M197L. Linearization with: NotI	Amp	Phleo	H. Reis

Abbreviations: Gent (Gentamicin), Amp (Ampicillin), Phleo (Phleomycin), Hygro (Hygromycin), Puro (Puromycin), Blas (Blasticidin), M (methionine), L (leucine).

2.2 Trypanosome culture and analyses

2.2.1 *Trypanosoma brucei brucei* strains

Table 3. Overview of parental *T. brucei* cell lines used in this study.

Name	Description/ Genotype	Constructs	Selection	Reference
MITat1.2 SM	BSF Lister 427, MITat1.2, clone 221a, TETR T7RNAP NEO	pHD328, pLew114hyg5'	G418	(Wirtz et al., 1999)
2T1	BSF Lister 427, MITat1.2, clone 221a, RRNA::hygΔstart PAC/ TUB::TetR BLE	pHD1313, ph3Ep	Phleo/Puro	(Alsford et al., 2005)
MITat1.6	BSF Lister 427, MITat1.6, clone 121	---	---	G. Cross, 1975
29-13	PCF Lister 427, TETR T7RNAP NEO HYG	pLew29, pLew13	G418/Hygro	(Wirtz et al., 1999)
427	PCF Lister 427 wild-type	---	---	S. Kramer

Abbreviations: MITat1.2 SM (Molteno Institute Trypanozoon Antigen Type 1.2 single marker), 2T1 (VSG221 expressing, Tagged, clone1), BSF (bloodstream form), PCF (procyclic form), TETR (tetracycline repressor), T7RNAP (T7 RNA polymerase), NEO (aminoglycoside phosphotransferase gene), BLE (phleomycin resistance gene), PAC (puromycin N-acetyltransferase gene), HYG (hygromycin phosphotransferase gene), RRNA (ribosomal RNA locus), TUB (tubulin), G418 (Neomycin), Phleo (Phleomycin), Hygro (Hygromycin), Puro (Puromycin).

Table 4. Overview of transgenic *T. brucei* cell lines generated in this study.

Name	Genotype	Constructs	Selection	Reference
SM TelBP1 RNAi	TETR T7RNAP NEO/ RDNA::TelBP1-RNAi^{Ti} BLE	pHD328, pLew114hyg5', pTrypRNAiGate TelBP1	G418/Phleo	H. Reis
2T1 TelBP1 Nt-RNAi	TUB::TetR BLE/ RRNA::TelBP1-Nt-RNAi^{Ti} HYG	pHD1313, ph3Ep, pGL2084_Nt-TelBP1	Phleo/Hygro	H. Reis
2T1 TelBP1 Ct-RNAi	TUB::TetR BLE/ RRNA::TelBP1-Ct-RNAi^{Ti} HYG	pHD1313, ph3Ep, pGL2084_Ct-TelBP1	Phleo/Hygro	H. Reis
SM TelBP1 OE	TETR T7RNAP NEO/ RDNA::TelBP1^{Ti} BLE	pHD328, pLew114hyg5', pLew100v5b1d_ TelBP1	G418/Phleo	H. Reis
SM ΔTelBP1	TETR T7RNAP NEO/ ΔTelBP1::HYG loxed/ ΔTelBP1::PAC loxed	pHD328, pLew114hyg5', pyrFEKO-HYG-TelBP1, pyrFEKO-PUR-TelBP1	G418	H. Reis
29-13 TelBP1 Ct-RNAi	TETR T7RNAP NEO HYG/ RDNA::TelBP1-RNAi^{Ti} BLE	pLew29, pLew13, pTrypRNAiGate TelBP1	G418/Hygro/ Phleo	H. Reis
29-13 TelBP1 Nt-RNAi	TETR T7RNAP NEO HYG/ RDNA::TelBP1-RNAi^{Ti} BLE	pLew29, pLew13, pTrypRNAiGate TelBP1	G418/Hygro/ Phleo	H. Reis
29-13 TelBP1 OE	TETR T7RNAP NEO HYG/ RDNA::TelBP1^{Ti} BLE	pLew29, pLew13, pLew100v5b1d_ TelBP1	G418/Hygro/ Phleo	H. Reis
427 PCF ΔTelBP1	ΔTelBP1::HYG/ ΔTelBP1::PAC	pyrFEKO-HYG TelBP1, pyrFEKO-PUR-TelBP1	Hygro/Puro	H. Reis
2T1 TbTRF RNAi	TUB::TetR BLE/ RRNA::TbTRF-RNAi^{Ti} HYG	pHD1313, ph3Ep, pGL2084_TbTRF	Phleo/Hygro	H. Reis
SM TbTRF -/Ty1	TETR T7RNAP NEO/ TbTRF::Ty1 PAC/ ΔTbTRF::BLE	pHD328, pLew114hyg5', pLew82 PCR, pMOTag 2T PCR	G418/Puro/ Phleo	M. Schwebs

Name	Genotype	Constructs	Selection	Reference
427 TbTRF -/ Ty1	TbTRF::Ty1 PAC/ ΔTbTRF::BLE	pLew82 PCR, pMOTag 2T PCR	Puro/Phleo	M. Schwebs
29-13 TelBP1 Ct-Ty1	TETR T7RNAP NEO HYG/ RDNA::TelBP1-Ty1^{Ti} BLE	pLew29, pLew13, pLew100v5b1d_ TelBP1-Ty1	G418/Hygro/ Phleo	H. Reis
29-13 TelBP1 Nt-Ty1	TETR T7RNAP NEO HYG/ RDNA::Ty1-TelBP1^{Ti} BLE	pLew29, pLew13, pLew100v5b1d_ Ty1-TelBP1	G418/Hygro/ Phleo	H. Reis
29-13 TelBP1 M1L	TETR T7RNAP NEO HYG/ RDNA::TelBP1_M1L^{Ti} BLE	pLew29, pLew13, pLew100v5b1d_ TelBP1_M1L	G418/Hygro/ Phleo	H. Reis
29-13 TeLBP1 M212L	TETR T7RNAP NEO HYG/ RDNA::TelBP1_M212L^{Ti} BLE	pLew29, pLew13, pLew100v5b1d_ TelBP1_M212L	G418/Hygro/ Phleo	H. Reis
29-13 TelBP1 M1L/M197L/M212L	TETR T7RNAP NEO HYG/ RDNA::TelBP1_M1L-M197L-M212L^{Ti} BLE	pLew29, pLew13, pLew100v5b1d_ TelBP1_M1L/M197L/M212L	G418/Hygro/ Phleo	H. Reis
SM-Rluc(pro)-Fluc(tel)	TETR T7RNAP NEO/ BES1pro::RLUC HYG/ Ψ221::FLUC BSD	pHD328, pLew114hyg5', pFG14n, pCJ25A	G418/Hygro/ Blas	H. Reis
SM ΔTelBP1-Rluc(pro)-Fluc(tel)	TETR T7RNAP NEO/ ΔTelBP1::HYG loxed/ ΔTelBP1::PAC loxed/ BES1pro::RLUC HYG/ Ψ221::FLUC BSD	pHD328, pLew114hyg5', pyrFEKO-HYG-TelBP1, pyrFEKO-PUR-TelBP1pFG14n, pCJ25A	G418/Hygro/ Blas	H. Reis
SM ΔTelBP1-Rluc(pro)-Fluc(tel) rescue	TETR T7RNAP NEO/ ΔTelBP1::HYG loxed/ ΔTelBP1::PAC loxed BES1pro::RLUC HYG/ Ψ221::FLUC BSD/ RDNA::TelBP1^{Ti} BLE	pHD328, pLew114hyg5', pyrFEKO-HYG-TelBP1, pyrFEKO-PUR-TelBP1pFG14n, pCJ25A, pLew100v5b1d_ TelBP1	G418/Hygro/ Blas/Phleo	H. Reis

Abbreviations: SM (single marker), TETR (tetracycline repressor), T7RNAP (T7 RNA polymerase), NEO (aminoglycoside phosphotransferase gene), BLE (phleomycin resistance gene), PAC (puromycin N-acetyltransferase gene), HYG (hygromycin phosphotransferase gene), BSD (Blasticidin resistance gene), RRNA (ribosomal RNA locus), G418 (Neomycin), Phleo (Phleomycin), Hygro (Hygromycin), Blas (Blasticidin), Puro (Puromycin), RDNA (ribosomal DNA locus), TUB (tubulin), Ti (Tetracycline inducible), Δ (Deletion), BES1pro (promoter region of Bloodstream form expression site 1), Ψ221 (VSG pseudogene of BES1), RLUC (Renilla luciferase gene), FLUC (Firefly luciferase gene), pro (promoter), tel (telomere), TK (Thymidine kinase gene)

2.2.2 Trypanosome growth

Bloodstream form (BSF) trypanosomes were cultured in HMI-9 medium (for 10L: 176.6 g Iscove's modified Dulbecco's Medium (IMDM), 30.24 g $NaHCO_3$, 1.36 g hypoxanthine, 282 mg bathocuproine sulfonate, 2 mM β-mercaptoethanol, 390 mg thymidine, 100 ml penicillin/streptomycin solution (Invitrogen), 1.82 g L-cysteine, 1 L FCS (Sigma)) (Hirumi and Hirumi, 1989) supplemented with appropriate drug selection (Table 5) at 37°C and 5% CO_2. BSF cell densities were kept under $1x10^6$ cells/ml to ensure cell growth in logarithmic growth phase. Procyclic form (PCF) cells were maintained in SDM-79 medium (SDM-79 basic medium (Brun and Schönenberger, 1979), modified by M. Boshart (SDM79 CGGGPPTA) for 10 L: 20 g $NaHCO_3$,18.642 g dextrose, 5.134 g L-glutamine, 6.15 g L-proline, 1 g sodium pyruvate, 4.068 g L-threonine, 105 mg sodium acetate anhydr., 224.2 mg L-glutamic acid, pH 7.3; 900 ml of SDM79 medium is complemented with 7.5 mg/ml hemin, 10 mM glycerol, 10 ml penicillin/streptomycin solution (Invitrogen), 100 ml heat-inactivated FCS (Sigma)) with appropriate drug selection at 27°C and 5% CO_2. PCF cell densities were kept between $5x10^5$ and $1x10^7$ cells/ml.

BSF and PCF cells were counted using the particle Coulter Counter Z2 (Beckman Coulter).

Table 5. Drug selection used for trypanosome culture.

Drug	Marker	Stock (mg/ml)	Final conc. (µg/ml) BSF	Final conc. (µg/ml) PCF	Company
G418	NEO	10	2	15	Applichem
Hygromycin	HYG	10	3	25	Applichem
Phleomycin	BLE	10	2.5	2.5	Invivogen
Puromycin	PAC	1	0.1	1	Applichem
Blasticidin	BSD	10	5	5	Invivogen
Tetracycline	---	10	1	1	Applichem
Ganciclovir	HSV-TK	10	50	---	Sigma

2.2.3 Stabilate preparation and retrieval

$2x10^6$ BSF or $2x10^7$ PCF cells were harvested (1500 g, 10 min, 4°C), the pellet resuspended in 500 µl freezing medium (HMI-9/ SDM-79 supplemented with 10% glycerol) and transferred into cryotubes. Stabilates were stored at -80°C.

To thaw out stabilates, cryotubes containing the cells were briefly placed into a 37°C water bath. Then, the cells were transferred into pre-warmed 10 ml HMI-9 or SDM-79 medium and centrifuged at 1500 g, 10 min, RT. Cell pellets were taken into a culture flask, containing medium with appropriate selection.

2.2.4 Stable transformation of trypanosomes

$2.5x10^7$ BSF cells were harvested (1500 g, 10 min, RT), washed once with 10 ml pre-warmed TDB (5 mM KCl, 80 mM NaCl, 1 mM $MgSO_4$, 20 mM Na_2PO_4, 2 mM NaH_2PO_4, 20 mM glucose, pH 7.4) (1500 g, 10 min, RT) and the pellet resuspended in 400 µl pre-warmed transfection buffer (90 mM Na_2PO_4, 5 mM KCl, 0.15 mM $CaCl_2$, 50 mM HEPES, pH 7.3). 10 µg linearized plasmid DNA or 3 µg PCR product were added to cells and mixed carefully. DNA-cell mixture was then transferred into a BTX cuvette and electroporated using the AMAXA nucleofector (Lonza) choosing the program 'X001 free choice'. The transfected cells were then put in pre-warmed medium containing the parental selection. 1:10 dilution was prepared and plated on two 24-well plates (1 ml/well). 6-8 h after transfection, drugs were added to select for positively transfected cells as cells have to divide at least once to recover from the transfection procedure.

PCF cells were transfected as described above with minor modifications. In short, after harvesting PCF cells, cells were washed in 10 ml PBS (10 mM Na_2HPO_4, 1.8 mM KH_2PO_4 pH 7.4, 140 mM NaCl, 2.7 mM KCl). After electroporation, cells were transferred into 20% conditioned SDM-79 medium and diluted 1:10, 1:100 and 1:1000. Each dilution was plated on one 24-well plate (1 ml/well). The selection was added 12 h post transfection. Conditioned SDM-79 medium was prepared by centrifugation (1500 g, 10 min, 4°C) of PCF culture and sterile filtration of the supernatant.

2.2.5 Transient transformation of BSF trypanosomes

In this study, the plasmid pLew100Cre-EP1 was transiently transfected in SM ΔTelBP1 cells to remove the resistance marker cassettes. For this purpose HMI-9 without thymidine was used.

$6x10^7$ SM ΔTelBP1 cells were harvested (1500 g, 10 min, RT) and the pellet resuspended in 800 µl pre-warmed transfection buffer. The cell suspension was split into two BTX cuvettes. 20 µg of pLew100Cre-EP1 was added to each 400 µl cell suspension and mixed well. Electroporation was carried out as described in 2.2.4. For each transfection four 50 ml falcons were prepared for serial dilutions (1:10, 1:100, 1:1000), one falcon containing 30 ml HMI-9 and three falcons with 27 ml HMI-9. For the first transfection, the prepared falcons were supplemented with 1 µg/ml tetracycline to induce Cre recombinase expression. For the second transfection, which served as control, no tetracycline was added to HMI-9. The transfected cells were diluted and each dilution plated on 24-well plates (1 ml/well). 8-9 h post transfection GCV (50 µg/ml final conc.) was added to the cells to select for the loss of the HSV-TK. No cells of the control plates should survive the GCV treatment.

2.2.6 Differentiation of monomorphic bloodstream form to procyclic form trypanosomes

To differentiate BSF cells to PCF cells, BSF trypanosomes were grown to a cell density of $1.5x10^6$ cells/ml in HMI-9. $2.5x10^7$ cells were harvested (1500 g, 10 min, RT) and resuspended in 5 ml DTM (For 1 l: 6.8 g NaCl, 0.4 g KCl, 0.2 g $CaCl_2$*2H2O, 0.14 g NaH_2PO_4*H2O, 0.2 g $MgSO_4$*$7H_2O$, 7.94 g HEPES, 2.2 g $NaHCO_3$, 10 mg Phenol red, 14 mg hypoxanthine, 1 mg biotin, 640 mg proline, 0.235 g glutamate, 1.63 g L-glutamine, 7.5 mg hemin, 20 ml MEM aminoacids solution 043-01130 (50x), 10 ml MEM non-essential amino acids solution 043-01140 (100x), 10 ml MEM vitamin solution 043-0140 (100x), 14 µl β-mercaptoethanol, 730 µl glycerol, 114 mg sodium pyruvate, 182 mg cysteine, 28.2 mg bathocuproine, 15% (v/v) heat inactivated FCS) containing 6 mM cis-aconitate (Sigma) (Overath et al., 1986). Trypanosomes were then cultured at 27°C with 5% CO_2 and diluted using SDM-79.

2.2.7 Isolation of genomic DNA of *T. brucei*

To purify genomic DNA of *T. brucei* for PCR amplifications the High Pure PCR Template Preparation kit (Roche) was used. Briefly, $5x10^6$ cells were harvested (1500 g, 10 min, RT) and the pellet resuspended in 200 µl of PBS buffer. 200 µl of Binding Buffer and 40 µl Proteinase K were added, mixed and incubated at 70°C for 10 min. Then, 100 µl of isopropanol was added, mixed and the sample loaded onto a column. By centrifugation (8000 g, 1 min, RT) genomic DNA was bound to the column and washed with 500 µl of Inhibitor Removal Buffer (8000 g, 1 min, RT). A second wash with 500 µl of Wash Buffer (8000 g, 1 min, RT) followed. Finally, the DNA was dried by full-speed centrifugation (21,000 g, 10 sec, RT) and eluted with 200 µl pre-warmed Elution Buffer (8000 g, 1 min, RT).

To purify genomic DNA of *T. brucei* for telomeric southern blot, a phenol/chloroform extraction method was used. Briefly, $5x10^8$ cells were harvested (1500 g, 10 min, 4°C) and the pellet snap frozen in liquid nitrogen and stored until use at -80°C. Cell pellet was quickly thawed out at RT and dissolved in 1 ml TNE (10 mM Tris pH 7.4, 100 mM NaCl, 10 mM EDTA), transferred into a 15 ml falcon tube containing 1 ml TNES (10 mM Tris pH 7.4, 100 mM NaCl, 10 mM EDTA, 1% (w/v) SDS) supplemented with 100 µg/ml Proteinase K (Thermo Fisher Scientific) and incubated overnight at 37°C. Then, 2 ml of phenol:chloroform:isoamyl alcohol (Roth) was added, the tube inverted until the mixture appeared milky and centrifuged (13,000 g, 5 min, RT). The water-phase was then transferred into a 15 ml falcon tube containing 220 µl 3M NaAc. 2 ml of isopropanol was added, the tube gently inverted several times and DNA precipitated (20,000 g, 5 min, RT). The DNA pellet was washed twice with ice-cold 70% EtOH (20,000 g, 5 min, 4°C) and the pellet air-dried for 10 min. 300 µl of TNE supplemented with 100 µg/ml RNaseA (Thermo Fisher Scientific) was added to the dry pellet and incubated at 37°C for 2.5 h. After 30 min, DNA was gently resuspended. An incubation with

additional 300 µl of TNES supplemented with 100 µg/ml Proteinase K followed at 37°C for 1 h. 600 µl of phenol:chloroform:isoamyl alcohol was added, the mixture inverted, and centrifuged (21,000 g, 5 min, RT). The upper phase was then transferred to a 1.5 ml tube containing 66 µl 3 M NaAc. 600 µl of isopropanol was added and the tube was inverted. DNA was precipitated (20,000 g, 5 min, RT) and washed twice with 500 µl of 70% EtOH. The pellet was air-dried for 10 min, dissolved in 100 µl TE (10 mM Tris pH 7.4, 10 mM EDTA) and incubated at 37°C for 30 min. DNA samples were stored at -20°C.

2.2.8 Isolation of RNA from *T. brucei* and cDNA synthesis

RNA from *T. brucei* was purified using the RNAeasy Mini kit (Quiagen). Briefly, $1x10^8$ BSF or PCF cells were harvested (1500 g, 10 min, 4°C) and the cell pellet resuspended in 2 ml of FCS-free HMI-9 or SDM-79, respectively. Resuspended cells were transferred into RNase-free tubes and centrifuged (1500 g, 10 min, 4°C). The supernatant was removed, pellets were snap frozen in liquid nitrogen and stored at -80°C until use. Cell pellets were thawed out very shortly at 37°C in a heating block, resuspended in 600 µl of buffer RLT supplemented with β-mercaptoethanol (0.01% (v/v) final conc.) while it was melting and pipetted up and down 20 times. Following purification steps were carried out according to the manufacturer's instructions.
For cDNA synthesis, the RevertAid First Strand cDNA Synthesis kit (Thermo Fisher Scientific) was used according to the manufacturer's instructions.

2.2.9 Immunofluorescence analysis

$1x10^7$ BSF trypanosomes were harvested (1500 g, 10 min, RT) and the cell pellet was dissolved in 1 ml HMI-9. To fix the cells formaldehyde was added to a final concentration of 2% and incubated for 5 min at RT. Cells were then washed three times with 1 ml PBS (10 mM Na_2HPO_4, 1.8 mM KH_2PO_4 pH 7.4, 140 mM NaCl, 2.7 mM KCl) (1000 g, 5 min, 4°C). After the last wash step, the cells were resuspended in 500 µl PBS. 100 µl of cell suspension was dropped on poly-L-lysine coated slides (Sigma). The cells were settled down for 30 min. After that, cells were permeabilized with 0.2% Igepal CA-630 in PBS for 5 min at RT. Two washes with PBS for 5 min at RT followed. To block unspecific binding sites, 1% BSA in PBS was dropped on cells and incubated in a humid chamber at 37°C for 1 h. BSA/PBS solution was removed and the primary antibody diluted in 0.1% BSA in PBS was applied in a humid chamber at RT for 1 h. Prior adding the secondary antibody the slides were washed three times with PBS. The secondary antibody and Hoechst 33258 were diluted in 0.1% BSA in PBS, dropped on the cells and incubated for 30 min at RT in the dark. Then, slides were washed three times with PBS and the cells embedded in 5 µl Vectashield (Vecta Laboratories Inc.). A coverslip was placed on top and was sealed with nail polish. Images were captured by using an IMIC microscope (TILL Photonics, Gräfelfing, Germany) and deconvolved using the Huygens Essential software 4.1 (Scientific Volume Imaging).

Table 6. Overview of used antibodies and nuclear counterstain for immunofluorescence.

Name	Isotype	Clonality	Dilution for IF	Reference
Anti-TbTRF 6F5	Rat	Monoclonal	1:2	E. Kremmer
Anti-TelBP1 2E6	Mouse	Monoclonal	1:2	E. Kremmer
Alexa Fluor® 488 anti-rat	Goat	Polyclonal	1:2,000	Thermo Fisher Scientific
Alexa Fluor® 594 anti-mouse	Goat	Polyclonal	1:2,000	Thermo Fisher Scientific
Hoechst 33258	---	---	1:1,000	Serva Feinbiochemica

2.2.10 Dual-Luciferase assay

The Dual-Luciferase Reporter Assay kit (Promega) was used in this study to measure the luciferase activity of dual-luciferase reporter cells. Briefly, per assay $1x10^6$ cells were harvested (1500 g, 10 min, 4°C) and washed once with 1 ml ice-cold PBS (10 mM Na_2HPO_4, 1.8 mM KH_2PO_4 pH 7.4, 140 mM NaCl, 2.7 mM KCl) (1500 g, 10 min, 4°C). The cell pellet was dissolved in 100 µl of 1x Passive Lysis Buffer and 10 µl of cell lysate was added to 45 µl of LARII (Luciferase Assay Substrate dissolved in Luciferase Assay Buffer II) in a 96-well plate. Subsequently, the luminescence of the firefly luciferase was measured using the Tecan Infinite M200. The integration time was set to 1000 ms. By adding 45 µl of 1x Stop&Glo substrate the activity of the firefly luciferase was stopped and the luminescence resulting from the activity of the renilla luciferase was measured using the same settings.

2.3 DNA methods

2.3.1 Polymerase Chain Reaction (PCR)

For PCR amplification a 50 µl reaction was set up containing either 10 ng of plasmid DNA or 100 ng of genomic DNA, specific forward (fw) and reverse (rv) primer (0.5 µM each) (synthesized by Sigma-Aldrich), 1x HF buffer or 1x GC buffer, 200 µM dNTP Mix (Thermo Fisher Scientific), 1 U Phusion Polymerase (Thermo Fisher Scientific) and dH_2O. The cycling parameters were adjusted to the melting temperature of the used primers and to the length of the amplified DNA fragment: 98°C/10 min - [98°C/30 sec - x°C/20 sec - 72°C/x sec] 30 cycles - 72°C/10 min.

To perform integration PCR directly on BSF or PCF cells, the Phusion Human Specimen Direct PCR Kit (Thermo Fisher Scientific) was used. Briefly, $1x10^6$ cells were harvested (1500 g, 10 min, 4°C) and the cell pellet resuspended in 20 µl dilution buffer supplemented with 0.5 µl of DNA release additive. After mixing well, the cell suspension was incubated for 5 min at RT and then, for 2 min at 98°C. The released DNA was separated from cell debris by centrifugation (2000 g, 5 min, 4°C), and 0.5 µl of the supernatant was taken as a template in a 20 µl PCR reaction. The PCR reaction was set up according to the manufacturer's instructions. Briefly, the 20 µl reaction was prepared as followed: 1x Phusion Human Specimen PCR buffer, fw and rv primer (0.5 µM each), 0.4 µl Phusion Human Specimen DNA Polymerase, 0.5 µl template and to 20 µl dH_2O. The cycling parameters were as followed: 98°C/10 min - [98°C/1 sec - x°C/5 sec - 72°C/x sec] 30 cycles - 72°C/1 min.

Table 7. Oligonucleotides used for PCR, EMSA and probe labeling for Southern blot.

Name	Sequence (5'-3')	Description
KT9	CGAATTCCCTCGCGAAAGTGGTGGTGGCGTAAGTATTGCCTAATGTTG	EcoRI-NruI pFG14 (without Neo) fw
KT10	CGAATTCCCTCGCGACATAAGCACTAGCCGTGTCAACTCACAGCGAC	EcoRI-NruI pFG14 (without Neo) rv
SB1	CTGTGCTTTGTGGCACATTTCTCACC	TelBP1 5'UTR fw, PvuII restriction site
SB2	CCCAAGCTTCCCCGTAAGAGAGGGTCA CACTAGC	TelBP1 5'UTR rv, HindIII restriction site
SB3	CGCGGATCCCTAACATGTTTGCTGCGC GCCCAC	TelBP1 3'UTR fw, BamHI restriction site
SB4	GCGCCCTGCAGGCAGCGTTGCCCAGCG GTATCACTAC	TelBP1 3'UTR rv, SdaI restriction site
SB9	GGGGACAAGTTTGTACAAAAAAGCAGGCTATGGTGAAGTGTTTGGATCA GG	attB1 TelBP1 fw (634-1203)
SB12	GGGGACCACTTTGTACAAGAAAGCTGGGTTCAAGACAGGGGTATGTCCT CGC	attB2 TelBP1 rv (634-1203)
SB20	CGAATTCCAGGATCCCTCAGTCAAGTGGGTCCTGGTTAGTATGGACCTCA GACAGGGGTATGTCCTCGCAAG	TelBP1-Ty1 rv, EcoRI-BamHI
F29	GGGGACAAGTTTGTACAAAAAAGCAGGCTGCTAACTTACTGGTGGACGA	attB1 TelBP1 fw (187-627)
F30	GGGGACCACTTTGTACAAGAAAGCTGGGTTGTATTGACCGCAACGGAAC TC	attB2 TelBP1 rv (187-627)
HW74	CGAATTCCCCAAGCTTATGGAGTCATCGCTCGGTGCTTAC	TelBP1 ORF fw, EcoRI-HindIII
HW75	CGAATTCCAGGATCCCTCAAGACAGGGGTATGTCCTCGC	TelBP1 ORF rv, EcoRI-BamHI
HW91	GGGGACAAGTTTGTACAAAAAAGCAGGCTGTGATTCTCCTGAAGTAACG GAG	attB1 TbTRF fw (530-1143)
HW92	GGGGACCACTTTGTACAAGAAAGCTGGGTCGTTATTCTCCATATTGGAGG C	attB2 TbTRF rv (530-1143)
HR25	CGAATTCCCCAAGCTTTATG*GAGGTCCATACTAACCAGGACCCACTTGAC* GAGTCATCGCTCGGTGCTTACTG	OE of N-term Ty1 TelBP1, fw
HR26	CGAATTCCAGGATCCCGTTCAAGACAGGGGTATGTCCTCGC	OE of N-term Ty1 TelBP1, rv
HR29	CCCTAACCCTAACCCTAA	Labeling telomere probe
HR35	GCAGCGACCTACCTAGGTAAAGC	833 bp of VSG221 fw
HR36	GAATTGCTGCTTCCTGTGGTGTTTG	833 bp of VSG221 rv
HR39	CCGCATACTGCGAAGCAATCAGAC	SL fw
HR40	TCAAGACAGGGGGATGTCCTCGC	3'-end of TelBP1 ORF rv
HR45	TTAGGGTTAGGGTTAGGGTTAGGGTTAGGGTTAGGGTTAGGGTTAGGGTT AGGGTTAGGG	$(TTAGGG)_{10}$ fw for EMSA
HR46	AACCCTAACCCTAACCCTAACCCTAACCCTAACCCTAACCCTAACCCTAA CCCTAACCCT	$(TTAGGG)_{10}$ rv for EMSA
HR47	TTGACAGTGAGTGTGAGTGTGAGTGTGAGTGTGAGTGTGAGTGTGAGTGT GAGTGTGAGT	$(GTGAGT)_{10}$ fw for EMSA
HR48	AAACTCACACTCACACTCACACTCACACTCACACTCACACTCACACTCAC ACTCACTGTC	$(GTGAGT)_{10}$ rv for EMSA

Abbreviations: KT (Klara Thein), SB (Susanne Bury), F (Ferdinand Bucerius), HW (Helena Weitner), HR (Helena Reis), fw (forward), rv (reverse).

2.3.2 Site-directed mutagenesis

To introduce a mutation into a plasmid sequence, a PCR was performed over the entire vector using primers, which contain the desired mutation and anneal the same sequence in the opposite strand of the plasmid. Primers were designed according to the mutagenic primer design guidelines of the Stratagene-Quickchange manual. The PCR product was digested with DpnI overnight in order to get rid of the original vector. Then, the mutated plasmid was purified using the PCR clean up kit (Macherey-Nagel) and 5 µl of it were used to transform *E. coli* TOP10 cells.

Table 8. Primers used for site-directed mutagenesis.

Name	Sequence (5'-3')	Description
HW93	GTTGCGGTCAATACAATTAAACTGGTGAAGTGTTTGGATCAGG	TelBP1 M212L fw
HW94	CCTGATCCAAACACTTCACCAGTTTAATTGTATTGACCGCAAC	TelBP1 M212L rv
HR5	CCAAAAAGTAAAATTCACAAGCTTCTGGAGTCATCGCTCGGTGC	TelBP1 M1L fw
HR6	GCACCGAGCGATGACTCCAGAAGCTTGTGAATTTTACTTTTTGG	TelBP1 M1L rv

Abbreviations: HW (Helena Weitner), HR (Helena Reis), M (methionine), L (leucine), fw (forward), rv (reverse).

2.3.3 PCR purification

PCR products were purified using the NucleoSpin® Gel and PCR clean up kit (Macherey-Nagel) according to the manufacturer's instructions.

2.3.4 Restriction digest

The digest of DNA was carried out using restriction enzymes (Thermo Fisher Scientific or NEB) according to the manufacturer's instructions.

2.3.5 Isopropanol precipitation of DNA

Prior transfection of trypanosomes linearized plasmid DNA or PCR product was precipitated by adding 1 volume isopropanol and 0.1 volume 3 M NaAc (pH 5.2) to the DNA. After mixing well, DNA was incubated for at least 30 min at -20°C. Then, the DNA was pelleted by centrifugation (20,000 g, 30 min, 4°C) and was washed twice with 500 µl 70% EtOH (20,000 g, 10 min, 4°C). After the second wash, the supernatant was removed under the hood and was air-dried under sterile conditions. Finally, the DNA pellet was dissolved in sterile dH_2O.

2.3.6 Agarose gel electrophoresis and gel extraction

This method was used to separate DNA fragments according to size, for control of restriction digest or gel extraction. DNA was mixed with 6x DNA loading buffer (0.4% (w/v) Orange G, 15% Ficoll 400), loaded on a gel containing 1% agarose and 0.1 µg/ml ethidium bromide in 1xTAE buffer (40 mM Tris-HCl pH 8.0, 20 mM acetic acid, 1 mM EDTA). Separation was conducted in 1xTAE buffer at 120 V for 30-40 min. DNA molecules were visualized under UV-light and documented using the Intas imager (INTAS). The GeneRuler Mix (Thermo Fisher Scientific) was taken as molecular weight standard.
For DNA extraction, specific DNA fragments were cut out under UV-light and processed using the NucleoSpin® Gel and PCR clean up kit (Macherey-Nagel).

2.3.7 Measurement of DNA concentration

DNA and RNA quantification was performed using the Tecan Infinite M200. This instrument measured the absorption at 260 nm and at 280 nm. The ratio of OD260 and OD280 provides information about the purity of DNA.

2.3.8 Ligation

For vector and insert ligation a molar ratio of 1:3 was used, respectively. The amount of insert was calculated referring to the 50 ng vector used per ligation. A 20 µl reaction was prepared containing 1x Ligase buffer and 2 µl T4 DNA ligase (Therm oFisher Scientific). The ligation mix was incubated at 16°C overnight. 10 µl of the ligation were taken for transformation of *E. coli* TOP10.

2.3.9 DNA sequencing

Sequencing was carried out by the company GATC (Konstanz, Germany). Per sequencing, a 20 µl volume of plasmid DNA with a DNA concentration of 80-100 ng/µl and 20 µl of sequencing primer with a concentration of 10 µM were sent to the company. Sequencing results were analyzed using the CLC Software (CLC bio, Quiagen).

Table 9. Primers used for sequencing.

Name	Sequence (5'-3')	Description
HW80	CTCACATGTTCTTTCCTGC	pyrFEKO 5'UTR seq fw
HW81	TCCTGGATTACGACCAATC	pyrFEKO 3'UTR seq rv
HW97	CTGTGTTGATAAGGGACG	pGL2084 seq fw
HW98	GGAAGATATCCACACACG	pGL2084 seq rv
GPEET	CTGAGTTTAACATGTTCTCG	pLew100 seq fw
LP27	GTGCCATCAGATTACTCC	pLew100 seq rv
tb44	CTGGTTAGTATGGACTTCTCTAGA	binds in Ty1, pyrFEKO seq rv

Abbreviations: HW (Helena Weitner), HR (Helena Reis), LP (Lena Pfaller), fw (forward), rv (reverse).

2.3.10 Telomere and VSG southern blot

For telomere southern blots, genomic DNA of *T. brucei* was extracted as described in 2.2.7. Then, 20 µg of genomic DNA were digested using the frequently cutting restriction enzymes AluI (10 U), HinfI (15 U) and RsaI (15 U) (Thermo Fisher Scientific). After overnight incubation at 37°C, the reaction was heat-inactivated at 80°C for 20 min.

DNA restriction fragments (10 µg) were separated on a 0.7% 0.5xTBE agarose gel (19 cm x 25 cm) in 0.5x TBE buffer (45 mM Tris-borate, 1 mM EDTA pH 8.0). The separation was first run at 30 V for 1 h and then at 45 V overnight. On the next day the run was continued at 120 V until the 2 kb marker almost ran off. To induce depurination the gel was immersed in 0.25 M HCl for 30 min. The denaturation step was conducted by immersing the gel in 1.5 M NaCl, 0.5 M NaOH for 30 min. After that the gel was neutralized in 3 M NaCl, 0.5 M Tris-HCl (pH 7.0) for 1 h. Gel remained in the neutralization solution while the transfer was prepared.

For Southern blotting, two thick and two thin Whatman paper were soaked into 20xSSC (3 M NaCl, 0.3 M sodium citrate, pH 7.0), the Hybond N+ membrane (GE Healthcare) was first floated on top of dH_2O before soaking it in 20xSSC. The gel chamber was filled with 20xSSC, a glass dish was put in it (to increase the height), the gel slide was put backwards in the glass and the blotting sandwich was

assembled from bottom to top: two thick Whatman paper, the first dipping into the tray, gel, Hybond N+ membrane, two wet thin Whatman paper, two dry thin Whatman paper, stack of paper towels, glass plate, 1 kg weight. The transfer was performed overnight. On the next day, the membrane was washed for 10 min in 2x SSC and the DNA UV cross-linked using the UV Stratalinker® 1800 (Stratagene).

To block unspecific binding the membrane was incubated in church mix (0.5 M NaPi pH 7.2, 1 mM EDTA pH 8.0, 7% (w/v) SDS, 1% (w/v) BSA) for 1 h at 65°C. In the mean while the probe was prepared. To visualize the telomeric DNA 200 ng of the 162 bp fragment of EcoRI-cut pTH5 was incubated with 5 ng of $(CCCTAA)_3$ oligonucleotide (HR29) in 29 µl total volume for 5 min at 95°C, cooled on ice and supplemented with 5 µl of 10xOLB (0.5 M Tris pH 6.8, 0.1 mM MgOAc, 1 mM DTT, 10 mg/ml BSA) containing dATP, dGTP and dTTP (each 0.6 mM final conc.), 5 µl of α-P^{32} CTP (Hartman Analytic) and 1 µl Klenow Polymerase (5 U, DecaLabel DNA Labeling Kit, Thermo Fisher Scientific). The reaction was mixed and incubated at RT for 90 min or longer. To stop the reaction 50 µl of TNES (10 mM Tris pH 7.4, 100 mM NaCl, 10 mM EDTA, 1% (w/v) SDS) was added and heated to 65°C for 10 min. For one membrane half of the probe was boiled at 95°C for 5 min. The church mix used for blocking was replaced by fresh 25 ml of church mix and the probe was added immediately after boiling. The hybridization was carried out at 65°C overnight. On the next day, the membrane was washed three times in church wash (40 mM NaPi pH 7.2, 1 mM EDTA pH 8.0, 1% (w/v) SDS) for 30 min at 65°C and dried between two Whatman paper. The dry membrane was then wrapped in plastic wrap and exposed to a phosphorimager screen overnight at RT. The screen was scanned using a Typhoon scanner.

To detect telomeres of the active BES, a VSG probe was used. The VSG221 probe was prepared by PCR amplification using the primer pair HR35/36 on genomic DNA of MITat1.2 SM cells. Then, the PCR product was purified and labeled with α-P^{32} CTP using the DecaLabel DNA Labeling Kit (Thermo Fisher Scientific) according to the manufacturer's instructions. The VSG probe was hybridized at 65°C overnight.

2.4 Protein methods

2.4.1 Telomere pull-down

The telomere pull-down was carried out by Falk Butter. Telomere pull-downs were done as previously described in (Casas-Vila et al., 2015). Briefly, oligonucleotides with either TTAGGG or TGTGAG repeats were chemically synthesized and annealed with their complementary strand. The resulting dsDNA was then phosphorylated with 100 U PNK (Thermo Fisher Scientific) for 2 h at 37°C and ligated overnight using 20 U of T4 ligase (Thermo Fisher Scientific) at RT. DNA was purified by chloroform-phenol extraction and incubated with biotin-dATP (Jena Biosciences) and 60 U Klenow fragment (Thermo Fisher Scientific) at 37°C overnight. To re-buffer the DNA a G50 Spin column (GE Healthcare) was used according to the manufacturer's instructions. Per pull-down 25 µg biotinylated DNA was immobilized on Streptavidin Dynabeads MyOne C1 (Thermo Fisher Scientific) and incubated with whole cell lysates from PCF trypanosomes. To prepare cell lysates, $2x10^8$ cells were harvested (1500 g, 10 min, 4°C), washed once in PBS (10 mM Na_2HPO_4, 1.8 mM KH_2PO_4 pH 7.4, 140 mM NaCl, 2.7 mM KCl) (1500 g, 10 min, 4°C) and lysed by using 1 ml of modified RIPA buffer (50 mM Tris-HCl, pH 7.5, 150 mM NaCl, 1% Igepal CA-630, 0.1% Sodium Deoxycholate, Protease inhibitor cocktail (Roche)). The binding reaction was carried out in protein binding buffer (PBB) (150 mM NaCl, 50 mM Tris-HCl pH 7.5, 5 mM $MgCl_2$, 0.5% Igepal CA-630) in the presence of 10 µg

sheared salmon sperm DNA (Ambion) at 4°C for 2 h under slight agitation. Three washes with PBB followed and the bound fraction was eluted with 1xLDS buffer (Thermo Fisher Scientific).

2.4.2 Co-Immunoprecipitation

30 µl of Protein G Sepharose Fast Flow bead slurry (GE Healthcare) were used per IP. First, the bead slurry was once washed in 1 ml PBS (10 mM Na_2HPO_4, 1.8 mM KH_2PO_4 pH 7.4, 140 mM NaCl, 2.7 mM KCl) (500 g, 1 min, 4°C) and twice in PBS/1% BSA. To block unspecific binding beads were incubated in PBS/1% BSA for 1 h at 4°C under slight agitation on a rotator. The block solution was removed after centrifugation (500 g, 1 min, 4°C) and the antibody added to the beads (2 ml of anti-TelBP1 mouse 2E6 antibody or 1.5 ml of anti-Ty1 mouse (BB2) antibody per IP). The binding reaction was performed overnight at 4°C under agitation on a rotator. Unbound antibody was removed by washing three times in 1 ml PBS/0.1% BSA.

Per IP $2x10^8$ BSF or PCF trypanosomes were harvested (1500 g, 10 min, 4°C) and washed once in ice-cold TDB (5 mM KCl, 80 mM NaCl, 1 mM $MgSO_4$, 20 mM Na_2PO_4, 2 mM NaH_2PO_4, 20 mM glucose, pH 7.4) or PBS, respectively. Lysis was carried out by adding 1 ml IP buffer (150 mM NaCL, 0.5% Igepal CA-630, 20 mM Tris-HCl pH 8.0, 10 mM $MgCl_2$, 1 mM DTT, Protease inhibitor cocktail (Roche)) and subsequent incubation for 20 min on ice. Cells were then sonicated (3 cycles, 30 s on and 30 s off) using a Biorupter (Diagenode). To clear the lysate a centrifugation step followed (10.000 g, 10 min, 4°C). Protein G sepharose beads with immobilized anti-TelBP1 mouse antibody or anti-Ty1 mouse antibody were washed with IP buffer prior incubation with the cell lysate. The incubation was performed overnight at 4°C under slight agitation. Unbound proteins were washed with IP buffer three times 5 min on ice. Bound proteins were eluted by boiling the beads in 50 µl 1x sample buffer (NuPAGE®LDS Sample buffer, 100 mM DTT) at 70°C for 10 min. The eluates were analyzed by mass spectrometry.

2.4.3 Mass spectrometry and data analysis

Mass spectrometry and data analyses were performed by Falk Butter. Samples were separated on a 4-12 % Novex NuPage gel (Thermo Fisher Scientific). The in-gel digest was performed according to a standard protocol (Shevchenko et al., 2006). The gel pieces were minced, incubated with 10 mM DTT/0.05 M ammonium bicarbonate pH 8 for 1 h min at 56°C and proteins subsequently alkylated with 55 mM iodoacetamide/ 0.05 M ammonium bicarbonate pH 8 for 30 min in the dark. The proteins were digested with 1 µg trypsin (Promega or Sigma) overnight at 37°C. The tryptic peptides were desalted using a StageTip (Rappsilber et al., 2007) and stored in the fridge until mass spectrometric measurement.

The telomere pull-down, the gel was sliced into 4 fractions per lane and each fraction was measured on an LTQ-Orbitrap XL (Thermo Fisher Scientific) coupled to an Easy-nLC system (Proxeon). The peptides were eluted in a 105 min nonlinear gradient of 2-60% acetonitrile with a Top10 acquisition method using CID fragmentation for MS/MS. For the protein co-IPs a single fraction per lane was measured on a Q Exactive Plus mass spectrometer coupled to an Easy-nLC 1000 (Thermo Fisher Scientific) with a 75 min non-linear gradient of 2-60% acetonitrile with a Top10 method using HCD fragmentation for MS/MS.

The MS spectra were processed with MaxQuant (version 1.5.2.8) (Cox and Mann, 2008) using LFQ quantitation (Cox et al., 2014) with preset setting except match between runs was activated. For the search a trypanosome brucei TREU 927 protein database (ver8.1; 11,567 entries) downloaded from www.tritrypdb.org was used. The data of the protein group file was filtered for contaminants, reverse

hits and used to generate the volcano plot by calculating median and a p-value (Welch t-test) for each protein group. The data was visualized using the ggplot2 package of R.

2.4.4 Preparation of cell lysates for SDS PAGE

BSF or PCF cells were harvested by centrifugation (1500 g, 10 min, 4°C) and washed once in TDB (5 mM KCl, 80 mM NaCl, 1 mM $MgSO_4$, 20 mM Na_2PO_4, 2 mM NaH_2PO_4, 20 mM glucose, pH 7.4) or PBS (10 mM Na_2HPO_4, 1.8 mM KH_2PO_4 pH 7.4, 140 mM NaCl, 2.7 mM KCl), respectively (1500 g, 10 min, 4°C). Cell pellets were resuspended in 2x sodium dodecyl sulfate (SDS) loading buffer (126 mM Tris-HCl pH 6.8, 20% (v/v) glycerol, 4% (w/v) SDS, 0.02% (w/v) bromphenol blue, 60 mM DTT) to a final concentration of $5x10^5$ cells/µl and boiled at 95°C for 10 min. Cell lysates were stored at -20°C until use.

2.4.5 Sodium dodecyl sulfate polyacrylamide gel electrophoresis (SDS-PAGE)

SDS-PAGE was conducted to separate proteins according to their molecular mass. Stacking gels consisted of 5% (v/v) acrylamid/bisacrylamid (5:1) in stacking gel buffer (500 mM Tris-HCl pH 6.8, 0.4% (w/v) SDS) and the separation gels of 15% (v/v) acrylamid/bisacrylamid (5:1) in separation buffer (1.5 M Tris-HCl pH 8.8, 0.4% (w/v) SDS). A prestained protein marker (Thermo Fisher Scientific) was used for size estimation of separated protein samples. The electrophoresis was carried out in SDS-running buffer (25 mM Tris, 192 mM glycine, 0.1% (w/v) SDS) at 180 V using the Consort EV265 electrophoresis power supply (Hoefer).

2.4.6 Coomassie staining

Protein gels were transferred in water and boiled for 1 min using a microwave oven. After discarding the water the gels were stained with Coomassie solution (0.02% (w/v) Coomassie Brilliant Blue G-250 (Applichem), 10% (v/v) EtOH, 5% (w/v) aluminiumsulfate-(14-18)-hydrate, 2% (v/v) orthophosphoric acid) for 3 h at RT. Destaining was performed using water.

2.4.7 Western blot

Proteins separated by SDS-PAGE were blotted from the SDS gel onto an Immobilon® polyvinylidene fluoride (PVDF) membrane (Merck Millipore). For this purpose, a sandwich from bottom to top was assembled: two Whatman paper soaked in anode buffer (25 mM Tris-HCl pH 7.6, 20% (v/v) methanol), for 15 sec in Methanol activated PVDF membrane, SDS gel, and one Whatman paper soaked in cathode buffer (300 mM Tris-HCl pH 7.6, 20% (v/v) methanol, 40 mM ε-aminocaproic acid). The sandwich was placed in a semi-dry blotter (TRANS-BLOT SD, Bio-Rad) and the protein transfer was carried out at 55 mA (approximately 1 mA/cm^2 gel) for 1 h using the Consort EV265 electrophoresis power supply (Hoefer).

To block unspecific binding, the membrane was incubated with 5% (w/v) milk in PBS (10 mM Na_2HPO_4, 1.8 mM KH_2PO_4 pH 7.4, 140 mM NaCl, 2.7 mM KCl) overnight at 4°C. After blocking primary antibodies (Table 10) were applied in PBS/1% milk/0.1% Tween 20 for 1 h at RT. Unbound antibodies were removed by three washes with PBS/0.1% Tween 20 for 10 min at RT. Then, IRDye800- and 680-conjugated secondary antibodies (LI-COR Bioscience) were applied in PBS/1% milk/0.1% Tween 20/0.02% SDS for 1 h at RT in the dark. Again, three washes with PBS/0.1% Tween 20 were conducted for 10 min at RT. Blots were analyzed using a LI-COR Odyssey Imager and the ImageStudio™ software.

Table 10. Primary and secondary antibodies used for western blot.

Name	Isotype	Clonality	Dilution for WB	Reference
Anti-TbTRF 6F5	Rat	Monoclonal	1:200	E. Kremmer
Anti-TelBP1 13D9	Rat	Monoclonal	1:5	E. Kremmer
Anti-TelBP1 2E6	Mouse	Monoclonal	1:5	E. Kremmer
Anti-PFR L13D6	Mouse	Monoclonal	1:100	K. Gull
Anti-H3	Rabbit	Polyclonal	1:50,000	Pineda
Anti-Ty1 BB2	Mouse	Monoclonal	1:500	K. Gull
Anti-VSG221 ΔCRD	Rabbit	Polyclonal	1:100,000	G. Cross
IRDye800CW anti-rat IgG	Goat	Polyclonal	1:20,000	LI-COR Bioscience
IRDye800CW anti-rabbit IgG	Goat	Polyclonal	1:20,000	LI-COR Bioscience
IRDye680LT anti-rabbit IgG	Goat	Polyclonal	1:20,000	LI-COR Bioscience
IRDye680LT anti-mouse IgG	Goat	Polyclonal	1:20,000	LI-COR Bioscience

2.4.8 Electromobility shift assay (EMSA)

To anneal complementary oligonucleotides, they were mixed at a 1:1 molar ratio (each 1 µM final conc.). The reaction was set up in 100 µl volume containing dH_2O supplemented with Ligase buffer (1x final conc., Thermo Fisher Scientific). The oligo mixture was incubated at 95°C for 5 min and the heat was reduced to RT. Annealed oligos were stored at -20°C until use.

To analyze binding to telomeric DNA the complementary oligonucleotides HR45 and HR46 were used. The oligonucleotides HR47 and HR48 served as negative control.

For the binding reaction 12 µl EMSA buffer 1 (5% glycerin, 10 mM Tris-HCl pH 7.6, 1 mM EDTA pH 8.0, 5 mM DTT) was mixed with 1.5 µl (50 ng) of annealed oligonucleotides, 1-2 µg recombinant protein and EMSA buffer 2 (20 mM HEPES/KOH pH 7.6, 1 mM DTT) to 20 µl final volume. The binding reaction was carried out on ice for 30 min. A 5% native TAE polyacrylamide gel was prepared and pre-run in 1xTAE buffer (40 mM Tris-HCl pH 8.0, 20 mM acetic acid, 1 mM EDTA) at 70 V for 1 h at 4°C. The complete reaction was loaded on the gel. A 100 bp generuler (Thermo Fisher Scientific) was used as DNA standard. The gel was run at 70 V for 90 min at 4°C. Finally, the gel was stained by incubation in water containing EtBR (0.1 µg/ml final conc.) for 15 min. The gel was then analyzed under UV-light and documented using the Intas imager.

2.4.9 Recombinant protein expression

Recombinant proteins were obtained from Falk Butter (IMB Mainz). To express recombinant N-terminal His_6-MBP TbTRF and His_6-MBP TelBP1 proteins the pCoofy expression system was used (Scholz et al., 2013). For this aim, the coding sequences of TbTRF and TelBP1 were amplified from reverse transcribed trypanosomes mRNA and cloned into the pCoofy vector. The cloning of both genes was verified by Sanger sequencing. The pCoofy4 constructs were transformed into BL21 (DE3) pRare T1 cells. Protein expression was induced and cells were harvested and lysed with Avestin. The soluble fraction was subjected to affinity purification using a 1 ml MBP-TrapHP column (GE Healthcare) and His-Select Ni Affinity Gel (Sigma). Protein identity and purity was monitored by LC-ESI/MS on a micrOTOF instrument (Burker).

2.4.10 Antibody production

Recombinant His_6-MBP TbTRF (HisMBP-TbTRF) and His_6-MBP TelBP1 (HisMBP-TelBP1) proteins were used to immunize animals for antibody production. For anti-TbTRF antibody generation rats were immunized. For anti-TelBP1 antibody production a rat and a mouse were immunized. Antibody production was carried out by Elisabeth Kremmer at the Helmholtz Centre in Munich. Our laboratory tested different hybridoma supernatants by western blotting for their specificity to recognize endogenous TbTRF or TelBP1 proteins.

3 RESULTS

3.1 Identification of novel telomere-binding proteins in *Trypanosoma brucei*

As African trypanosomes diverged early from the main eukaryotic lineage (Stevens et al., 2001), sequence-based searches for shelterin proteins in *T. brucei* identified only a TRF homolog (Li et al., 2005). Other components of the telomere protein complex in *T. brucei* e.g. TbRAP1 and TbTIF2, were found by yeast two-hybrid screens or co-immunoprecipitation (Co-IP) experiments (Yang et al., 2009, Jehi et al., 2014b).

To find novel telomere-binding proteins in trypanosomes, we carried out two independent but complementary biochemical experiments (Figure 13). The first approach aimed to identify proteins that interact directly or indirectly with telomeric DNA using a pull-down assay with telomeric repeat oligonucleotides. The second approach intended to identify the interacting proteins of the telomeric protein TbTRF by Co-IP.

For the telomeric pull-down assay, whole lysates from procyclic form (PCF) cells were incubated with oligonucleotides consisting of telomeric repeats. This procedure was carried out in quadruplicates. Shuffled control oligonucleotides served as a negative control. The bound proteins were eluted and processed for label-free quantitative mass spectrometry (MS) analysis. The mass spectromic data of co-purified candidates of the telomere and control samples were then analyzed and compared using the software MaxQuant (Cox and Mann, 2008, Cox et al., 2014). The comparison of those samples is represented in the volcano plot (Figure 13A). From this experiment, we found among 210 interactions 17 proteins that were statistically significantly ($p<0.01$, S0>) enriched at the telomeric oligonucleotides (Table 11).

For the TbTRF Co-IP, a BSF cell line was generated that constitutively expressed a Ty1-tagged TbTRF from the endogenous locus. The second allele was knocked out. The Co-IP was performed in quadruplicates of TbTRF -/Ty1 cell extracts with an anti-Ty1 antibody. For the controls, lysates from wild-type (WT) cells without the tagged TbTRF were immunoprecipitated in parallel using the anti-Ty1 antibody. These samples contained unspecific interactions with the anti-Ty1 antibody and/or the Protein G sepharose beads, which were used to immobilize the antibody. The bound proteins were eluted and analyzed by label-free quantitative MS (Figure 13B). Five proteins were significantly ($p<0.01$, S0>) co-purified with TbTRF: Tb927.3.1560 (TbTIF2), Tb927.6.4330 (hypothetical protein, shown to associate with telomeres (Glover et al., 2016)), Tb927.9.4000/3930 (hypothetical proteins), Tb927.11.5550 (DNA polymerase theta) and Tb927.11.9870 (hypothetical protein). All of these five proteins and TbTRF were also significantly enriched at telomeric DNA as shown by the telomere pull-down. The whole data set of the two independent approaches is summarized in Table 11 and Table 12.

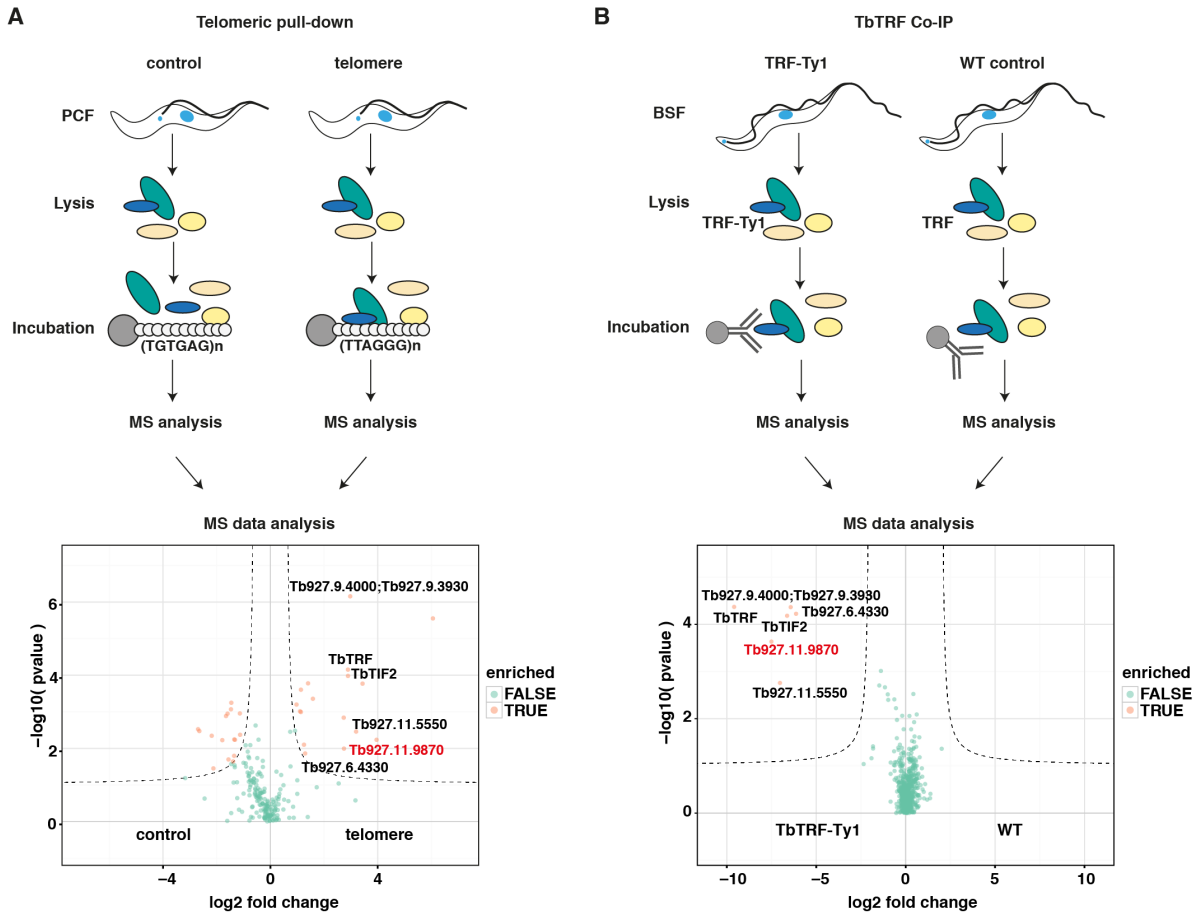

Figure 13. Identification of novel telomere-binding proteins in *T. brucei* using label-free quantitative mass spectrometry.

(**A**) Experimental design of the telomeric pull-down assay and volcano plot showing interactions with telomeric DNA. Quadruplicates of PCF cell lysates were incubated with TTAGGG-repeat oligonucleotides and as a negative control with TGTGAG-repeat oligonucleotides. The interacting proteins were eluted and analyzed by mass spectrometry. The comparison of control and telomeric DNA interacting proteins revealed 17 proteins to be significantly enriched at telomeric DNA. This enrichment is displayed by the x-axis which represents the log2-fold change between telomeric and control samples. The y-axis shows the -log10 (p-value). (**B**) Experimental workflow of the TbTRF Co-IP and volcano plot showing the TbTRF-interacting proteins. Lysates from BSF TbTRF-/Ty1 and wild-type (WT) cells were prepared, each in quadruplicates, and incubated with anti-Ty1 antibody. WT cells served as control. The co-purified proteins were eluted and analyzed by mass spectrometry. Six protein groups were significantly enriched in the TbTRF-/Ty1 sample: Tb927.9.4000/3930, Tb927.6.4330, TbTRF, TbTIF2, Tb927.11.9870, Tb927.11.5550. All these six proteins were also found in the telomeric pull-down experiment. In both plots, only the six overlapping candidates are displayed. The protein, which was selected for detailed analysis is highlighted in red (Tb927.11.9870).

Table 11. Overview of telomere DNA interactions found by the telomeric pull-down assay.

Gene ID	GeneDB Protein Description	Reference
Tb927.2.6100	hypothetical protein, conserved	
Tb927.3.1560	TRF-Interacting Factor 2 (TIF2)	(Jehi et al., 2014b)
Tb927.3.5150	exonuclease, putative	
Tb927.5.1700	replication Factor A 28 kDa subunit, putative	
Tb927.6.4330	hypothetical protein, conserved	(Glover et al., 2016)
Tb927.9.4000; Tb927.9.3930	hypothetical protein, conserved	
Tb927.9.5020	HMG-box domain containing protein, putative	
Tb927.9.8740	Double RNA binding domain protein 3 (DRBD3)	(Das et al., 2015)
Tb927.9.10770	polyadenylate-binding protein 2 (PABP2)	(Kramer et al., 2013)
Tb927.10.2200	hypothetical protein, conserved	
Tb927.10.2520	PrimPol-like protein 2 (PPL2)	(Rudd et al., 2013)
Tb927.10.4220	hypothetical protein, conserved	
Tb927.10.6220	5'-3' exoribonuclease D (XRND)	(Li et al., 2006)
Tb927.10.12850	ttaggg binding factor (TRF)	(Li et al., 2005)
Tb927.11.5550	DNA polymerase theta (POLQ)	
Tb927.11.9870	hypothetical protein, conserved	

Table 12. Overview of TbTRF interactions identified by Co-IP with BSF cells.

Gene ID	GeneDB Protein Description	Reference
Tb927.3.1560	TRF-Interacting Factor 2 (TIF2)	(Jehi et al., 2014b)
Tb927.6.4330	hypothetical protein, conserved	(Glover et al., 2016)
Tb927.9.4000; Tb927.9.3930	hypothetical protein, conserved	
Tb927.10.12850	ttaggg binding factor (TRF)	(Li et al., 2005)
Tb927.11.5550	DNA polymerase theta (POLQ)	
Tb927.11.9870	hypothetical protein, conserved	

3.2 Bioinformatic analysis of identified potential telomere-binding proteins

To gather more information about the found candidate proteins I searched for conserved domains (Table 13), mapped nuclear localization signals (NLSs) (Table 13), predicted protein functions (Table 14), predicted protein structure (Table 15), and for information from published high-throughput phenotyping approaches, proteomics and transcriptomics (Table 16).

Table 13. Overview of conserved domains and predicted NLS in the candidate proteins.

Gene ID	GeneDB Protein Description	Mol. weight [kDa]	Conserved Domains	NLS (Position in aa)
Tb927.2.6100	hypothetical protein, conserved	53	*No*	82, 83, 239
Tb927.3.1560	TIF2	42	*No*	*No*
Tb927.3.5150	exonuclease, putative	38	Exonuc_X-T; 3'-5' exonuclease ERI1-related; Polynucleotidyl transferase, Ribonuclease H-like	*No*
Tb927.5.1700	replication Factor A 28 kDa subunit, putative	28	Wingled helix' DNA-binding domain; OB-fold, tRNA/helicase-type; RPA, C-terminal	*No*
Tb927.6.4330	hypothetical protein, conserved	20	*No*	*No*
Tb927.9.4000; Tb927.9.3930	hypothetical protein, conserved	38	*No*	*No*
Tb927.9.5020	HMG-box domain containing protein, putative	44	High mobility group box (HMG)	*No*
Tb927.9.8740	DRBD3	37	RNA recognition motif, RNP-1; Polypyrimidine tract-binding protein 1	*No*
Tb927.9.10770	PABP2	62	RNA recognition motif, RNP-1; Polyadenylate-binding protein/ Hyperplastic disc protein	*No*
Tb927.10.2200	hypothetical protein, conserved	38	PD-(D/E)XK nuclease superfamily	93, 94, 95, 97
Tb927.10.2520	PPL2	82	*No*	*No*
Tb927.10.4220	hypothetical protein, conserved	34	*No*	*No*
Tb927.10.6220	XRND	91	XRN 5'-3' exonuclease N-terminus	623, 625, 758, 757, 777
Tb927.10.12850	TRF	42	Myb domain; TRFH domain	171
Tb927.11.5550	POLQ	93	DNA-directed DNA polymerase activity; DNA Polymerase I/A	42, 52, 53
Tb927.11.9870	hypothetical protein, conserved	45	*No*	282

In order to identify conserved domains in the found candidate proteins the Basic Local Alignment Search Tool (BLAST) was used. To predict nuclear localization signal motifs the cNLS mapper program was chosen (Kosugi et al., 2009). TriTryp Database provided the information about the molecular weight of the found candidates (Aslett et al., 2010).

Table 14. Overview of biological processes, function and cellular components.

Gene ID	GeneDB Protein Description	Biological process	Function	Cellular component
Tb927.2.6100	hypothetical protein, conserved	*No information*	*No information*	mitochondrion
Tb927.3.1560	TIF2	*No information*	*No information*	*No information*
Tb927.3.5150	exonuclease, putative	*No information*	Nucleic acid binding, exonuclease activity	intracellular
Tb927.5.1700	replication Factor A 28 kDa subunit, putative	*No information*	Nucleic acid binding	*No information*
Tb927.6.4330	hypothetical protein, conserved	*No information*	*No information*	*No information*
Tb927.9.4000; Tb927.9.3930	hypothetical protein, conserved	*No information*	*No information*	*No information*
Tb927.9.5020	HMG-box domain containing protein, putative	*No information*	*No information*	*No information*
Tb927.9.8740	DRBD3	mRNA stabilization; prosttranscriptional regulation of gene expression; RNA processing	mRNA binding; mRNA 3'UTR binding	ribonucleoprotein complex; cytosol; nucleus
Tb927.9.10770	PABP2	prosttranscriptional regulation of gene expression; RNA processing	Poly(A) binding; RNA binding	cytoplasmic mRNA processing body; Nuclear stress granule; Cytoplasmic stress granule; cytoplasm
Tb927.10.2200	hypothetical protein, conserved	*No information*	*No information*	*No information*
Tb927.10.2520	PPL2	Translesion synthesis; response to UV; Response to oxidative stress; Regulation of G2/M transition of mitotic cell cycle	DNA-directed DNA polymerase activity; Not DNA primase activtiy	site of double-strand break; nucleus
Tb927.10.4220	hypothetical protein, conserved	*No information*	*No information*	*No information*
Tb927.10.6220	XRND	RNA processing	Nucleic acid binding, exonuclease activity	nucleus; intracellular; nucleolus
Tb927.10.12850	TRF	*No information*	*No information*	*No information*
Tb927.11.5550	POLQ	Translesion synthesis	DNA-directed DNA polymerase activity	nucleus
Tb927.11.9870	hypothetical protein, conserved	*No information*	*No information*	*No information*

In order to yield information about the putative function of the found proteins the genome database GeneDB was used (Logan-Klumpler et al., 2012).

Table 15. Overview of predicted protein structure.

Gene ID	GeneDB Protein Description	Phyre2 top hit(s)
Tb927.2.6100	hypothetical protein, conserved	**Fold:** Methionine synthase domain-like **Superfamily:** TM0693-like **Modeled:** 23 residues (11.3% confidence)
Tb927.3.1560	TIF2	**Fold:** Regulator of G-protein signaling **Superfamily:** Regulator of G-protein signaling, RGS **Modeled:** 74 residues (64.5% confidence)
Tb927.3.5150	exonuclease, putative	**PDB header:** Hydrolase **PDB Molecule:** 3'-5' exonuclease eri1 **Modeled:** 206 residues (100% confidence)
Tb927.5.1700	replication Factor A 28 kDa subunit, putative	**PDB header:** Replication, DNA-binding protein **PDB Molecule:** replication protein a 32 kda subunit **Modeled:** 126 residues (100% confidence)
Tb927.6.4330	hypothetical protein, conserved	**PDB header:** Gene regulation **PDB Molecule:** heterochromatin protein 1-binding protein 3 **Modeled:** 16 residues (24.5% confidence)
Tb927.9.4000; Tb927.9.3930	hypothetical protein, conserved	**PDB header:** Lyase **PDB Molecule:** 3,4-hydroxy-2-butanone 4-phosphate synthase **Modeled:** 62 residues (51.9% confidence)
Tb927.9.5020	HMG-box domain containing protein, putative	**Fold:** HMG-box (Transcription factor) **Modeled:** 58 residues (96.3% confidence)
Tb927.9.8740	DRBD3	**PDB header:** RNA binding protein **PDB Molecule:** heterogeneous nuclear ribonucleoprotein **Modeled:** 179 residues (100% confidence)
Tb927.9.10770	PABP2	**PDB header:** RNA binding protein **PDB Molecule:** u4/u6 snRNA-associated-splicing factor prp24; **Modeled:** 340 residues (100% confidence)
Tb927.10.2200	hypothetical protein, conserved	**Fold:** Restriction endonuclease **Modeled:** 57 residues (69.0% confidence)
Tb927.10.2520	PPL2	**PDB header:** Transferase/dna **PDB Molecule:** DNA-directed primase/polymerase protein **Modeled:** 203 residues (99.4% confidence)
Tb927.10.4220	hypothetical protein, conserved	**PDB header:** Isomerase **PDB Molecule:** S-adenosylmethionine:tRNA ribosyltransferase **Modeled:** 62 residues (33.4% confidence)
Tb927.10.6220	XRND	**PDB header:** Hydrolase/ protein binding **PDB Molecule:** 5'-3' exoribonuclease 2 **Modeled:** 650 residues (100% confidence)
Tb927.10.12850	TRF	**Fold:** DNA/RNA-binding 3-helical bundle **Superfamily:** Homeodomain-like **Family:** DNA-binding domain of telomeric protein **Modeled:** 59 residues (98% confidence)
Tb927.11.5550	POLQ	**PDB header:** Transferase/dna, **PDB Molecule:** DNA polymerase nu **Modeled:** 551 residues (100% confidence)
Tb927.11.9870	hypothetical protein, conserved	**PDB header:** Oxidoreductase, **PDB Molecule:** Quinohemoprotein amine dehygrogenase 60 kDa **Modeled:** 33 residues (37.8% confidence) **Fold:** Bromodomain-like **Superfamily:** Bacillus cereus metalloprotein-like **Modeled:** 22 residues (30.3% confidence)

In order to predict the protein structure Phyre2 was used. Phyre2 is a portal for protein modeling, protein structure and function prediction (Kelley et al., 2015). Predicted models are derived from the Protein Data Bank (PDB).

Table 16. RNAi high-throughput phenotyping and comparative proteome and transcriptome data.

Gene ID	RIT-seq PCF	BSF d3	BSF d6	BSF diff.	Proteome BSF/PCF (Butter et al., 2013)	Proteome BSF/PCF (Urbaniak et al., 2012)	Transcriptome BSF/PCF (Siegel et al., 2010)
Tb927.2.6100	Normal	Abnormal	Abnormal	Abnormal	1.41	1.04	1.16
Tb927.3.1560	Normal	Abnormal	Abnormal	Normal		1.21	1.2
Tb927.3.5150	Normal	Normal	Normal	Abnormal			0.86
Tb927.5.1700	Normal	Abnormal	Normal	Normal	0.67	0.92	0.96
Tb927.6.4330	Abnormal	Abnormal	Abnormal	Abnormal			0.87
Tb927.9.4000; Tb927.9.3930	Normal	Normal	Normal	Normal			
Tb927.9.5020	Normal	Normal	Normal	Normal	.		
Tb927.9.8740	Abnormal	Abnormal	Abnormal	Abnormal	0.90	0.59	0.8
Tb927.9.10770	Abnormal	Abnormal	Abnormal	Abnormal	0.92	0.83	0.71
Tb927.10.2200	Normal	Normal	Normal	Normal			
Tb927.10.2520	Normal	Abnormal	Abnormal	Abnormal		0.59	
Tb927.10.4220	Abnormal	Normal	Abnormal	Abnormal	0.62	0.69	1.21
Tb927.10.6220	Abnormal	Abnormal	Abnormal	Abnormal		0.50	
Tb927.10.12850	Abnormal	Abnormal	Abnormal	Abnormal	1.23	1.17	0.92
Tb927.11.5550	Normal	Normal	Normal	Normal	.		
Tb927.11.9870	Normal	Normal	Normal	Normal	1.68	2.48	1.57

In order to gain more information about the potential telomere-binding proteins the data of RNAi target sequencing (RIT-seq) were analyzed for our candidates (Alsford et al., 2011). As this genome-scale RNAi screen was conducted with PCF, BSF and differentiated (diff) BSF it provides information if a gene is essential in those life cycle stages of the parasite. However, no observed effect in the screen can also be a false negative result and has to be validated. Abbreviations d3 and d6 indicate days after RNAi induction. The comparative proteomes show the ratio of protein amount calculated in BSF and PCF cells (BSF/PCF) and thus reflect the fold change of protein amount between both stages. The transcriptome data also show the ratio of BSF/PCF and represent the fold change of transcript amount in both life cycle stages.

We selected the protein Tb927.11.9870 for detailed characterization as it was found in both of our independent biochemical searches for telomere-binding proteins (Figure 13). Furthermore, this candidate was one of the six proteins for whom a NLS sequence motif was predicted. Interestingly, this protein was also described in the comparative proteome study where it showed a stage-specific regulation. Although bioinformatics of the amino acid sequence revealed neither annotated domains nor any homology to known telomere-binding proteins, we named the candidate Tb927.11.9870 telomere-binding protein 1 (TelBP1) as it was highly enriched in both of our telomeric interaction studies.

3.3 Tools for Tb927.11.9870 (TelBP1) characterization

The characterization of a protein with unknown functions starts mostly with answering the questions: Is the protein essential for cell viability? Where does the protein localize within the cell? What are the interacting proteins? To answer these questions I first had to prepare the appropriate tools, which are described in the following sections.

3.3.1 Production of TelBP1 and TbTRF monoclonal antibodies

First, monoclonal antibodies against the recombinant HisMBP-TelBP1 full-length protein were raised in mouse and rat. In addition, a monoclonal antibody against recombinant HisMBP-TbTRF full-length protein was raised in rat as marker for telomeres. E. Kremmer from the Helmholtz Center in Munich produced all these antibodies and provided us with the supernatants from the hybridoma cells. The specificity of the anti-TelBP1 antibodies was validated by western blot using cell lysates from BSF and PCF WT cells. The lysate from TelBP1 knockout mutant (ΔTelBP1) BSF cells (3.3.3) served as negative control and the recombinant protein as a positive control (Figure 14A, B).

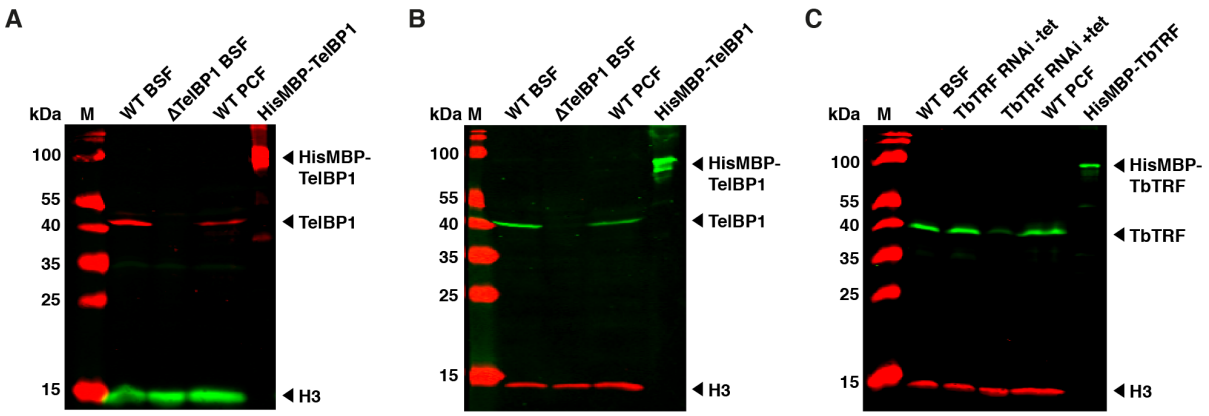

Figure 14. Specificity of anti-TelBP1 and anti-TbTRF monoclonal antibodies.
(**A**) Western blot showing specificity of the anti-TelBP1 monoclonal mouse antibody clone 2E6. Recombinant HisMBP-TelBP1 protein was used as a positive control as this protein was taken for animal immunization. Cell lysate from ΔTelBP1 BSF served as negative control. The antibody recognizes a protein of 45 kDa in trypanosome wild-type (WT) lysates and the recombinant HisMBP-TelBP1 protein (87.5 kDa). (**B**) Anti-TelBP1 monoclonal rat antibody clone 13D9 was analyzed under same conditions as described in the panel A. (**C**) Western blot analysis showing the specificity of the anti-TbTRF monoclonal rat antibody clone 6F5. TbTRF RNAi cell line was induced with tetracycline and taken as control for antibody specificity. Recombinant HisMBP-TbTRF was used as positive control. The antibody recognizes the recombinant protein (84 kDa) and a protein around 40 kDa. TbTRF has a molecular weight of 41.5 kDa. Histone H3 was used as loading control in all three western blots.

Both anti-TelBP1 monoclonal antibodies recognized the recombinant protein and in the WT cell lysates a protein with a molecular mass of appriximately 45 kDa. The specificity of the anti-TbTRF monoclonal rat antibody was analyzed by western blot as well (Figure 14C). For this purpose, WT cell lysates from BSF and PCF stage were taken. The lysate from TbTRF RNAi-induced cells and the recombinant TbTRF protein served as controls. The anti-TbTRF antibody recognized the recombinant TbTRF protein and a protein with a molecular mass of appriximately 40 kDa in WT cell lysates. The TbTRF RNAi-induced cells showed a downregulation of TbTRF protein expression confirming the specificity of the anti-TbTRF monoclonal antibody.

3.3.2 Generation of TelBP1 RNAi cell lines in both life cycle stages of the parasite

Next, inducible TelBP1 RNAi cell lines were generated in BSF and PCF cells to test whether TelBP1 is essential for cell growth. To generate TelBP1 RNAi cell lines the pTrypRNAiGate system was used (Kalidas et al., 2011). RNAi-mediated depletion of TelBP1 protein expression was confirmed by western blot using the anti-TelBP1 monoclonal rat antibody (Figure 15A). Three days after RNAi induction TelBP1 protein was undetectable in BSF parasites. In PCF parasites, the TelBP1 protein was not detectable already after day one post RNAi induction. Furthermore, growth analysis of induced TelBP1 RNAi cell lines revealed that TelBP1 is neither essential for the viability of BSF nor of PCF cells (Figure 15B, C). No significant growth difference was detected between induced and non-induced TelBP1 RNAi cell lines. PCF WT cells showed a faster growth compared to PCF RNAi cells in the first 24 h of the time course of the growth curve. Therefore, the growth curve of WT PCF cells runs above the curves of induced and non-induced RNAi parasites. However, no significant difference was detectable in the slopes of the curves.

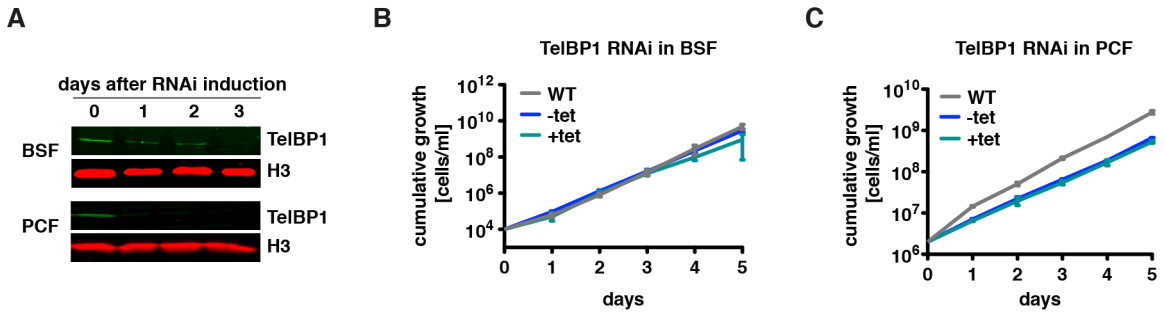

Figure 15. RNAi-mediated depletion of TelBP1 shows no effect on cell viability in both life cycle stages of the parasite.
(**A**) Western blot analysis confirmed downregulation of TelBP1 upon RNAi induction in both life cycle stages. Histone H3 was taken as a loading control. (**B**) Cumulative growth of wild-type BSF cells (WT), non-induced (-tet) and induced (+tet) TelBP1 RNAi BSF cells (n=3). (**C**) Cumulative growth of PCF cells after TelBP1 depletion (n=3). The bars represent the standard deviation (±SD).

3.3.3 Generation of TelBP1 BSF and PCF knockout mutants

As TelBP1 RNAi results suggested that the protein is not essential for cell growth, TelBP1 knockout mutants (ΔTelBP1) were generated in both life cycle stages of the parasite. For this aim, the pyrFEKO vector system was used (Kim et al., 2013a). The pyrFEKO vectors carry a resistance cassette fused with the thymidine kinase (TK). This dual marker cassette is flanked by loxP sites. Thus, cells harboring a TK cassette are sensitive for the nucleoside analog Ganciclovir (GCV). Replacement of TelBP1-alleles by selectable drug markers was validated by integration PCR on genomic DNA (Figure 16). Eight ΔTelBP1 BSF clones and one ΔTelBP1 PCF clone were obtained. To reuse the selectable drug markers, the resistance marker cassettes in ΔTelBP1 BSF cells (clone 7) were removed by transient transfection with pLew100Cre-EP1 and selection with 50 µg/ml GCV. Cells that have lost the resistance cassettes are GCV-resistant and hygromycin/puromycin-sensitive. The removal of the resistance cassette markers was confirmed by negative selection with hygromycin and puromycin.

To examine if TelBP1 deletion had an influence on cell viability the growth of ΔTelBP1 BSF and ΔTelBP1 PCF cells was investigated (Figure 17). While TelBP1 deletion in PCF cells had no effect on cell viability, growth of ΔTelBP1 BSF cells was mildly slowed with 7.0 h population doubling time (PDT) compared to WT cells with 6.4 h PDT.

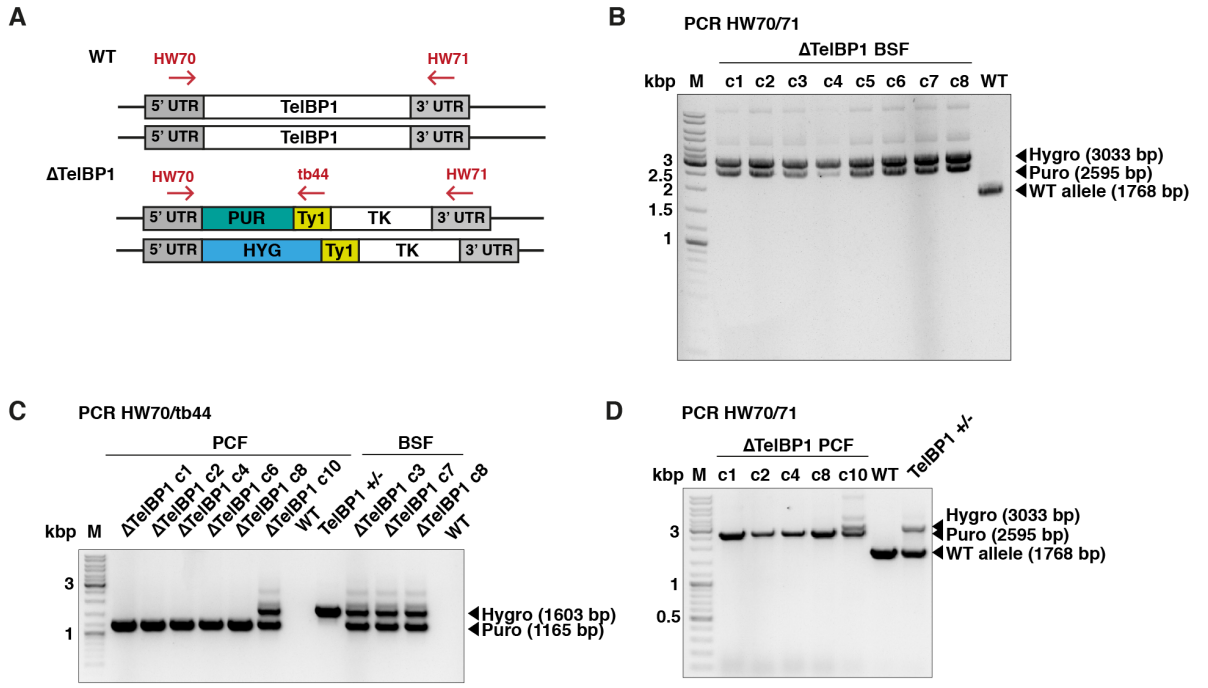

Figure 16. Deletion of TelBP1 gene in BSF and PCF cells.
(**A**) Illustration of endogenous TelBP1 gene locus in wild-type (WT) cells and TelBP1 knockout mutants. The first allele was replaced by the hygromycin resistance (HYG)-Ty1-thymidine kinase (TK) fusion cassette, and the second allele by the puromycin resistance (PUR)-Ty1-TK fusion cassette. Red arrows indicate primers used for integration PCRs. (**B**) Integration PCR with primers HW70/71 binding in the untranslated regions (UTRs) of TelBP1 gene to prove TelBP1 deletion in BSF cells. Eight clones were tested positive as no band at the height of the WT allele was detected. (**C**) Integration PCR with primer pair HW70/tb44 to control correct integration of resistance cassettes into the TelBP1 locus in PCF and BSF cells. HW70 is binding outside of the integration site and the tb44 primer anneals to the Ty1 sequence of the deletion constructs. ΔTelBP1 PCF c10 and ΔTelBP1 BSF c3, c7, c8 are positive for a TelBP1 knockout. (**D**) Integration PCR with primers HW70/71 to prove that no WT allele is present in TelBP1 PCF knockout mutants. PCR with primers HW70/71 on genomic DNA of ΔTelBP1 PCF c10 generates bands specific for HYG-TK and PUR-TK fusion cassettes.

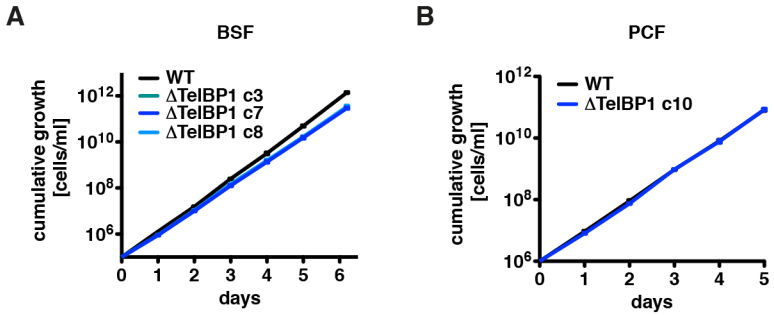

Figure 17. Growth of BSF and PCF TelBP1 knockout mutants.
(**A**) Cumulative growth of wild-type (WT), ΔTelBP1 c3, c7 and c8 BSF cells (n=3). (**B**) Cumulative growth of WT and ΔTelBP1 PCF c10 (n=3). The bars represent the standard deviation (±SD).

3.3.4 Overexpression of TelBP1 reveals TelBP1 processing into smaller isoforms

To test whether TelBP1 overexpression has an impact on cell viability, BSF and PCF cells were transfected with the pLew100v5b1d_TelBP1 construct. This construct enables inducible ectopic overexpression of TelBP1 from an rRNA spacer. To confirm TelBP1 protein increase after tetracycline-induced TelBP1 overexpression, a western blot using the anti-TelBP1 rat antibody was performed (Figure 18A, B). Quantification of the TelBP1 signal revealed that overexpression led to a 2-8-fold TelBP1 protein increase in BSF cells compared to WT level (Appendix Figure 36). A 20-40-fold increase of TelBP1 was observed in PCF cells compared to WT level (Appendix Figure 37). The

analysis of BSF and PCF growth after TelBP1 overexpression demonstrated that increase of TelBP1 expression had no impact on cell viability (Figure 18C, D). From these results and the results of TelBP1 knockdown or knockout, we can conclude that the viability of BSF and PCF parasites is independent of TelBP1 protein expression level under *in vitro* cell culture conditions.

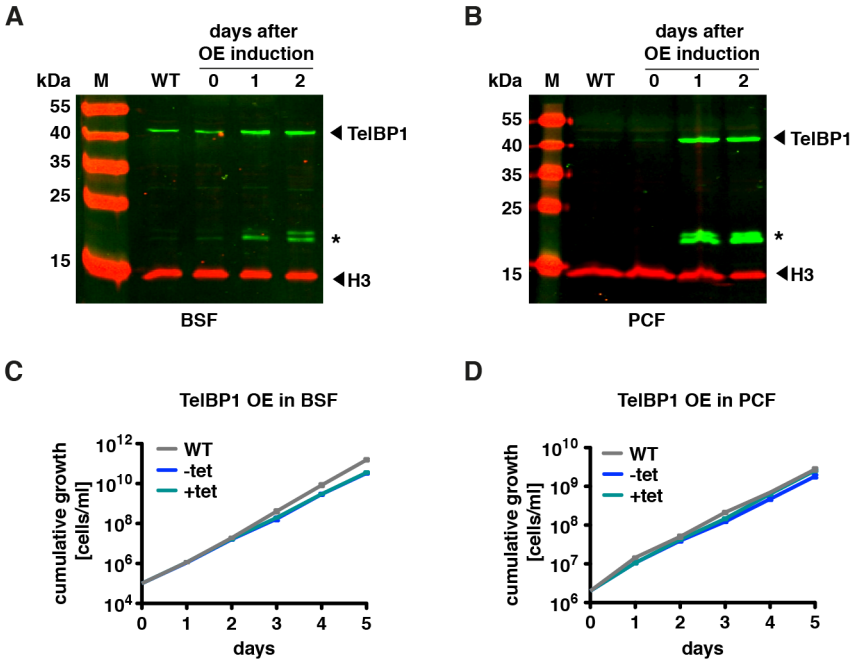

Figure 18. Inducible ectopic overexpression of TelBP1 in BSF and PCF shows no effect on cell viability. (**A**) Western blot analysis of TelBP1 overexpression in BSF and (**B**) in PCF cells using the TelBP1-specific rat antibody. Two additional bands (asterisk) are detectable after induction of ectopic TelBP1 overexpression. Histone H3 was used as loading control. (**C**) Cumulative growth of BSF and (**D**) PCF cells after induction of ectopic TelBP1 overexpression using 1 µg/ml tetracycline (+tet). The growth curves represent the cumulative mean cell number ±SD of three replicates.

Interestingly, two additional bands were strongly upregulated after TelBP1 overexpression in BSF and PCF cells. These bands were detected with a monoclonal anti-TelBP1 antibody indicating that these products must be TelBP1-specific.

3.3.5 Analysis of TelBP1 isoforms

To reveal the source of the observed additional bands, it was first essential to find out if these bands are also present in WT cells. For this purpose, an IP experiment using the anti-TelBP1 monoclonal mouse anti-body was conducted to enrich the smaller TelBP1 products, as their expression was undetectable in WT cells. ΔTelBP1 BSF cells were used as negative control. Western blot analysis of the immunoprecipitated material revealed an enrichment of the additional TelBP1 fragments, which were detected by the TelBP1-specific antibody (Figure 19). In ΔTelBP1 immunoprecipitate none of the bands was detected suggesting that these bands might be TelBP1 isoforms. We named these isoforms accordingly to their molecular mass p20 and p22.

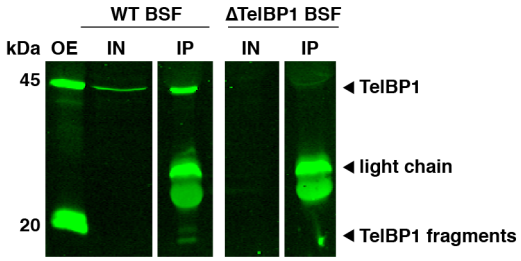

Figure 19. Western blot analysis of TelBP1 IP conducted with monoclonal mouse antibody.
The western blot was performed with the TelBP1 monoclonal rat antibody. Two additional bands are enriched and recognized by the TelBP1-specific antibody in WT cells but not in ΔTelBP1 cells. The lysate from TelBP1 overexpressing cells (OE) served as positive control for the smaller TelBP1 fragments. IN (input), IP (immunoprecipitate).

Thus, the question arose: How are these isoforms produced? Are the small TelBP1 products the result of proteolytic processing or of alternative splicing or of alternative ATG usage? To find out how the TelBP1 protein is processed into smaller fragments the TelBP1 open reading frame (ORF) either containing the Ty-1 epitope tag at the C-terminus (Ct) or at the N-terminus (Nt) was cloned into the pLew100v5b1d plasmid (Figure 20). Since TelBP1 overexpression led to higher expression levels of the isoforms in the PCF stage compared to BSF stage, 29-13 PCF parasites were transfected with those constructs. Induced ectopic expression of TelBP1 Ct-Ty1 and TelBP1 Nt-Ty1 was analyzed by western blot using the anti-TelBP1 rat and anti-Ty1 mouse antibodies. C-terminal tagging of TelBP1 showed that the isoforms comprise the C-terminus of the TelBP1 protein as they were detected with both the TelBP1-specific and the Ty1-specific antibody (Figure 20A). The N-terminal tagging indicated that TelBP1 is proteolytically processed (Figure 20B). The western blot analysis suggested that TelBP1 is cleaved somewhere in the middle of its protein sequence as below the full-length TelBP1-Ty1 fusion protein an additional band was detected using the anti-Ty1 antibody.

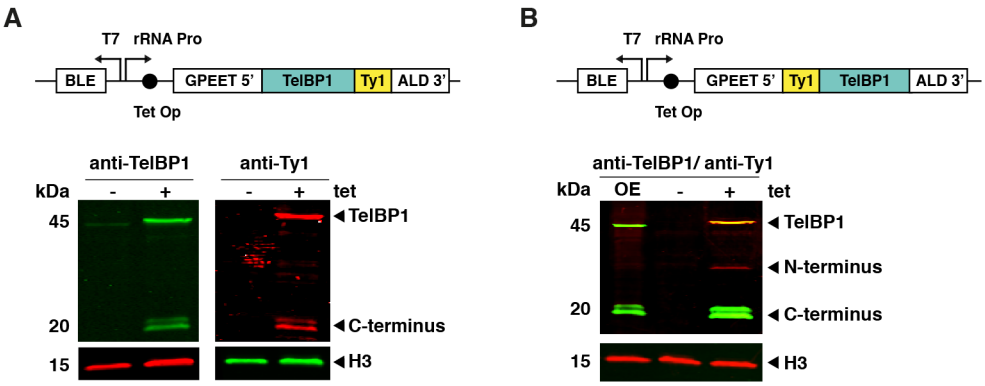

Figure 20. TelBP1 is processed into smaller isoforms.
(**A**) Scheme and western blot analysis of inducible C-terminally Ty1-tagged TelBP1 in PCF cells. The expression of TelBP1-Ty1 is controlled by an inducible rRNA promoter. TelBP1-Ty1 coding region is flanked by a GPEET 5'UTR (GPEET 5') and a Aldolase 3'UTR (ALD 3'). The expression of the resistance cassette is under control of a T7 promoter. C-terminal tagging of TelBP1 proved that the isoforms are TelBP1-specific and that the isoforms comprise the C-terminus of TelBP1. (**B**) N-terminal Ty1-tagging of TelBP1 indicated that TelBP1 is proteolytically processed. Below the full-length Ty1-TelBP1 fusion protein (yellow) an additional band is detected with an anti-Ty1 antibody (red). The isoforms are not detectable with an anti-Ty1 antibody. Histone H3 served as loading control.

In parallel, the data of spliced leader trapping (SLT) (Nilsson et al., 2010) and other high-throughput RNA sequencing experiments (Siegel et al., 2010, Kolev et al., 2010) were analyzed to find out if the expression of TelBP1 isoforms might be regulated on the transcriptional level. The database of SLT (http://splicer.unibe.ch) offers a summary of all identified splice acceptor sites (SASs) of three high-throughput RNA sequencing attempts performed by different groups (Siegel et al., 2010, Kolev et al.,

2010, Nilsson et al., 2010). The SLT database revealed five splice acceptor sites (SASs) in the 5' untranslated region (UTR) of TelBP1 and two ORF-internal SASs (Figure 21). To validate this data and to analyze if small transcripts are upregulated upon TelBP1 overexpression, RNA was isolated from WT, TelBP1 OE non-induced (-tet) and induced (+tet) BSF cells and from TelBP1 OE -tet/+tet PCF parasites. Each isolated RNA sample was transcribed into cDNA, which then was used for PCR with primers specific for the spliced leader (SL) sequence and the 3' end of the TelBP1 ORF (Figure 21B). All splice variants were expected to have the SL at the 5' end and the 3' end of the TelBP1 ORF. Analysis of PCR products suggested multiple splice variants of TelBP1. At the time point when this experiment was conducted the ΔTelBP1 cell line was not available yet. Therefore, a negative control is missing in this experiment. Thus, it remains elusive which of the smaller fragments are specific products and which of them are unspecific products. None of the smaller PCR fragments showed an upregulation in TelBP1 OE induced cells. However, an upregulation of the fragment around 1200-1300 bp was apparent in induced BSF and PCF cells indicating that a SAS at position approx. -100 must be used predominantly. As I was using the pLew100v5_b1d vector for overexpression this SAS is located within the GPEET 5'UTR. Kolev and colleagues detected most of the reads for splice products resulting from the SASs at position -126 and -40 (Kolev et al., 2010). Nilsson and colleagues detected most of the reads arising from the -40 SAS (Nilsson et al., 2010). In contrast, Siegel and Cross only found the splice products from -1378, -1357, and -126, whereby -1378 and -1357 showed the most hits (Siegel et al., 2010). Our data indicate that apart from the SAS in the GPEET 5'UTR a SAS within the TelBP1 ORF might be used, most likely at position +32.
Taken together, overexpression of TelBP1 increases the amount of splice products deriving from the SASs at the position -100 in the GPEET 5'UTR and at position +32 within the TelBP1 ORF, but the origin of the TelBP1 isoforms remains unknown.

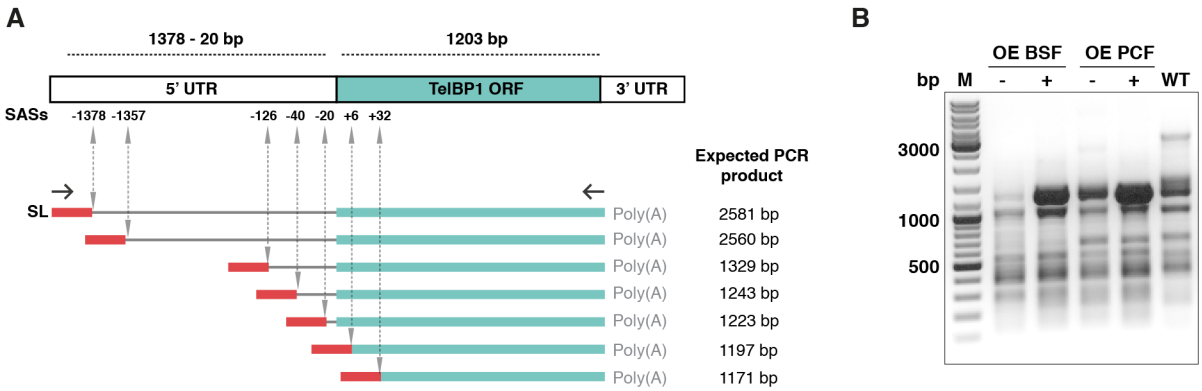

Figure 21. Different splice variants of TelBP1.
(**A**) Illustration of splice acceptor sites (SASs) in the 5'UTR and the open reading frame (ORF) of TelBP1 and the resulting mRNAs. The red boxes represent the splice leader (SL) and the green boxes the TelBP1 ORF. Splice leader trapping revealed five SASs in the 5'UTR of TelBP1 and two ORF-internal SASs (Nilsson et al., 2010). (**B**) PCR with SL and TelBP1-specific primers on cDNA of wild-type BSF (WT) and TelBP1 overexpressing (OE) cells (either induced (+) or non-induced (-)) suggested multiple splice variants of TelBP1.

Given that distinct transcript variants of TelBP1 are present, I aimed to rule out if a smaller transcript not detected by previous high-throughput sequencing approaches might exist. For this purpose I investigated if it is possible to selectively silence the expression of the full-length protein but not of the isoforms by RNAi. Therefore two different non-overlapping RNAi targeting constructs were designed (Figure 22A) and transfected into BSF and PCF cells. I obtained one clone for Nt-RNAi in PCF cells and two clones for Ct-RNAi in BSF cells and analyzed the resulting clones upon RNAi induction by western blot (Figure 22B).

Induction of TelBP1 Nt-RNAi in PCF cells led to full downregulation of full-length TelBP1 whereas the smaller TelBP1 fragment was still detectable by western blot. For the TelBP1 Ct-RNAi, the two obtained clones in the BSF were tested after RNAi induction. Here, clone 1 showed a downregulation of the full-length protein compared to the non-induced cells and the small fragment was still detectable. In contrast, clone 2 showed full downregulation of full-length TelBP1 and the isoform signal also got weaker compared to the non-induced cells.

However, no concrete conclusion could be made out of these results. The combination of a weak antibody and low abundance of the isoforms hampered this study.

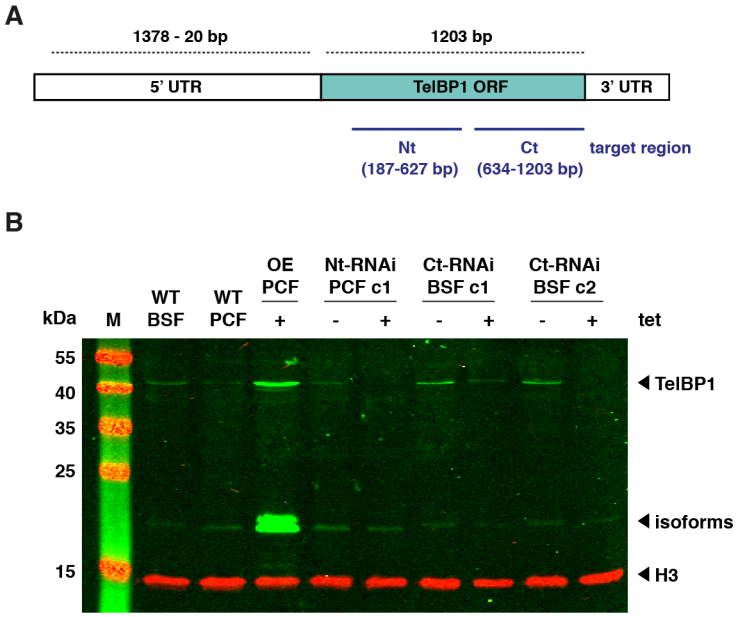

Figure 22. RNAi-mediated TelBP1 downregulation using two different non-overlapping targeting constructs.

(A) Illustration of TelBP1 RNAi targeting sequences. (B) Western blot analysis of TelBP1 expression upon induction of RNAi-mediated TelBP1 depletion using the TelBP1-specific monoclonal rat antibody. Wild-type BSF and PCF cells served as controls. In addition, induced TelBP1 overexpressing PCF cells were taken as control for TelBP1 isoform expression. An additional band is also seen in wild-type cells at the same height as the detected isoforms upon TelBP1 overexpression induction. Induction of Nt-RNAi in PCF cells led to downregulation of the full-length TelBP1 protein whereas the small band was still detectable. Induction of Ct-RNAi in BSF led to downregulation of full-length TelBP1 expression. Although this construct was expected to downregulate the expression of the isoforms they were still detectable as weak bands. Histone H3 served as loading control.

Next, I investigated if alternative ATG codons are used for TelBP1 isoform expression. The TelBP1 ORF contains eleven ATGs in frame (Table 17) with the last codon as stop codon.

Table 17. Analysis of the TelBP1 coding sequence.

ATG #	ATG position within TelBP1 CDS (nt)	Methionine position within full-length TelBP1 (aa)	Protein size (aa)	MW (kDa)
1 (start codon)	1	1	400	44.6
2	28	10	391	43.7
3	490	164	237	25.9
4	529	177	224	24.5
5	538	180	221	24
6	589	197	204	22.2
7	634	212	189	20.7
8	826	276	125	14.1
9	1021	341	60	6.8
10	1024	342	59	6.7
11	1153	385	16	1.8

Listed are the number (#) of found ATGs in frame and the resulting putative polypeptide products and the molecular weight. nt (nucleotide), aa (amino acid), MW (molecular weight), kDa (Kilodalton).

The usage of these ATGs would result in smaller TelBP1 products. In addition, the TelBP1 ORF contains 14 smaller ORFs with alternative stop codons within its coding sequence. However, these ORFs were neglected as C-terminal Ty1-tagging of TelBP1 indicated that the isoforms comprise the complete C-terminal end of TelBP1. We selected the first ATG and the seventh ATG at position 634 of the TelBP1 coding sequence for mutation studies, which correspond to methionines at position 1 and 212, respectively. The first methionine was chosen for mutation studies because if alternative splicing is the source, the small bands should be still detected. Are the isoforms degradation products they should be undetectable when the full-length TelBP1 is not expressed anymore. The methionine 212 was selected since translation from the corresponding ATG would result in a protein of around 20 kDa like the found isoforms. To this end, a point mutation of adenosine to cytosine was introduced in the first ATG codon in the pLew100v5b1d_TelBP1 construct leading to the mutation of the first methionine to leucine (M1L). As both amino acids are nonpolar, the mutated amino acid was not expected to influence protein properties. Induction of TelBP1-M1L was analyzed by western blot using the TelBP1-specific antibody. Although the first ATG was mutated cells still expressed the full-length TelBP1 protein (Figure 23B). The mutation of M212L also did not affect the isoform expression (Figure 23C, D). Several different clones were analyzed by western blot. Those, which expressed the full-length TelBP1, also expressed the two isoforms. In addition a cell line overexpressing TelBP1-M1L-M197L-M212L was generated and analyzed by western blot after induction of overexpression (Appendix Figure 38). Again, TelBP1 full-length and isoforms were still expressed indicating that the second ATG might be used as start codon, which would give rise to a 44 kDa-protein. However, the source of the isoforms remained unknown.

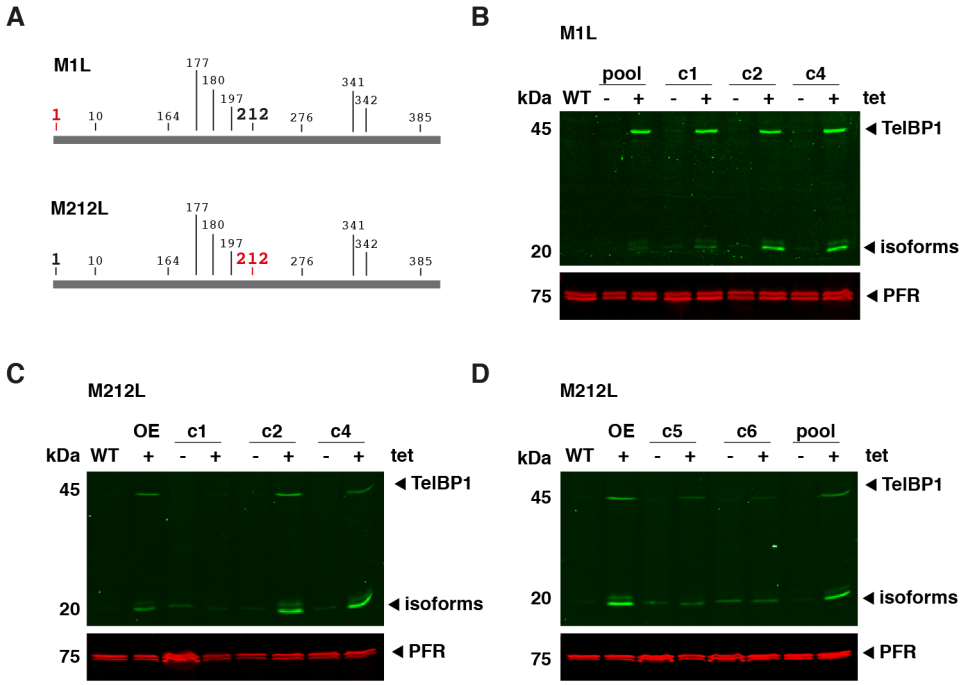

Figure 23. Mutation of methionine to leucine in the TelBP1 protein sequence has no effect on isoform expression.
(**A**) Overview of methionines found in the protein sequence of TelBP1. Red indicates which methionine was mutated. The pLew100-TelBP1 construct was used to introduce the mutations. (**B**) Western blot analysis of clones with mutation of methionine 1 to leucine (M1L). Induction of TelBP1 M1L expression (+tet) still leads to the expression of the full-length TelBP1 protein and the isoforms. Paraflagellar rod (PFR) served as loading control. (**C**)(**D**) Western blot analysis of clones with mutation of methionine 212 to leucine (M212L). Some clones express two isoforms (c2, c4) some only one isoform (c5, c6).

Analysis of TelBP1 transcripts and mutational studies of potential alternative ATGs did not solve the origin of the TelBP1 isoforms. Knowing the amino acid sequence of the isoforms would provide information about their origin. In the case that the fragments start with a methionine alternative ATG usage or splicing would be most likely the source of the isoforms. Another amino acid would be a sign for proteolytic degradation. In order to investigate the amino acid sequence of the TelBP1 isoforms MS analysis was used. The isoforms were first enriched by TelBP1 IP with PCF cells overexpressing TelBP1 and then separated by SDS-PAGE to subsequently cut out the bands containing the isoforms. However, TelBP1 isoforms were not detectable using Coomassie for protein staining. Therefore, the TelBP1 IP was repeated. This time, the immunoprecipitated material and whole cell lysates from induced TelBP1 OE PCF cells were separated by SDS PAGE and the gel was cut in the middle. While the half containing the IP sample was stained with Coomassie, the other half was taken for western blot with the TelBP1-specific rat antibody. Using the western blot image the height of the isoforms was estimated on the Coomassie gel to cut out the isoforms for MS analysis (Figure 24). The MS analysis was performed by Falk Butter and revealed that the isoforms are TelBP1-specific and comprise the C-terminus (Figure 24C). A conclusion about the first amino acid of the TelBP1 isoforms was not possible due to technical limitations. Prior to MS analysis the protein was digested with trypsin to smaller peptides. As the resulting peptides behaved differently in the mass spectrometer not all peptides were detected. Thus, the MS analysis did not reveal the complete amino acid sequence of the TelBP1 protein isoforms.

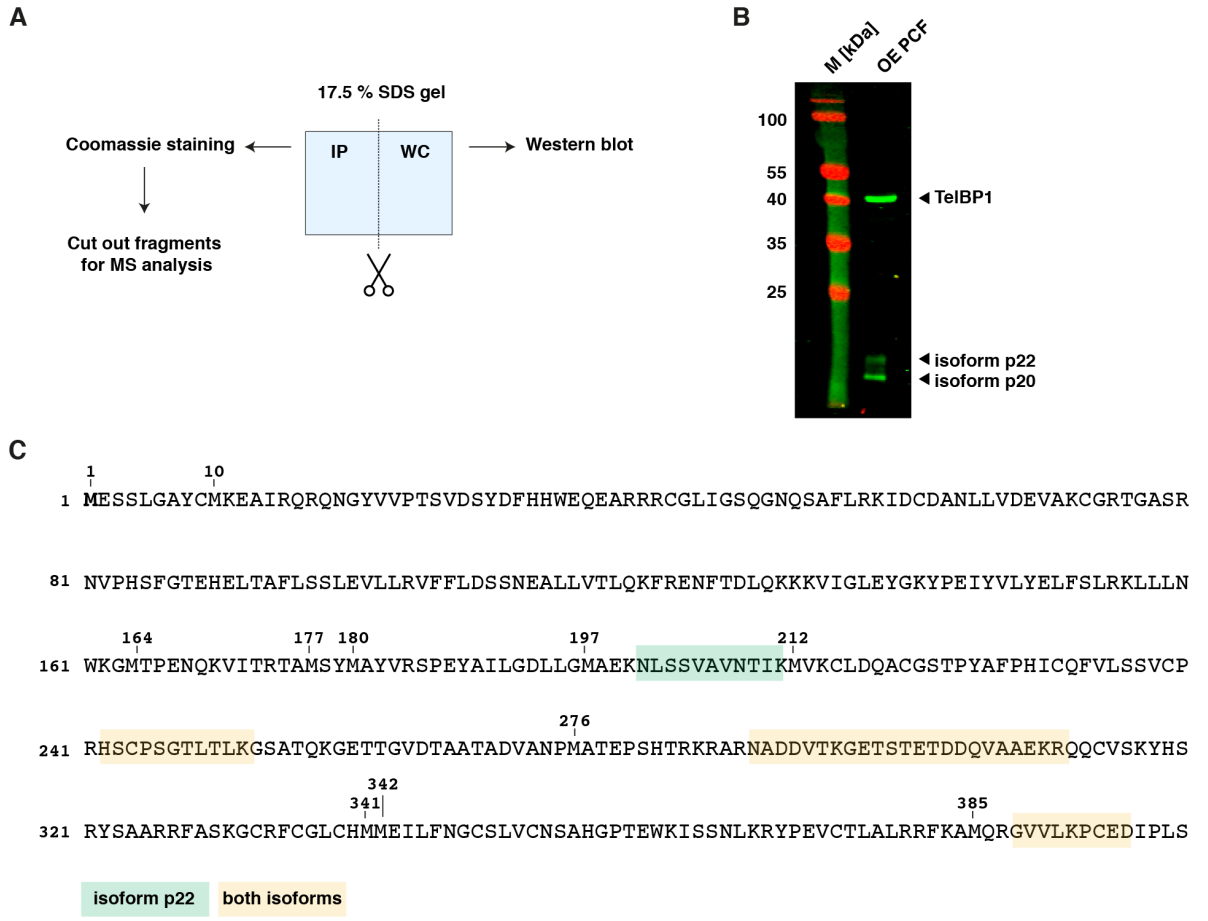

Figure 24. Mass spectrometry analysis of TelBP1 isoforms confirms the TelBP1 specificity of the fragments.
(**A**) Experimental design. By TelBP1 IP enriched isoforms and whole cell lysate (WC) of TelBP1 overexpressing PCF cells were loaded on an SDS gel. After electrophoretic separation, the gel was cut in the middle and the half containing the enrichment of TelBP1 isoforms was stained with Coomassie and the other half was used for western blot analysis (**B**). Using the western blot as orientation two bands were cut out from the Coomassie stained gel and analyzed by mass spectrometry. (**C**) The result of mass spectrometry analysis showing the protein sequence of TelBP1 and the detected peptides. Methionines present in the TelBP1 protein sequence are marked by numbers. Green-marked peptides were found only in the isoform p22 and the yellow marked peptides in both isoforms.

Taken together, all the experiments, which were conducted to determine the source of TelBP1 isoforms implicate that the expression might be regulated on multiple levels. It seems that proteolytic processing and alternative splicing act together to produce those smaller TelBP1 fragments. However, the precise source and the function of those TelBP1 isoforms are still unknown.

3.4 TelBP1 is a component of the *T. brucei* telomere protein complex

TelBP1 was found in the telomere pull-down assay and in the TbTRF Co-IP. Before proceeding with the functional analysis of TelBP1, it was, therefore, essential to validate that TelBP1 is a true telomere-binding protein. I used two independent approaches to confirm the association of TelBP1 with telomeres. The first approach aimed to show where TelBP1 is localized and the second with which proteins TelBP1 is interacting. TbTRF is a published telomere-binding protein and served as telomere marker (Li et al., 2005).

First, to investigate if TelBP1 is a telomere-binding protein an immunofluorescence (IF) analysis with the TelBP1-specific mouse antibody was performed in BSF cells (Figure 25A). The DNA was stained with Hoechst.

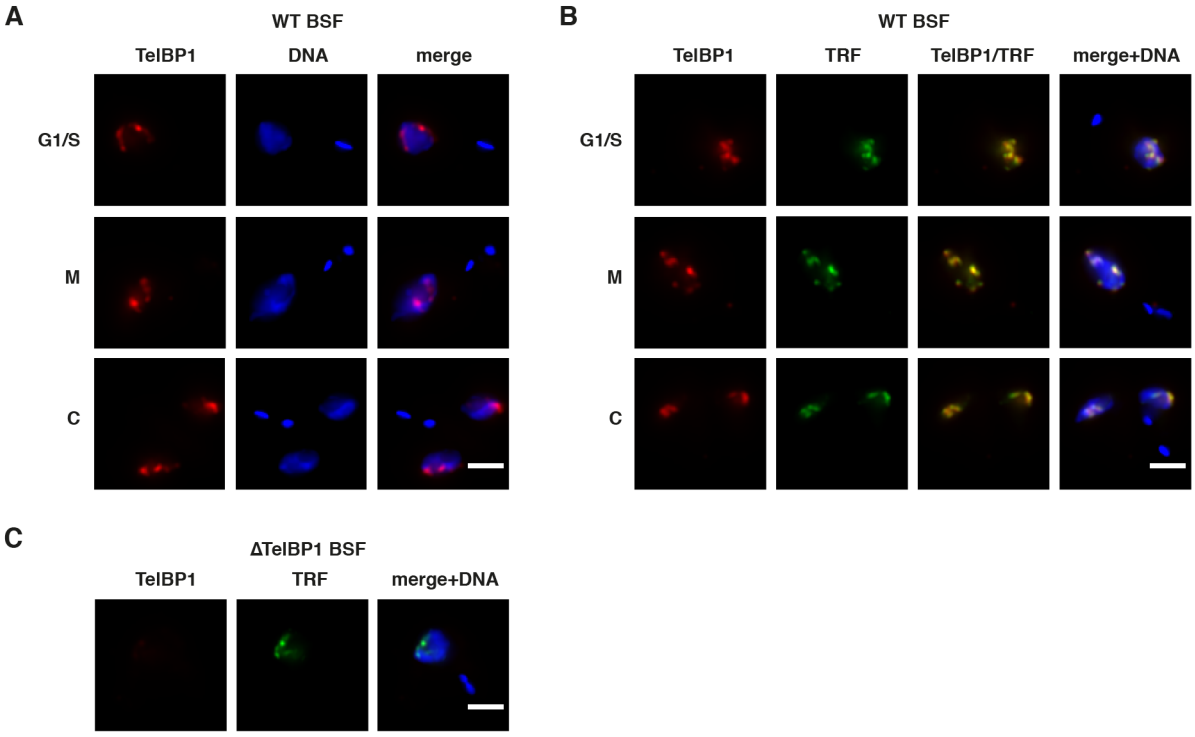

Figure 25. TelBP1 is a nuclear protein and co-localizes with TbTRF in BSF cells.
(**A**) Indirect immunofluorescence (IF) analysis of TelBP1 localization in BSF cells using monoclonal mouse antibody specific for TelBP1 (red). DNA was stained using Hoechst (blue). Different cell cycle stages were analyzed. (**B**) Indirect IF analysis of BSF cells using the TelBP1-specific mouse antibody and monoclonal rat antibody recognizing TbTRF (green). (**C**) Indirect IF of ΔTelBP1 BSF cells with TelBP1- and TbTRF-specific antibodies served as negative control and confirmed the specificity of the TelBP1 signal. Scale bar 2 µm. G1 (gap1 phase), S (synthesis phase), M (mitosis), C (cytokinesis).

The IF showed that TelBP1 is a nuclear protein, which is present through out the cell cycle of the parasite. In G1/S phase of the cell cycle, TelBP1 was mainly detected in the nuclear periphery. In cells undergoing mitosis (M), TelBP1 showed redistribution in a few clusters located in the center of the nucleus. In cells undergoing cytokinesis (C), TelBP1 localized at opposite poles of the dividing cell. Minichromosomes show a comparable redistribution throughout the cell cycle (Ersfeld and Gull, 1997, Ogbadoyi et al., 2000). They are abundant and a large proportion of the DNA consists of telomeric repeats (5-10%) (reviewed in Horn and Barry, 2005). Therefore, it is likely that TelBP1 associates with telomeres. In order to find out if the observed TelBP1 localization was restricted to telomeres a Co-IF using the TelBP1-specific mouse and the TbTRF-specific rat antibody was conducted in BSF cells (Figure 25B) while ΔTelBP1 BSF cells were taken as negative control (Figure 25C). The antibody staining of both proteins revealed identical distribution of TbTRF and TelBP1 throughout the cell cycle indicating that TelBP1 is a component of the telomere protein complex in trypanosomes. To validate TelBP1 as a telomere-binding protein and in order to learn more about the components of the telomere protein complex, the interactions of TelBP1 were analyzed. Interacting proteins, which are already described, can reflect the local distribution within the cell and the function of an uncharacterized protein. To this end, a Co-IP using the anti-TelBP1 mouse antibody and whole cell lysates from BSF parasites was conducted. To exclude unspecific binding to the TelBP1-specific antibody or the Protein G sepharose beads ΔTelBP1 BSF were chosen as a control. The experiment was performed in quadruplicates and the precipitated material of all replicates was

eluted and analyzed by label-free quantitative MS. The results of all replicates are presented in a volcano plot (Figure 26A). The x-axis of the volcano plot represents the log2-fold difference between the mean of peptide counts found in WT samples and the mean of peptide counts found in ΔTelBP1 samples. The y-axis shows how statistically significant the enrichment of the identified proteins is by showing the -log10(p-value). Seven protein groups were statistically significantly co-purified with TelBP1 including the already known telomere-binding proteins like TbTRF, TbTIF2, TbRAP1 and Tb927.6.4330 (Glover et al., 2016, Jehi et al., 2014b, Yang et al., 2009, Li et al., 2005). The whole data set is summarized in Table 18.

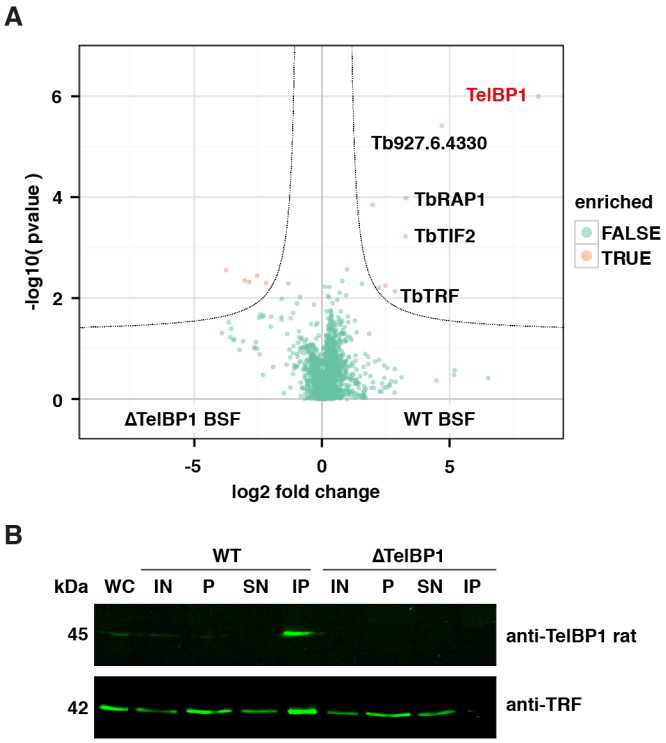

Figure 26. TelBP1 is part of the telomere complex in BSF trypanosomes.
(**A**) Volcano plot displaying the interaction partners of TelBP1. A Co-IP was carried out in four biological replicates of wild-type (WT) and ΔTelBP1 BSF cells using the TelBP1 monoclonal mouse antibody coupled to Protein G sepharose beads. Eluted proteins were analyzed by quantitative mass spectrometry. The x-axis represents the log2 fold change of detected proteins in the WT and ΔTelBP1 samples. The y-axis shows the p-value. Both axes together show which proteins were significantly co-purified with TelBP1. TelBP1 and known telomere proteins are displayed in the volcano plots. (**B**) Western blot analysis of TelBP1 Co-IP confirmed the association of TelBP1 with TbTRF. Two separate western blots were carried out. One western blot was incubated with anti-TelBP1 rat antibody and the other with anti-TbTRF rat antibody. 20-fold more of the pellet and IP sample was loaded compared to IN and SN samples. 13% of the TbTRF input was co-precipitated with TelBP1. WC (whole cell lysate), IN (input), P (pellet), SN (supernatant), IP (immunoprecipitate).

Table 18. Overview of TelBP1 co-purified proteins.

Gene ID	GeneDB Protein Description	Reference	TRF Co-IP (BSF)	Telomere (PCF)
Tb927.3.1560	TRF-Interacting Factor 2 (TIF2)	(Jehi et al., 2014b)	✔	✔
Tb927.6.4330	hypothetical protein, conserved	(Glover et al., 2016)	✔	✔
Tb927.9.4000; Tb927.9.3930	hypothetical protein, conserved		✔	✔
Tb927.10.2520	PrimPol-like protein 2 (PPL2)	(Rudd et al., 2013)		✔
Tb927.10.12850	ttaggg binding factor (TRF)	(Li et al., 2005)	✔	✔
Tb927.11.370	Repressor activator protein 1 (RAP1)			
Tb927.11.5550	DNA polymerase theta (POLQ)		✔	✔
Tb927.11.9870	hypothetical protein, conserved		✔	✔

Besides the MS analysis, the precipitates were examined by western blot using TelBP1-specific and TbTRF-specific antibodies (Figure 26B). During the Co-IP experiment, western blot samples were prepared after each step of purification. The input (IN) sample contained the soluble starting material, the pellet (P) sample the insoluble cell fraction after lysis, the supernatant (SN) sample the unbound protein fraction and the IP sample the protein fraction bound to TelBP1. Whole cell lysates served as control for western blot. 20-fold more of the pellet and IP sample was loaded compared to other samples. Western blot analysis of the IP samples with TelBP1-specific rat antibody showed that nearly all of the TelBP1 protein of the input sample was precipitated. Quantitative western blot analysis of the IP samples using the TbTRF-specific antibody revealed that 13% of TbTRF were co-purified with TelBP1 (Appendix Figure 39). The MS analysis and the western blot analysis of the Co-IP further supported the finding that TelBP1 is a component of the telomere complex in *T. brucei*. However, it is not clear if TelBP1 interacts directly or indirectly with TbTRF, TbTIF2, TbRAP1, Tb927.6.4330 and the other candidates found in the Co-IP.

Alternatively, it is possible that the found TelBP1 interactions are DNA-dependent. To rule this out, the TelBP1 Co-IP was combined with DNase I treatment. Prior to the Co-IP, DNase I activity was confirmed in the Co-IP buffer (Figure 27A). The Co-IP experiment was carried out in quadruplicates. Briefly, the Co-IP was performed as the previous one with minor modifications. After the lysate-antibody incubation, the unbound fraction was removed by centrifugation and the precipitated material was incubated with DNase I for 10 min at 37°C. Four replicates were prepared without DNase I treatment as a control. These control samples were also incubated at 37°C for 10 min. DNA-dependent interactions should dissociate from the precipitate after DNase I incubation. The DNase I-treated and untreated samples were then washed and the bound proteins eluted and analyzed by MS. MS analysis revealed that none of the found TelBP1 interactions had dissociated from the TelBP1 complex as none of the candidates was significantly enriched in the DNase I-untreated samples (Figure 27B).

Apart from that, the samples were analyzed by western blot using antibodies specific for TelBP1 and TbTRF (Figure 27C). Western blot analysis with the TelBP1-specific antibody confirmed that the 37°C incubation step had no effect on the TelBP1 antigen-antibody interaction. Western blot analysis using the TbTRF-specific antibody proved the TelBP1-TbTRF association after DNase I treatment. Taken all results together leads us to the conclusion that the TelBP1 interactions are likely DNA-independent.

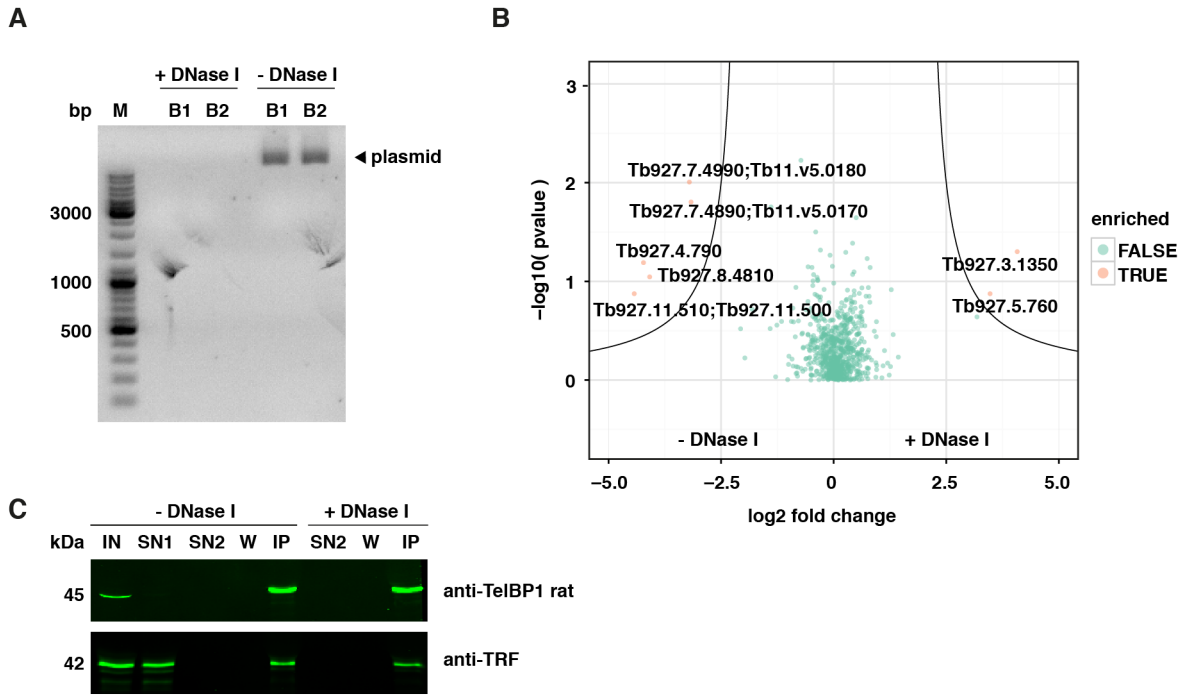

Figure 27. Analysis of DNA-dependence of TelBP1 interactions.
(**A**) Agarose gel showing DNase I activity in the used IP buffer. 1 µg of plasmid DNA was incubated with and without 1 unit DNase I in IP buffer 1 (B1; pH 7.5) or in IP buffer 2 (B2; pH 7.8) at 37°C for 10 min. 80 ng of plasmid DNA were then analyzed. (**B**) Volcano plot showing the result of TelBP1 Co-IP with and without DNase I treatment. None of the found TelBP1 interaction proteins has dissociated from the precipitated telomere complex after DNase I treatment. (**C**) Western blot analysis of TelBP1 Co-IP samples either treated or not treated with DNase I using the TbTRF-specific antibody suggests that the TelBP1-TbTRF interaction is DNA-independent. IN (input), P (pellet), SN (supernatant), W (Wash), IP (immunoprecipitate).

3.5 Recombinant TelBP1 does not interact directly with telomeric DNA

Although TelBP1 was identified by the telomeric pull-down assay it is not clear whether TelBP1 is a direct DNA-binding protein or not. To solve this question an electromobility shift assay (EMSA) was performed using recombinant HisMBP-TelBP1 protein. Recombinant HisMBP-TbTRF protein was taken as positive control. To establish the EMSA experiment different telomeric probes were tested (Figure 28A).

The pTH5 plasmid was digested with EcoRI to release a 162 bp fragment containing TTAGGG repeats. This double-stranded telomeric DNA was incubated with recombinant TbTRF. The interaction was confirmed by native PAGE, which showed a DNA shift (Figure 28A lane 1 and 2) after ethidium bromide (EtBr) staining. Nevertheless, the negative control using denatured recombinant TbTRF protein showed a DNA shift as well (lane 3). In contrast to the DNA shift observed in lane 1 and 2, the DNA signal was weaker. The incubation of recombinant TbTRF with double-stranded telomeric oligonucleotides revealed a DNA shift. Neither the incubation of denatured TbTRF protein with telomeric oligonucleotides nor the incubation of recombinant TbTRF with shuffled control oligonucleotides caused a DNA shift. Thus the telomeric and shuffled control oligonucleotides were used in the EMSA to examine the DNA-binding property of recombinant TelBP1 protein (Figure 28B). No DNA shift was observed after incubation of telomeric DNA with recombinant TelBP1 protein, while the positive control with TbTRF displayed a clear shift. The telomeric oligonucleotides were still detected at the bottom of the gel in samples containing recombinant TelBP1 protein. The bands

detected in the pockets are most probably large protein/DNA aggregates as these bands are missing in the samples containing denatured protein.

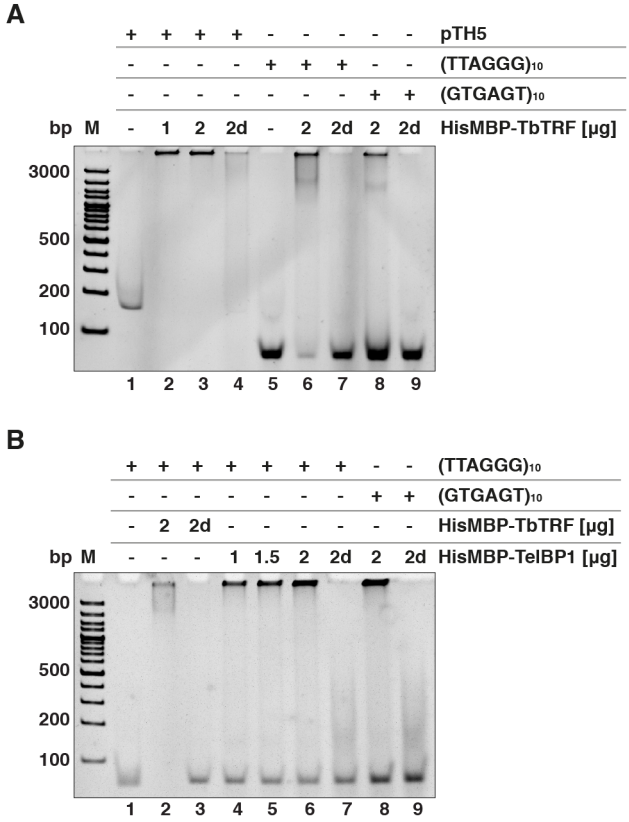

Figure 28. Recombinant HisMBP-TelBP1 protein does not directly bind to telomeric DNA.
(**A**) Electromobility shift assay (EMSA) with recombinant HisMBP-TbTRF. TbTRF was either incubated with 38 ng of the 162 bp fragment containing 27 TTAGGG repeats which was cut out from the pTH5 plasmid using EcoRI or with 50 ng of the double-stranded oligonucleotides containing TTAGGG (HR45/46) or GTGAGT repeats (HR47/48). Either 1 or 2 µg of recombinant protein or 2 µg of denatured (d) protein was used for DNA-protein interaction studies. After incubation of DNA with recombinant protein, the reaction was separated on a native polyacrylamide gel. To visualize the interaction the gel was stained with EtBr. A shift was observed using the native TbTRF protein with the pTH5 fragment (lane 2 and 3) and with TTAGGG repeat oligonucleotides (lane 6). (**B**) EMSA with recombinant HisMBP-TelBP1. Recombinant HisMBP-TbTRF served as positive control (lane 2). Different HisMBP-TelBP1 protein amounts were incubated with 50 ng of telomeric repeat oligonucleotides (lane 4-6). 2 µg of recombinant HisMBP-TelBP1 was incubated with shuffled oligonucleotides as a negative control (lane 8).

These data indicate that TelBP1 associates with telomeres rather through interaction with other telomere-binding proteins than through direct DNA-binding. However, we cannot exclude that TelBP1 might need accessory factors or post-translational modifications for a direct telomere interaction. In addition it is not clear if the selected conditions were appropriate for TelBP1-DNA interaction.

3.6 TelBP1 seems to be dispensable for telomere maintenance in BSF cells

The deletion of each single shelterin component in human cells leads to telomere shortening and affects cell viability. In trypanosomes, the known telomere-binding proteins are essential for proper telomere function and cell viability, too. Here, we have found a novel telomere-binding protein and want to study if this protein is required for telomere maintenance in trypanosomes as well. To monitor telomere length changes, WT and ΔTelBP1 BSF cells were cultivated for a period of 12 weeks while stabilates were prepared weekly. After 12 weeks all stabilates were thawed out and genomic DNA was isolated. The long cultivation period enables monitoring telomere length changes as the telomeres of trypanosomes are elongated by 6-12 bp with each replication (Pays et al., 1983a,

Bernards et al., 1983). To this end, the isolated genomic DNA was cut using frequently cutting restriction enzymes, which do not cut within the telomeric sequence. The restriction fragments were then analyzed by southern blot using a telomere-specific probe (Figure 29A).

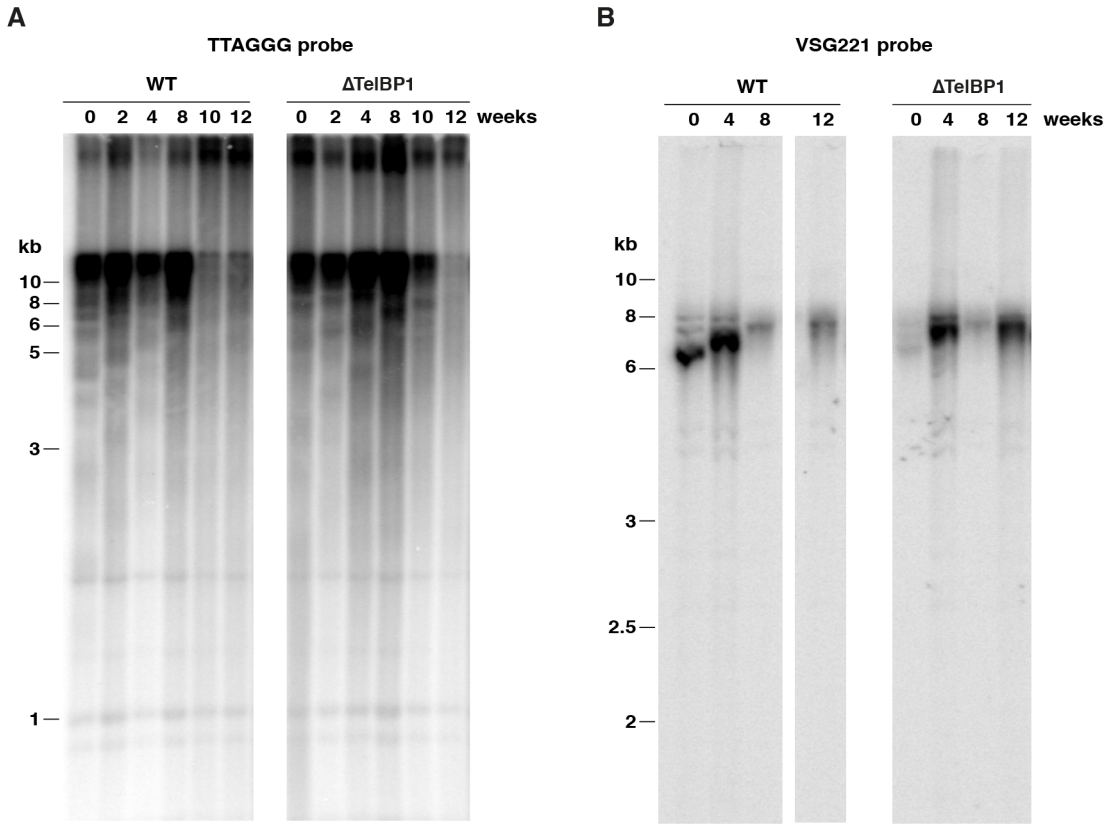

Figure 29. TelBP1 seems not to be involved in telomere length maintenance.
(**A**) Southern blot analysis of telomere restriction fragments of genomic DNA isolated from wild-type (WT) and ΔTelBP1 trypanosomes. Genomic DNA was digested with AluI, HinfI and RsaI and separated on a 0.7% agarose gel. Southern blot was hybridized with a radiolabeled (TTAGGG) probe. (**B**) Genomic DNA of WT and ΔTelBP1 cells was digested with EcoRI and hybridized with a radiolabeled VSG221 probe.

Although the telomere blot revealed that the majority of the genomic DNA was not digested telomere shortening could not be observed in ΔTelBP1 BSF cells. To analyze the telomere length of the active BES the genomic DNA was cut with EcoRI restriction enzyme and the southern blot carried out with a VSG221-specific probe (Figure 29B). In WT cells, an increase of telomere length is observed over the time course of 12 weeks. In ΔTelBP1 BSF cells, telomere shortening of the active BES was not observed. The time points 0 and 8 weeks show only a weak signal. However, the comparison of time point 4 and 12 weeks suggests the conclusion that TelBP1 deletion does not affect telomere maintenance mechanisms.

Interestingly, TelBP1 is not essential for cell viability compared to known telomere complex components. TbTRF, TbTIF2 and TbRAP1 are all essential for cell growth and indispensable for telomere integrity and stability in both life cycle stages of the parasite. Which role does TelBP1 play for the telomere complex in trypanosomes? Since TelBP1 does not seem to affect the telomere length and the function of the known telomere-binding proteins we speculate that the function of TelBP1 might be uncoupled from the function of TbTRF, TbTIF2 and TbRAP1.

3.7 Expression of TelBP1 is stage-specifically regulated

TelBP1 exhibits a differential protein expression pattern in comparative proteome studies (Butter et al., 2013, Urbaniak et al., 2012). In these studies, the protein expression profiles between BSF and PCF life cycle stages were compared and revealed a 1.68-fold (Butter et al., 2013) and 2.48-fold (Urbaniak et al., 2012) upregulation of TelBP1 in the BSF stage. To elucidate the function of TelBP1, we first wanted to verify the observed developmentally regulated expression pattern. To compare TelBP1 expression levels between BSF and PCF parasites, a quantitative western blot with whole cell lysates was performed (Figure 30A, B). TelBP1 expression was detected using the TelBP1-specific rat antibody. Quantification of the TelBP1 signal revealed a 4.39-fold upregulation (n=4, SD±1.15) in BSF parasites compared to PCF stages (Figure 30B).

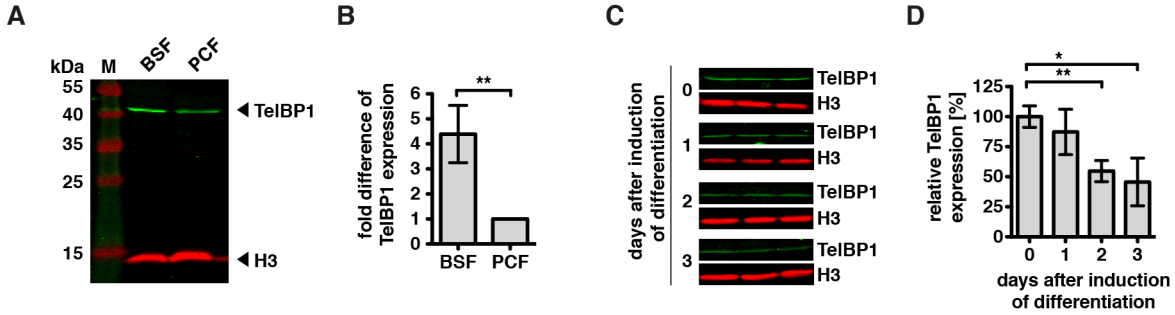

Figure 30. TelBP1 protein expression is stage-specifically regulated.
(**A**) Western blot analysis of TelBP1 expression in both life cycle stages of the parasite revealed a 4.39-fold upregulation in BSF cells. Histone H3 served as loading control. A representative blot of four independent experiments and (**B**) their quantification is shown. TelBP1 signal intensity was normalized to histone H3 protein. PCF expression level was set to 1. Error bars represent the standard deviation of 4 replicates. (**C**) Western blot analysis and (**D**) its quantification of TelBP1 expression during the developmental transition of BSF to PCF cells. The differentiation was conducted in three biological replicates. TelBP1 signal intensity was normalized to Histone H3 protein. Error bars represent the standard deviation of 3 replicates. Statistical significance was determined by an unpaired t-test * $p<0.05$, ** $p<0.01$.

Moreover, TelBP1 expression pattern was monitored during the developmental transition of BSF to PCF stage, as TelBP1 was not described in a recent differentiation proteome (Dejung et al., 2016). Differentiation of BSF cells was induced by replacing HMI-9 medium by DTM medium, adding 6 mM cis-aconitate and decreasing the cultivation temperature to 27°C. Differentiation was performed with three biological replicates of MITat1.2 SM cells. During the differentiation process cell lysates were prepared after different time points and analyzed by quantitative western blot (Figure 30C). The quantitative analysis of TelBP1 expression revealed that TelBP1 downregulation starts early during the developmental transition (Figure 30D). The protein amount is decreased about 50% already 48 h after differentiation induction.

3.8 Telomere protein complex composition is stage-specifically regulated

As TelBP1 expression is stage-specifically regulated we asked whether the telomere complex composition might be differentially regulated as well. To solve this question we searched for interaction partners of TelBP1 and TbTRF in PCF cells by Co-IP and quantitative MS (Figure 31) as previously performed with BSF parasites. For this aim, a procyclic cell line expressing a TbTRF-Ty1 fusion protein from the endogenous locus was prepared by Marie Schwebs. The second TbTRF allele was knocked out using a PCR-based method for allele deletion (Master thesis, Marie Schwebs, 2017).

Surprinsingly, no TelBP1-TbTRF interaction was observed by quantitative MS neither in the TelBP1 nor in the TbTRF Co-IP in PCF parasites

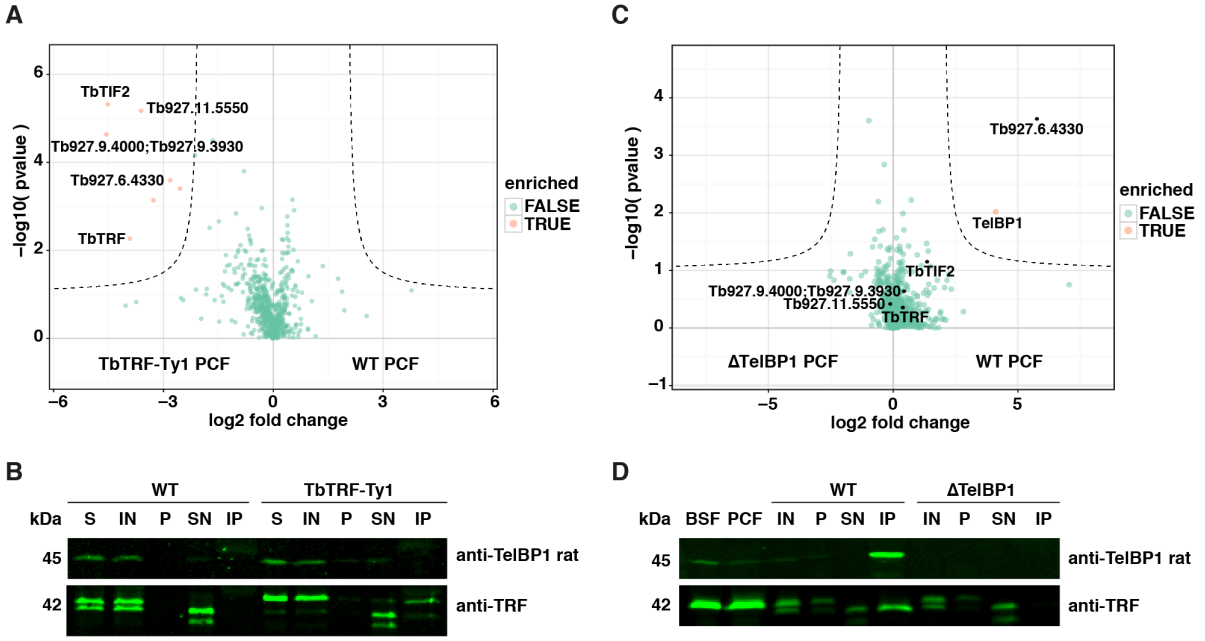

Figure 31. Identification of TbTRF and TelBP1 interacting proteins in procyclic cells using label-free quantitative interactomics.

Co-immunoprecipitations were carried out in four biological replicates and the eluted interacting proteins were analyzed by mass spectrometry. (**A**) Volcano plot showing TbTRF interacting candidates in PCF cells. Six proteins were significantly co-purified with TbTRF-Ty1 including four proteins known from TbTRF-Ty1 Co-IP in BSF cells: TbTIF2, Tb927.11.5550, Tb927.9.4000/3930, Tb927.6.4330. These proteins are displayed in the volcano plot. The whole data set is summarized in Table 19 (**B**) Western blot analysis of TbTRF-Ty1 Co-IP with anti-TelBP1 and anti-TbTRF antibodies. TbTRF was proteolytically degraded during the IP experiment as additional shorter bands appeared which were detected by the monoclonal TbTRF antibody. Nevertheless, Ty1 epitope-tagged TbTRF was precipitated. TbTRF-Ty1 runs higher in the SDS-gel than the wild-type TbTRF. Using the TelBP1-specific antibody for western blot revealed no TelBP1 in the eluate. 20-fold more of the IP sample was loaded compared to IN and SN samples. (**C**) Volcano plot presenting TelBP1 interacting proteins in PCF parasites. Only Tb927.6.4330 was significantly co-purified with TelBP1. (**D**) Western blot analysis of TelBP1 Co-IP with anti-TbTRF antibody detected interaction of TelBP1 with TbTRF in PCF stage. Again, TbTRF was proteolytically processed after cell lysis. A smaller TbTRF fragment was co-purified with TelBP1. BSF and PCF whole cell lysates served as control and showed only one TbTRF product. 20-fold more of the pellet and IP sample was loaded compared to IN and SN samples. 5% of TbTRF input was co-purified with TelBP1. S (starting material after lysis), IN (input), P (pellet), SN (supernatant), IP (immunoprecipitate).

The TbTRF MS-IP using TbTRF-/Ty1 PCF cells and the anti-Ty1 antibody revealed the known TbTRF interactions observed in the BSF stage (Figure 31A). Only TelBP1 was not co-purified. TelBP1 was not detected at all. Western blot analysis of the Co-IP samples with TelBP1- and TbTRF-specific antibodies confirmed the MS results (Figure 31B). The western blot using the TbTRF-specific antibody indicated proteolytic degradation of TbTRF upon cell lysis as two bands were detected.

While Tb927.6.4330 was significantly co-purified with TelBP1 in PCF cells, previously found TelBP1 interactions including TbTRF in the BSF stage showed a shift towards the zero point of the x-axis (Figure 31C). TbRAP1 was not found in the MS data at all. In contrast to the volcano plot, western blot analysis of the Co-IP samples using antibodies specific for TelBP1 and TbTRF revealed a co-purification of TbTRF with TelBP1 (Figure 31D). The band that was detected by the TbTRF-specific antibody runs slower in the SDS-PAGE compared to the detected protein in whole BSF and PCF cell lysates.

Nevertheless, the Co-IP data indicate that the protein-protein interactions within the telomere complex change in the PCF stage. The protein Tb927.6.4330 seems to be the strongest interaction partner of TelBP1 in the BSF and PCF life cycle stages. Although TelBP1 expression is

downregulated during differentiation to PCF stage, TelBP1 remains associated with telomeres in PCF cells as TelBP1 was found by the telomeric pull-down assay using PCF parasites (Figure 13A).

Table 19. Overview of TbTRF co-purified proteins in PCF cells.

Gene ID	GeneDB Protein Description	Reference
Tb927.3.1560	TRF-Interacting Factor 2 (TIF2)	(Jehi et al., 2014b)
Tb927.6.4330	hypothetical protein, conserved	(Glover et al., 2016)
Tb927.9.4000; Tb927.9.3930	hypothetical protein, conserved	
Tb927.9.15360	40 S ribosomal protein S6, putative	
Tb927.10.6030	Proteosome subunit alpha type-1, putative	
Tb927.10.12850	ttaggg binding factor (TRF)	(Li et al., 2005)
Tb927.11.5550	DNA polymerase theta (POLQ)	

3.9 TelBP1 regulates BES silencing kinetics during developmental differentiation of BSF to PCF cells

The function of TelBP1 seems to be uncoupled from the function of currently known components of the trypanosomal telomere complex. Nevertheless, we expected a contribution to VSG regulation as this has been reported for TbTRF, TbTIF2 and TbRAP1. Since TelBP1 is stage-specifically regulated we focused on the question if there might be a link between the developmentally regulated TelBP1 expression and the developmental silencing of the active VSG-BES.

Consequently, we studied BES silencing of WT and ΔTelBP1 BSF cells during the differentiation process to PCF parasites. The investigation of VSG protein expression provides indirect information about the transcriptional status of the active BES during the developmental transition. VSG expression during the differentiation process is influenced by multiple mechanisms such as mRNA (Berberof et al., 1995) and protein stability (Ziegelbauer et al., 1993, Gruszynski et al., 2006). In addition, BES promoter activity affects the VSG gene transcription directly (Landeira and Navarro, 2007).

To examine the BES transcriptional activity during early events of the differentiation process, WT and ΔTelBP1 BSF cells were differentiated in three biological replicates and whole cell lysates prepared after 0, 5, 24 and 48 h post differentiation induction. Then, a quantitative western blot using anti-VSG211 and anti-paraflagellar rod (PFR) antibodies was conducted to monitor VSG expression during the differentiation (Figure 32A, B). The quantitative analysis of the western blot revealed a faster VSG downregulation in ΔTelBP1 BSF cells compared to WT cells. The most significant difference of VSG expression between WT and ΔTelBP1 BSF cells was detected at the time points 5 h ($p<0.01$) and 24 h ($p<0.05$) after differentiation induction. At time point 24 h after induction of differentiation ΔTelBP1 BSF cells expressed 3-fold less VSG protein compared to WT cells. This outcome implies that TelBP1 influences VSG expression early during the differentiation process to PCF stage and that loss of TelBP1 appears to increase BES silencing kinetics. Notably, TelBP1 loss did not affect growth or cell viability during the differentiation event (Figure 32C).

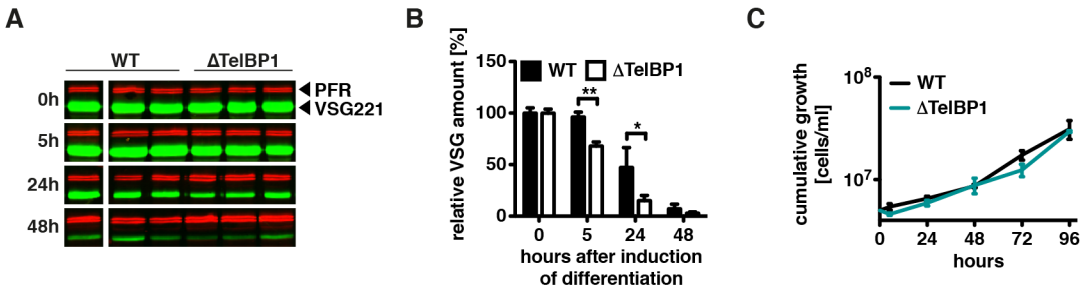

Figure 32. Silencing of VSG expression during differentiation from BSF to PCF stage is faster in ΔTelBP1 cells.
(**A**) Western blot and (**B**) its quantitative analysis of VSG221 expression in WT and ΔTelBP1 cells during differentiation. The experiment was conducted in triplicates. VSG221 signal intensity was normalized to paraflagellar rod (PFR) signal intensity. Statistical significance was determined by an unpaired t-test * $p<0.05$, ** $p<0.01$. (**C**) Cumulative growth of wild-type (WT) and ΔTelBP1 cells during the developmental transition. The growth curves represent the cumulative mean cell number ±SD of three replicates.

It has been described previously that the UTRs of a gene can impact protein expression levels during differentiation and in different life cycle stages of the parasite ((Berberof et al., 1995, Ziegelbauer et al., 1993, Gruszynski et al., 2006, Siegel et al., 2010, Clayton, 2013)). To distinguish if the faster VSG silencing in ΔTelBP1 cells is regulated on mRNA- or chromatin-based mechanisms a luciferase reporter assay was established. To this end, luciferase reporter genes were used flanked by UTRs that do not influence mRNA stability or translation during the differentiation process. The active BES of WT and ΔTelBP1 BSF cells was doubly marked using two different luciferase reporter genes. The Renilla luciferase (Rluc) reporter gene was inserted downstream of the RNA polymerase I promoter and the Firefly luciferase (Fluc) reporter gene upstream of the VSG221 gene (Figure 33A). The Rluc gene expression is regulated by tubulin UTRs and the Fluc gene expression by an actin 3'UTR and an aldolase 5'UTR, which do not influence mRNA stability or translation during differentiation (Garcia-Salcedo et al., 2004, Hug et al., 1993). To ensure that the reporter constructs integrate into the active BES, drug concentrations for selection after transfection were increased about 10-fold compared to standard culture conditions. As shown previously (Figueiredo et al., 2008), these extremely high drug concentrations prohibit survival of cells with reporter integration into inactive BESs because the transcriptional activity of these sites is very low compared to an active BES (Kassem et al., 2014). The usage of a dual BES luciferase reporter system enables us to monitor simultaneously BES silencing kinetics during differentiation at the BES promoter and at the telomere region. WT and ΔTelBP1 reporter cells were differentiated and the luciferase activity measured at different time points post induction (Figure 33B). Changes of Rluc and Fluc activity is presented as relative light unit (RLU) per 10^5 cells in %. The measurement at the time point 0 h was set to 100%. WT and ΔTelBP1 reporter cells start with comparable absolute values (Appendix Table 20) indicating that TelBP1 loss has no effect on the transcriptional activity of the active BES in BSF parasites. In the first 24 h post differentiation induction WT cells showed an increase in luciferase activity at both regions, downstream of the Pol I promoter and proximal to the telomere. The increase was stronger at the BES promoter. This peak has been already observed in previous studies and the source for this effect is still elusive. 48 h after differentiation induction the luciferase activity measured at both marked regions dropped. The decline of Fluc activity was more prominent than the Rluc activity indicating that BES silencing happened earlier at the telomere. The comparison of ΔTelBP1 and WT reporter cells revealed that the decrease of both luciferase activities started earlier in ΔTelBP1 reporter cells. The most significant difference ($p<0.001$) is seen at 24 h after differentiation induction (1.5-fold difference). Thus, our data indicate that BES silencing kinetic is faster in ΔTelBP1 cells compared to WT cells and point out the influence of TelBP1 on the BES transcriptional activity during early differentiation.

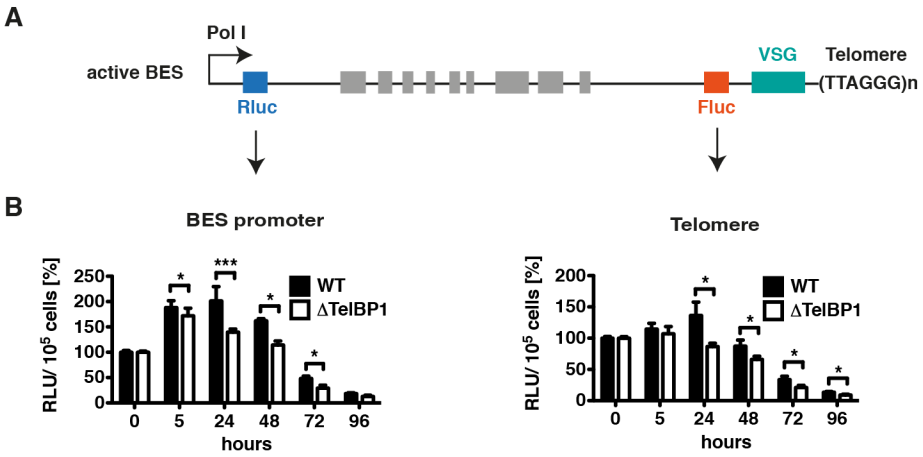

Figure 33. Dual luciferase reporter in the active expression site reveals faster silencing kinetics during differentiation in ΔTelBP1 cells.
(**A**) Illustration of the dual luciferase reporter. The active BES of wild-type (WT) and ΔTelBP1 cells was marked with a Renilla luciferase (Rluc) reporter gene downstream of the BES promoter and a Firefly luciferase (Fluc) gene upstream of the VSG221 gene. The graphic is not to scale. (**B**) Analysis of luciferase activity at the Pol I promoter of the BES and at the telomere region during the developmental transition of WT and ΔTelBP1 reporter cell lines. Differentiation of reporter cell lines (n=3) was induced and luciferase activity measured in a dual luciferase assay at the time points indicated. Luciferase activity is presented as relative light units (RLU) ± SD. Starting time point 0 h was set as 100%. Statistical significance was determined by an unpaired t-test * p<0.05, ** p<0.01, *** p<0.001.

To approve that the observed effect on the BES transcriptional activity during differentiation was TelBP1-specific, the protein was reintroduced into ΔTelBP1 reporter cells (Figure 34). To this end, ΔTelBP1 reporter cells were transfected with the pLew100v5b1d_TelBP1 construct to ectopically express TelBBP1 by tetracycline induction. This rescue cell line was named ΔTelBP1R. TelBP1 expression was confirmed by western blot using the TelBP1-specific rat antibody (Figure 34A). Full induction of ectopic TelBP1 expression resulted in a 2-fold higher protein level compared to WT cells. 24 h after induction of TelBP1 expression in ΔTelBP1R reporter cells, these cells were differentiated to PCF parasites and the luciferase activity was compared with non-induced ΔTelBP1R reporter cells (Appendix Table 21). This experiment was conducted with one clone in triplicates for +tet and -tet conditions. The analysis of the luciferase assay revealed higher values in induced ΔTelBP1R reporter cells at the promoter and the telomere region compared to the non-induced ΔTelBP1R cells (Figure 34C). To compare the luciferase activities of rescue cells with WT cells, WT values shown in Figure 33 were included in the graphs. Induced ΔTelBP1R reporter cells reached WT kinetics of developmental BES silencing indicating that only the TelBP1 loss was responsible for the transcriptional effects observed in ΔTelBP1 reporter cells during the developmental transition.

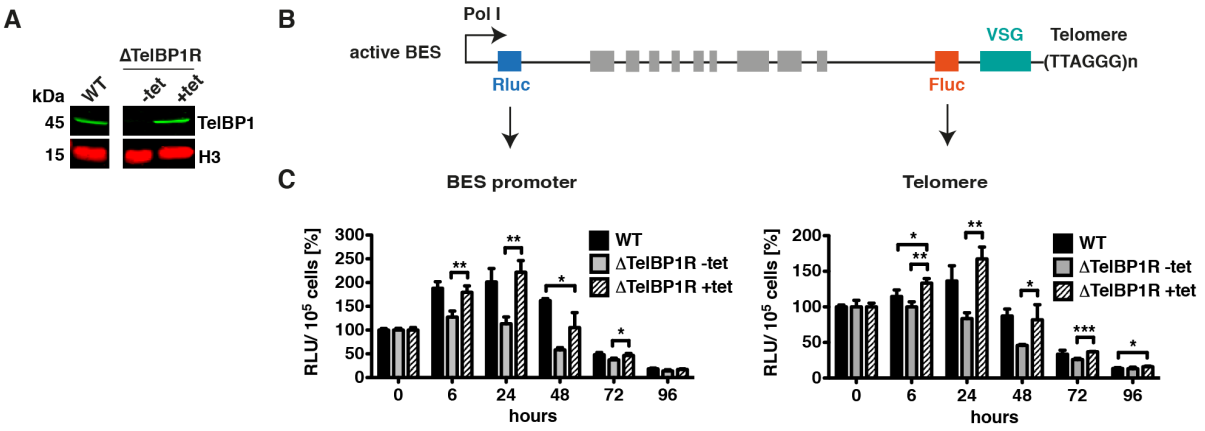

Figure 34. Reintroduction of TelBP1 in ΔTelBP1 reporter cell line slows down BES silencing kinetics during differentiation.

(**A**) Western blot analysis of TelBP1 expression in wild-type (WT), non-induced (-tet) and induced (+tet) ΔTelBP1 rescue (ΔTelBP1R) dual luciferase reporter cells. Ectopic TelBP1 expression leads to a 2-fold increase of TelBP1 protein amount compared to WT cells. (**B**) Scheme of the dual luciferase reporter. (**C**) Analysis of luciferase activity at the BES promoter and at the telomere during differentiation of ΔTelBP1R non-induced and induced reporter cells. One clone was analyzed in triplicates. WT values of the experiment shown in Figure 33 were included in the graphs. Ectopic expression of TelBP1 in ΔTelBP1 reporter cells leads to WT kinetics of BES silencing during developmental differentiation. Statistical significance was determined by an unpaired t-test * $p<0.05$, ** $p<0.01$, *** $p<0.001$.

Parallel to the luciferase assay, cell lysates from induced and non-induced ΔTelBP1R reporter cells were prepared to analyze VSG221 protein expression during differentiation (Figure 35A, B). The quantitative western blot (Figure 35B) revealed no significant difference between induced and non-induced ΔTelBP1R cells. Considering the observed complementation effect in luciferase reporter cells we also expected to get a slower downregulation of VSG221 protein amount upon induction of TelBP1 expression compared to non-induced cells. Therefore, we expected a higher VSG protein amount in induced TelBP1R cells compared to non-induced TelBP1R cells. But at time point 24 h post induction, the VSG amount of non-induced cells was comparable with that of WT and induced cells. However, western blot analysis of non-induced ΔTelBP1R cells showed already a weak signal detected with the TelBP1-specific antibody (Figure 35C).

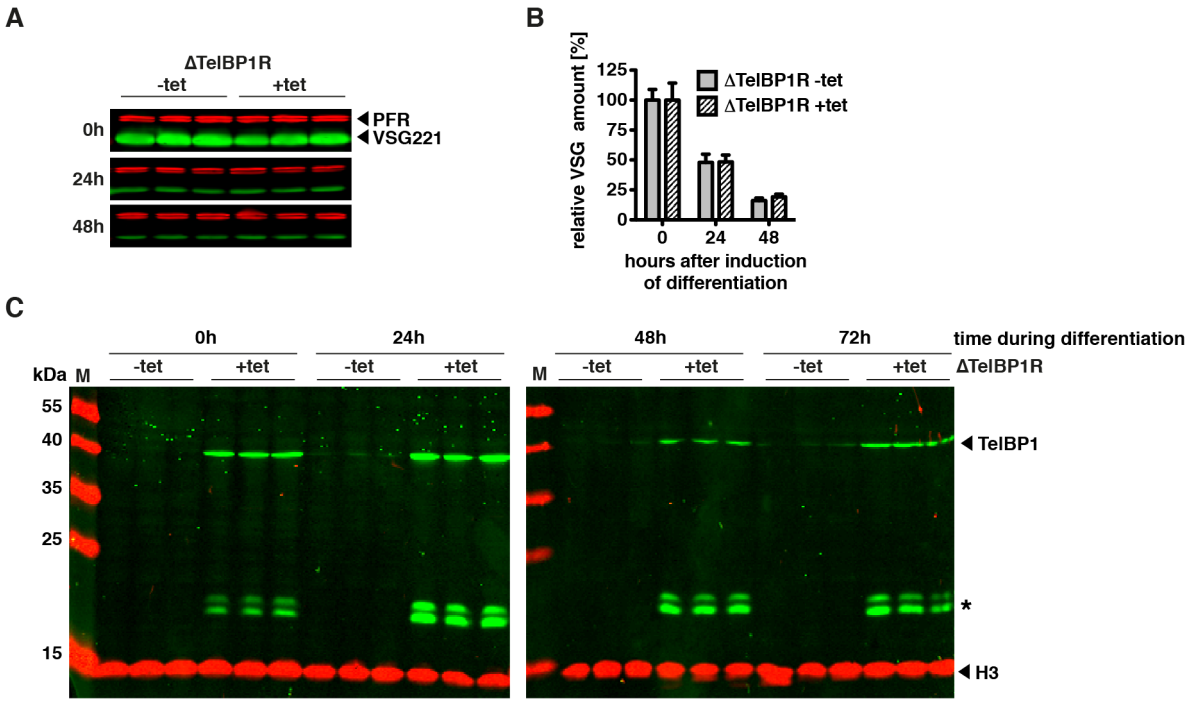

Figure 35. VSG silencing in ΔTelBP1R reporter cell line during differentiation.
(**A**) Western blot and (**B**) its quantitative analysis of VSG221 expression in induced and non-induced ΔTelBP1R reporter cells. The VSG signal intensity was normalized to paraflagellar rod (PFR) signal intensity. (**C**) Western blot analysis of TelBP1 expression in induced and non-induced ΔTelBP1R reporter cells confirms the reintroduction and presence of TelBP1 during differentiation. Two additional bands (asterisk) are detectable after ectopic TelBP1 expression. Histone H3 protein served as loading control.

In summary, by using the dual luciferase reporter system we have shown that TelBP1 reintroduction slows down BES silencing kinetics during differentiation to WT levels. This indicates that the observed silencing phenotype is TelBP1-specific.

Our data strongly indicate that the stage-specifically regulated protein TelBP1 is a regulator of BES silencing during early differentiation events in *T. brucei*. To our knowledge, this is the first evidence that telomere-binding proteins influence transcriptional activity of the BES during developmental differentiation of African trypanosomes. Furthermore, TelBP1 illustrates that developmental silencing is a fine-tuned process, which involves stage-specific changes in telomere complex composition.

4 DISCUSSION

The telomeric chromatin architecture is crucial for the transcriptional control of VSG genes in *T. brucei*. Compared to mammals and yeast, where telomeres are extensively studied, less is known about the structural components of the telomeres in trypanosomes. Previous research revealed three functional homologs of the mammalian shelterin members in trypanosomes (TbTRF, TbTIF2 and TbRAP1), and elucidated the importance of telomere biology for antigenic variation (Li et al., 2005, Yang et al., 2009, Pandya et al., 2013, Jehi et al., 2014a, Jehi et al., 2014b, Jehi et al., 2016, Nanavaty et al., 2017). However, how exactly these proteins impact the transcription of VSG genes remains elusive. Moreover, less is known about telomeres and their contribution to developmental differentiation of BSF to PCF parasites. In order to gain insights into the telomere-mediated regulation of antigenic variation and developmental silencing it was therefore important to determine the complete composition of the telomere protein complexes. So far, no systematic approach has been performed in trypanosomes to identify all telomere complex components.
To this end, we conducted a systematic search for novel telomere-binding proteins in *T. brucei* using label-free quantitative proteomics and discovered 17 new potential telomere-associated factors including already known telomere-binding proteins such as TbTRF and TbTIF2. For detailed characterization the protein Tb927.10.9870 was selected and named TelBP1. All in all, the characterization of TelBP1 uncovered two novel aspects of telomere biology of trypanosomes. Firstly, the telomere complex composition is dynamic and changes during the developmental transition of trypanosomes from the BSF to the PCF stage. Secondly, telomere-binding proteins control the dynamic of developmental BES repression.

4.1 Biochemical approach to identify novel telomere-binding proteins in *T. brucei*

A pull-down assay with telomeric DNA as bait was carried out, from which 17 telomeric interaction partners were found including the known direct and indirect telomeric DNA binders TbTRF (Li et al., 2005) and TbTIF2 (Jehi et al., 2014b), respectively. The recently identified telomere-associated protein Tb927.6.4330 was also found using this biochemical approach (Glover et al., 2016). The identification of previously reported telomere-binding proteins validates that our screening method is suitable for the discovery of novel telomere DNA-binding proteins and their interaction partners. Although TbRAP1 interacts with TbTRF (Yang et al., 2009), it was not found by our approach. Like TbTIF2, TbRAP1 does not bind telomeric DNA directly. It associates with telomeres solely through its weak interaction with TbTRF, which has been shown by Co-IP and Chromatin Immunoprecipitaiton (ChIP) experiments carried out by Yang and colleagues (Yang et al., 2009). In the Co-IP experiment only 3%-14% of endogenously FLAG-HA-HA-tagged TbRAP1 were co-purified with TbTRF. In the ChIP experiment, using an antibody specific for TbRAP1 and formaldehyde cross-linked material, Yang and colleagues observed an association of TbRAP1 with telomeric DNA. Whereas, samples in which proteins were not cross-linked to DNA showed no significant enrichment of telomeric DNA with TbRAP1. The weak interaction between TbRAP1 and TbTRF might be the reason why tbRAP1 was not detected using our method. Alternatively, another approach to find DNA-interacting proteins, such as proteomics of isolated chromatin segments (PICh) could be used to support and to increase the current dataset of potential telomere-binding proteins. In mammals for instance, a telomere proteome of around 200 proteins has been discovered using this method (Dejardin and Kingston, 2009).

The telomeric role of the found potential telomere binders is unclear. Therefore, detailed work on these candidates is necessary. To additionally validate some of the identified candidates a TbTRF Co-IP with BSF cells was carried out and resulted in the co-purification of five proteins with TbTRF. All these five proteins were also discovered by the telomeric pull-down assay indicating that these five candidates are bona fide telomere-binding proteins.

4.2 Distinct telomere-binding protein complexes are present in *T. brucei*

In 1995, the first attempt to identify telomere-binding proteins in *T. brucei* was reported by Eid and Sollner-Webb (Eid and Sollner-Webb, 1995). In that study two distinct telomere complexes were isolated from BSF and PCF cell extracts with telomeric DNA, and three complexes with subtelomeric DNA. However, their composition remained unsolved. They only found out that a 39-kDa protein, ST-1, had a selective affinity for the C-rich strands of both the 29-bp subtelomeric repeats and the telomeric repeats. Furthermore, they demonstrated that ST-1 was binding as a dimeric complex. Two years later, Eid and Sollner-Webb identified a second telomere-binding protein complex, the ST-2 complex, which exhibited complementary binding characteristics to those of ST-1 (Eid and Sollner-Webb, 1997). They reported that the ST-2 complex was composed of five polypeptides ranging between 35 and 55 kDa in their molecular mass. Moreover, Cano and colleagues identified three protein complexes (complexes C1-C3) associated with single-stranded telomeric DNA (Cano et al., 2002). However, the components of these complexes remained also unknown. Consistent with these studies (Eid and Sollner-Webb, 1995, Eid and Sollner-Webb, 1997, Cano et al., 2002), our Co-IP results suggest that different telomere protein complexes might be present at telomeres in trypanosomes.

The PrimPol-like protein 2 (PPL2) (Rudd et al., 2013), was identified in the TelBP1 Co-IP, but not in the TbTRF Co-IP, which might indicate that a separate TelBP1-PPL2 complex exists in BSF cells. Tb927.6.4330 might also be member of this complex as the TelBP1 Co-IP in the PCF cells suggests direct interaction of TelBP1 and Tb927.6.4330. The second and main complex might contain TbTRF, TbRAP1, TbTIF2, Tb927.11.5550, Tb927.6.4330, Tb927.9.4000/3930 and TelBP1 as all these candidates were discovered in the TbTRF and TelBP1 BSF Co-IPs. However, we cannot exclude that sub-complexes of these proteins are present. To this aim, detailed analyses and reciprocal Co-IPs with different candidates are necessary. Further hints that distinguishable telomere protein complexes are present in trypanosomes are provided by comparison of TbTRF and TelBP1 Co-IPs in PCF cells. These data show that a TbTRF complex and a TelBP1 complex exist. In PCF cells, TelBP1 interacts only with Tb927.6.4330 and is absent in the TbTRF complex as demonstrated by the TbTRF Co-IP data. Furthermore, considering these results, we assume that Tb927.9.4000/3930, which are nearly identical in their amino acid sequence and encode 38-kDa proteins, are ST-1. Both proteins were purified in the telomeric pull-down as well as in the BSF Co-IPs with TbTRF and TelBP1 and in the PCF Co-IP with TbTRF.

Two studies have also demonstrated that sub-complexes of shelterin are present at mammalian telomeres (Liu et al., 2004, Kim et al., 2008). Three TIN2 sub-complexes were found at mammalian telomeres. However, the function of these sub-complexes is still elusive. In addition, a trimeric CST complex containing CTC1, STN1 and TEN1 associates with single-stranded telomeric DNA (reviewed in Rice and Skordalakes, 2016). Orthologs of the CST complex members have also been characterized in *S. cerevisiae* and *S. pombe* (reviewed in Kupiec, 2014, Martin et al., 2007). Complexes equivalent to the mammalian or yeast CST complex have not yet been discovered in *T. brucei*. However, it is reasonable that the proteins of the complexes C1-C3 resemble a CST-like complex in trypanosomes as these complexes were found at single-stranded telomeric DNA (Cano et

al., 2002). The telomeric architecture is highly dynamic, as a variety of different cell biological events have to be coordinated at telomeres during the cell cycle. These events include recruitment and regulation of telomerase activity, replication of highly repetitive telomeric DNA and protection against unwanted DNA repair, recombination and degradation. Thus, it is not surprising that different telomere complexes bind telomere DNA in mammals and yeast to facilitate these numerous tasks. Our data indicate that different telomere protein complexes might also bind telomeres in trypanosomes. This would make sense, as a trypanosomal cell has to deal with comparable tasks during the cell cycle. The question of how many sub-complexes of the identified candidates TbTRF, TbRAP1, TbTIF2, Tb927.11.5550, Tb927.9.4000/3930, Tb927.6.4330 and TelBP1 exist at trypanosome telomeres should be in the focus of future research.

4.3 Stage-specific regulation of telomere protein complexes in trypanosomes

Strikingly, the study of TelBP1 revealed that the telomere protein complex composition is developmentally regulated. The characterization of TelBP1 is to our knowledge the first evidence for dynamic changes of telomere complexes during the developmental transition of BSF to PCF parasites. Quantification of TelBP1 expression showed that TelBP1 is 4.39-fold upregulated in the BSF stage and that it is downregulated during the differentiation process to the PCF stage. Thereby, the stage-specific expression of TelBP1 relies on differential protein stability as RNA sequencing data and ribosome profiling revealed no developmentally regulated TelBP1 transcript abundance or translation efficiency, respectively (Siegel et al., 2010, Vasquez et al., 2014). The analyses of the interaction partners of TelBP1 and TbTRF in both life cycle stages of the parasite leads us not only to the conclusion that distinguishable telomere complexes might bind to telomeres but also that the composition of the telomere complexes may differ between the BSF and the PCF stage of the parasite. While TelBP1 is part of the TbTRF complex in BSF cells, it seems to interact only with Tb927.6.4330 and is missing in the TbTRF complex in PCF cells. Therefore, it is possible that TelBP1 dissociates from the main telomere complex containing TbTRF and is degraded during differentiation to PCF. It is also conceivable that TelBP1 assembles its own complex already in BSF cells, which stays at telomeres upon differentiation to PCF stage. However, it remains unclear how the TelBP1 complex is combined in the BSF stage. It is conceivable that a complex composed of TelBP1, PPL2, Tb927.6.4330, and maybe other not yet identified proteins is present. In the PCF stage PPL2 was not co-purified with TelBP1. Therefore, it would be interesting to carry out a reciprocal Co-IP with PPL2 in PCF cells to find further telomere complex changes accompanying developmental differentiation. Furthermore, a telomeric pull-down assay with BSF cell extracts would provide an additional comparison of the telomeric architecture between BSF and PCF cells. Expression levels of TbTRF and TbRAP1 only change slightly during developmental differentiation compared to TelBP1. According to a recently published comparative proteome (Butter et al., 2013), TbRAP1 is 1.26-fold upregulated in the PCF stage and TbTRF displays a 1.23-fold upregulation in BSF parasites. No information is available for TbTIF2 expression levels in this report while the study conducted by Urbaniak and colleagues revealed a 1.21-fold upregulation of TbTIF2 in BSF cells (Urbaniak et al., 2012). To our knowledge TelBP1 is the first telomere-associated protein, which is highly stage-specifically regulated in trypanosomes.

What is the reason for different telomere complexes in the BSF and PCF cells? It has been reported already that chromatin structure and nuclear architecture differ between BSF and PCF cells, indicating that chromatin restructuring occurs during developmental transition (Schlimme et al., 1993, Burri et al., 1994, Rout and Field, 2001). Chromatin restructuring can be regulated by histone modifications and the arrangement of nucleosomes (reviewed in Figueiredo et al., 2009). In *T. brucei*

for instance, it has been shown that the histone H3 trimethylase DOT1B is essential for the developmental chromatin restructuring (Dejung et al., 2016). Thus, the changed chromatin structure might offer altered binding sites for telomere-binding proteins. It is also possible that telomere-binding proteins itself are involved in the restructuring process during differentiation. Therefore, different telomere complexes might be necessary in BSF and PCF parasites. Various studies support the idea of developmentally regulated telomere structure in trypanosomes (reviewed in Alsford et al., 2012). First, telomeric DNA modifications are different between BSF and PCF cells. A modified nucleotide β-D-glucosyl-hydroxymethyluracil (base J) replaces a part of the thymidines in the telomeric DNA of BSF cells but not of PCF cells (Gommers-Ampt et al., 1993, van Leeuwen et al., 1996, van Leeuwen et al., 1997). Jehi and colleagues have demonstrated that TbTRF binding to telomeric DNA is not affected by base J (Jehi et al., 2014a). However, it is still unknown whether base J influences the binding affinity of other telomere-binding proteins. Second, telomeric silencing of reporter constructs displays differences between BSF and PCF parasites. In BSF cells the transcription from three different promoters inserted in an inactive BES nearby telomeres was silenced (Horn and Cross, 1995). In contrast, in PCF cells only the BES promoter remained repressed indicating a developmentally regulated silencing effect of telomeres. Finally, the chromatin accessibility of inactive BESs in BSF cells alters upon the differentiation to PCF parasites (Navarro et al., 1999). In PCF parasites, the chromatin of inactive BES becomes inaccessible suggesting tighter packaging of chromatin in this stage. Thus, chromatin remodeling is developmentally regulated as well. The current hypothesis is that these differences are facilitated by distinct composition or regulation of telomeric complexes in BSF and PCF parasites.

4.4 TelBP1 is a novel telomere-binding protein and might function independently from TbTRF, TbTIF2 and TbRAP1

In this study, I focused on the characterization of TelBP1 as this protein was discovered in the telomeric pull-down assay as well as in the BSF TbTRF Co-IP. In addition, TelBP1 was described in the comparative proteome study as a developmentally regulated protein (Butter et al., 2013, Urbaniak et al., 2012). Therefore, TelBP1 was an interesting candidate to analyze.

I demonstrated that TelBP1 is a novel telomere-binding protein based on its localization within the nucleus and its interaction partners. Furthermore, EMSA studies using the recombinant TelBP1 protein indicated that TelBP1 localizes to telomeres through protein-protein interactions rather than through direct telomere DNA-binding. In mammals a shelterin member fulfills the following criteria: firstly, it is abundant at telomeres and does not accumulate elsewhere; secondly, it binds telomeres either directly or indirectly throughout the cell cycle; and thirdly, its function is restricted to telomeres (reviewed in de Lange, 2005). So far, TelBP1 meets these three criteria suggesting that TelBP1 is a component of the trypanosome telomere complex. However, the full function of TelBP1 remains elusive.

Interestingly, functional analyses revealed that TelBP1 is not essential for cell viability in BSF and PCF parasites. This might be an indication that the function of TelBP1 is uncoupled from the function of the known telomere-binding proteins TbTRF, TbTIF2 and TbRAP1, which are all indispensable for cell viability (Li et al., 2005, Yang et al., 2009, Jehi et al., 2014b). The observation of a TbTRF-independent TelBP1 complex in PCF cells supports this hypothesis. Furthermore, I used quantitative mass spectrometry to analyze changes of VSG expression pattern in TelBP1 null-mutant cells. Thereby, neither derepression of silent VSG genes nor enhanced VSG switching rates was observed (data not shown). TbRAP1 RNAi cells served as a control, which shows derepression of ES-linked silent VSG genes (Yang et al., 2009). The studies carried out by Cestari and Stuart, demonstrate

clearly the consequences of affecting TbRAP1 and TbTRF interactions and functions (Cestari and Stuart, 2015). They observed derepression of silent BESs upon knockdown of the TbRAP1- and TbTRF-associated protein, TbPIP5-Pase. This observed derepression phenotype was similar to the reported phenotype upon TbRAP1 downregulation. In contrast, TelBP1 loss does not result in this phenotype. This additionally supports the hypothesis that the function of TelBP1 might be separated from the function of the known telomere-binding proteins.

4.5 TelBP1 is processed into smaller isoforms

Interestingly, TelBP1 overexpression drew our attention to smaller TelBP1 fragments. These smaller TelBP1 products are also present in wild-type cells, but at low abundance. Our data showed that these fragments are indeed TelBP1-specific and comprise the C-terminus of TelBP1. The exact source of these fragments remained unknown. However, our data indicate that alternative *trans*-splicing events and specific protease cleavage might be involved in TelBP1 isoform expression. However, no specific protease involved or a cleavage site could be predicted. TelBP1 overexpression suggests that the information for TelBP1 isoform production must be in the TelBP1 ORF and/or amino acid sequence, as for overexpression other UTRs than the endogenous ones were used.

Alternative ATG usage downstream of the SAS can shorten the sequence of a gene. Thereby, a signal peptide may be excluded leading to altered cellular targeting of the translated protein (reviewed in Siegel et al., 2011). IF analysis of TelBP1 isoform overexpressing cells showed no changed cellular targeting (Master thesis, Susanne Bury, 2014). Indeed, TelBP1 isoforms were detected in the nucleus. This is in concordance with the predicted NLS, which resides in the C-terminus of TelBP1. To investigate if TelBP1 and the isoforms display distinct localization within the nucleus it is essential to selectively tag the isoforms at their N-terminal end as the monoclonal TelBP1-specific antibody recognizes both. To this end, it is necessary to know the N-terminal amino acid sequence of the isoforms. For this purpose, Edman degradation could be used. It is a method of sequencing amino acids in a peptide (Pham et al., 2003).

Interestingly, splice variants of mammalian shelterin components have been described as well. For instance, a study performed by Kaminker and colleagues described a second TIN2 isoform (termed TIN2L for long), which contains additional 97 amino acids (Kaminker et al., 2009). The authors showed that the previously described TIN2 (now termed TIN2S for short) and the TIN2L isoform result from alternative *cis*-splicing. The shorter TIN2S isoform derives by retention of a small intron, which introduces a stop codon. Both isoforms are expressed at similar levels as shown by western blotting and interact with TRF1, TRF2 and TPP1. Furthermore, TIN2S and TIN2L display distinct distribution within the nucleus. Thereby, TIN2L strongly associates with the nuclear matrix indicating a role in the organization and attachment of telomeres to the nuclear periphery. Splice variants for the human POT1 have also been reported. There are five POT1 splice variants, which show different DNA-binding properties (Baumann et al., 2002). Based on this differential interaction with telomeric DNA the authors speculated that the POT1 variants might have distinct functions *in vivo*. Alternate transcripts generated from the TRF1 gene were identified, too (Lages et al., 2004). In this case, alternative splicing gives rise to the proteins TRF1 and Pin2, which show no functional differences (Shen et al., 1997, Young et al., 1997). Furthermore, two additional splice variants were found lacking the N-terminal part of TRF1 and Pin2, referred to as t-TRF1 and t-Pin2, resulting in loss of the N-terminal interaction partners (Lages et al., 2004). The mRNA levels for t-TRF1 and t-Pin2 were about $1/10^{th}$ to $1/100^{th}$ compared to those for TRF1 and Pin2, depending on the cell type.

Alternative *cis*-splicing has also been observed for the human TERT gene, which encodes the telomerase catalytic subunit (Kilian et al., 1997). Strikingly, distinct splicing patterns were observed in various tumors, cell lines and even normal tissues. Thereby, alternative splicing contributes to telomerase activity regulation by producing inactive or dominant-negative forms of TERT (Yi et al., 2000).

To sum up, alternative splicing gives rise to proteins with different biochemical properties and functions. Thus, differential isoforms might enable forming discrete complexes to execute the functional variety of shelterin at telomeres.

The future prospective will be to discover how TelBP1 isoforms are produced exactly and to which extent alternative splicing plays a role. This could be analyzed for example by real-time PCR and Northern blot in order to rule out how many TelBP1 transcript variants are present and which of them are upregulated upon TelBP1 overexpression. In addition, it remains to be elucidated whether the observed TelBP1 isoforms are functional and if their function differs from the full-length TelBP1. Furthermore, it would be interesting to analyze if full-length TelBP1 and the isoforms form differential protein complexes and thus influence distinct processes at chromosome ends or elsewhere. However, in order to characterize the isoforms it is first essential to know the complete amino acid sequence of the isoforms and the complete function of TelBP1 full-length protein.

4.6 TelBP1 fine tunes developmental silencing of the active BES

During developmental transition, many biological processes such as energy metabolism, morphology, motility, and surface proteins have to adapt to changing conditions in order to ensure parasite survival in different environments (reviewed in Matthews, 2005, Fenn and Matthews, 2007). Such a differentiation process requires a tightly coordinated gene expression during life cycle progression of the parasite. It is conceivable that telomere-binding proteins contribute to the developmentally regulated expression of VSG genes.

Here, I provide the first direct evidence for a telomere-binding protein playing a role in the regulation of developmental silencing of the VSG BES. Telomere-binding proteins have been shown to be involved in monoallelic expression and switching of VSG genes (Yang et al., 2009, Jehi et al., 2016). None information is available about their role during the differentiation process. The study of TbTRF, TbTIF2 and TbRAP1 during the differentiation is difficult due to the necessity of these proteins for cell viability. In contrast, TelBP1 is not essential and thus, provides an advantage to investigate its role in developmental silencing of VSG BES.

To this end, I compared BES silencing kinetics between wild-type and TelBP1 null-mutant cells during the differentiation event. Loss of TelBP1 led to faster BES silencing during the differentiation to PCF parasites compared to wild-type cells suggesting that TelBP1 is involved in the regulation of BES silencing kinetics during the early differentiation.

TelBP1 reintroduction experiments confirmed that this phenotype was TelBP1-specific. The effect of reintroducing TelBP1 back into ΔTelBP1 reporter cells was analyzed by luciferase assays and quantitative western blot using the VSG221-specific antibody. Comparing both datasets revealed a discrepancy. While the luciferase assay showed a complementation effect upon TelBP1 reintroduction, the quantitative western blot revealed no significant difference between induced and non-induced ΔTelBP1R cells. Considering the observed rescue effect in ΔTelBP1R luciferase reporter cells we also expected to get higher VSG amounts upon induction of TelBP1 expression. But at time point 24 h after induction of differentiation, the VSG amount of non-induced cells is comparable with that of wild-type and induced cells. In addition, western blot analysis of non-induced ΔTelBP1R cells showed a weak band detectable with the TelBP1-specific antibody

suggesting that our inducible TelBP1 expression system is leaky. The observed discrepancy between both approaches to analyze BES silencing might rely on the different dynamic ranges of the used methods. A luciferase assay is more sensitive and exhibits a substantially broader dynamic range, which enables detecting small differences.

The current hypothesis is that TelBP1 transiently maintains an open chromatin status early during the differentiation event to coordinate transcriptional silencing of the BES with other cellular processes or environmental cues. However, mechanistic information about the observed phenotype upon TelBP1 loss during differentiation is missing. The used luciferase reporters indicate that the transcription of the active BES is influenced. The transcriptional activity of the BES could be regulated on the promoter level or the chromatin structure level. Comparison of transcript levels and FAIRE (Formaldehyde-assisted isolation of regulatory elements) enrichment of the active VSG gene would provide information about the type of silencing mechanism. Transcript levels would reflect the promoter activity and FAIRE the status of chromatin conformation. FAIRE is a technique, which allows the purification and quantification of nucleosome-depleted DNA regions (Figueiredo and Cross, 2010). Thus, FAIRE enrichment indicates an open chromatin conformation. Using these techniques Aresta-Branco and colleagues showed that during differentiation, the decrease in mRNA levels of the active BES occurs earlier and it is more pronounced than changes in chromatin conformation (Aresta-Branco et al., 2016). Although transcription was halted the chromatin still adopted an open conformation, indicating that chromatin does not close immediately after transcription is stopped. After this intermediate state, chromatin condensation takes place, which relies on epigenetic regulation.

Several studies in yeast and mammals suggest that telomere-binding proteins influence the epigenetic status of telomeric DNA (reviewed in de Lange, 2005, Blasco, 2007, Fojtova and Fajkus, 2014). It has been reported that the length of telomeres can modulate heterochromatin formation and the telomeric silencing (reviewed in Blasco, 2007). However, the observed effect of TelBP1 on BES silencing kinetics during differentiation seems not to be based on telomere length-mediated regulation, as TelBP1 loss does not affect telomere length maintenance. Another explanation for the observed effect of TelBP1 on BES silencing might be a crosstalk between chromatin factors and TelBP1 leading to fine tuning of silencing initiation and heterochromatin establishment at the active BES during the differentiation process. Studying the interaction partners of TelBP1 could shed light on the underlying mechanisms.

4.7 Conclusion and future perspective

Here, we provide a set of novel potential telomere-binding proteins in *T. brucei*. These novel candidates might be helpful to answer specific questions of telomere biology and parasitology. Therefore the characterization of these candidates should be the focus of future research.

The initial characterization of one of the found candidates, TelBP1, revealed that telomere-binding proteins are involved in the regulation of developmental transcriptional silencing of VSG genes. Thus, TelBP1 demonstrates the first link between telomere-binding proteins and developmental differentiation of BSF to PCF trypanosomes. Changes in the cell biology upon differentiation induction must be regulated and interconnected. The developmental program of the parasite is temporally ordered. First, the replacement of the VSG coat by EP procyclin takes place in the first 5 h, second, kinetoplast repositioning occurs between 6-12 h after differentiation initiation, and finally the cells reenter the cell cycle and turn on the mitochondrial-based energy production after 14-24 h (reviewed in Matthews, 1999). This requires coordination of different events (reviewed in Matthews, 2005). All these developmental changes were not investigated during differentiation of TelBP1 null-mutant cells,

as the strain used in this study (Lister 427) is not suitable to analyze differentiation *in vivo*. These so-called monomorphic cells are culture-adapted and very useful for reverse genetics. However, differentiation initiation is quite inefficient and asynchronous. Therefore, they are very helpful for initial characterization of candidate proteins, but for detailed investigation of the implications of chromatin dynamics during differentiation the more laborious pleomorphic AnTat1.1 trypanosomes should be used.

It would be also interesting to study the telomere complex composition in these pleomorphic trypanosomes during the differentiation event by using pull-down assays and Co-IP experiments as our data suggest that the conformation of telomeres is dynamic and changes during differentiation from BSF to PCF stage reflecting that telomeres have to carry out distinct functions in both life cycle stages of the parasite.

5 REFERENCES

ABREU, E., ARITONOVSKA, E., REICHENBACH, P., CRISTOFARI, G., CULP, B., TERNS, R. M., LINGNER, J. & TERNS, M. P. 2010. TIN2-tethered TPP1 recruits human telomerase to telomeres in vivo. *Mol Cell Biol,* 30**,** 2971-82.

ALARCON, C. M., SON, H. J., HALL, T. & DONELSON, J. E. 1994. A monocistronic transcript for a trypanosome variant surface glycoprotein. *Mol Cell Biol,* 14**,** 5579-91.

ALSFORD, S., DUBOIS, K., HORN, D. & FIELD, M. C. 2012. Epigenetic mechanisms, nuclear architecture and the control of gene expression in trypanosomes. *Expert Rev Mol Med,* 14**,** e13.

ALSFORD, S. & HORN, D. 2008. Single-locus targeting constructs for reliable regulated RNAi and transgene expression in Trypanosoma brucei. *Mol Biochem Parasitol,* 161**,** 76-9.

ALSFORD, S. & HORN, D. 2012. Cell-cycle-regulated control of VSG expression site silencing by histones and histone chaperones ASF1A and CAF-1b in Trypanosoma brucei. *Nucleic Acids Res,* 40**,** 10150-60.

ALSFORD, S., KAWAHARA, T., GLOVER, L. & HORN, D. 2005. Tagging a T. brucei RRNA locus improves stable transfection efficiency and circumvents inducible expression position effects. *Mol Biochem Parasitol,* 144**,** 142-8.

ALSFORD, S., KAWAHARA, T., ISAMAH, C. & HORN, D. 2007. A sirtuin in the African trypanosome is involved in both DNA repair and telomeric gene silencing but is not required for antigenic variation. *Mol Microbiol,* 63**,** 724-36.

ALSFORD, S., TURNER, D. J., OBADO, S. O., SANCHEZ-FLORES, A., GLOVER, L., BERRIMAN, M., HERTZ-FOWLER, C. & HORN, D. 2011. High-throughput phenotyping using parallel sequencing of RNA interference targets in the African trypanosome. *Genome Res,* 21**,** 915-24.

AMIGUET-VERCHER, A., PEREZ-MORGA, D., PAYS, A., POELVOORDE, P., VAN XONG, H., TEBABI, P., VANHAMME, L. & PAYS, E. 2004. Loss of the mono-allelic control of the VSG expression sites during the development of Trypanosoma brucei in the bloodstream. *Mol Microbiol,* 51**,** 1577-88.

APARICIO, O. M., BILLINGTON, B. L. & GOTTSCHLING, D. E. 1991. Modifiers of position effect are shared between telomeric and silent mating-type loci in S. cerevisiae. *Cell,* 66**,** 1279-87.

ARESTA-BRANCO, F., PIMENTA, S. & FIGUEIREDO, L. M. 2016. A transcription-independent epigenetic mechanism is associated with antigenic switching in Trypanosoma brucei. *Nucleic Acids Res,* 44**,** 3131-46.

ARMSTRONG, C. A. & TOMITA, K. 2017. Fundamental mechanisms of telomerase action in yeasts and mammals: understanding telomeres and telomerase in cancer cells. *Open Biol,* 7.

ASLETT, M., AURRECOECHEA, C., BERRIMAN, M., BRESTELLI, J., BRUNK, B. P., CARRINGTON, M., DEPLEDGE, D. P., FISCHER, S., GAJRIA, B., GAO, X., GARDNER, M. J., GINGLE, A., GRANT, G., HARB, O. S., HEIGES, M., HERTZ-FOWLER, C., HOUSTON, R., INNAMORATO, F., IODICE, J., KISSINGER, J. C., KRAEMER, E., LI, W., LOGAN, F. J., MILLER, J. A., MITRA, S., MYLER, P. J., NAYAK, V., PENNINGTON, C., PHAN, I., PINNEY, D. F., RAMASAMY, G., ROGERS, M. B., ROOS, D. S., ROSS, C., SIVAM, D., SMITH, D. F., SRINIVASAMOORTHY, G., STOECKERT, C. J., JR., SUBRAMANIAN, S., THIBODEAU, R., TIVEY, A., TREATMAN, C., VELARDE, G. & WANG, H. 2010. TriTrypDB: a functional genomic resource for the Trypanosomatidae. *Nucleic Acids Res,* 38**,** D457-62.

AUTY, H., TORR, S. J., MICHOEL, T., JAYARAMAN, S. & MORRISON, L. J. 2015. Cattle trypanosomosis: the diversity of trypanosomes and implications for disease epidemiology and control. *Rev Sci Tech,* 34**,** 587-98.

BARRY, J. D., GINGER, M. L., BURTON, P. & MCCULLOCH, R. 2003. Why are parasite contingency genes often associated with telomeres? *Int J Parasitol,* 33**,** 29-45.

BARRY, J. D., GRAHAM, S. V., FOTHERINGHAM, M., GRAHAM, V. S., KOBRYN, K. & WYMER, B. 1998. VSG gene control and infectivity strategy of metacyclic stage Trypanosoma brucei. *Mol Biochem Parasitol,* 91**,** 93-105.

BATRAM, C., JONES, N. G., JANZEN, C. J., MARKERT, S. M. & ENGSTLER, M. 2014. Expression site attenuation mechanistically links antigenic variation and development in Trypanosoma brucei. *Elife,* 3**,** e02324.

BAUMANN, P. & CECH, T. R. 2001. Pot1, the putative telomere end-binding protein in fission yeast and humans. *Science,* 292**,** 1171-5.

BAUMANN, P., PODELL, E. & CECH, T. R. 2002. Human Pot1 (protection of telomeres) protein: cytolocalization, gene structure, and alternative splicing. *Mol Cell Biol,* 22**,** 8079-87.

BENETTI, R., SCHOEFTNER, S., MUNOZ, P. & BLASCO, M. A. 2008. Role of TRF2 in the assembly of telomeric chromatin. *Cell Cycle,* 7**,** 3461-8.

BENMERZOUGA, I., CONCEPCION-ACEVEDO, J., KIM, H. S., VANDOROS, A. V., CROSS, G. A., KLINGBEIL, M. M. & LI, B. 2013. Trypanosoma brucei Orc1 is essential for nuclear DNA replication and affects both VSG silencing and VSG switching. *Mol Microbiol,* 87**,** 196-210.

BERBEROF, M., VANHAMME, L., TEBABI, P., PAYS, A., JEFFERIES, D., WELBURN, S. & PAYS, E. 1995. The 3'-terminal region of the mRNAs for VSG and procyclin can confer stage specificity to gene expression in Trypanosoma brucei. *EMBO J,* 14**,** 2925-34.

BERMEJO, R., LAI, M. S. & FOIANI, M. 2012. Preventing replication stress to maintain genome stability: resolving conflicts between replication and transcription. *Mol Cell,* 45**,** 710-8.

BERNARDS, A., DE LANGE, T., MICHELS, P. A., LIU, A. Y., HUISMAN, M. J. & BORST, P. 1984. Two modes of activation of a single surface antigen gene of Trypanosoma brucei. *Cell,* 36**,** 163-70.

BERNARDS, A., MICHELS, P. A., LINCKE, C. R. & BORST, P. 1983. Growth of chromosome ends in multiplying trypanosomes. *Nature,* 303**,** 592-7.

BERNARDS, A., VAN DER PLOEG, L. H., FRASCH, A. C., BORST, P., BOOTHROYD, J. C., COLEMAN, S. & CROSS, G. A. 1981. Activation of trypanosome surface glycoprotein genes involves a duplication-transposition leading to an altered 3' end. *Cell,* 27**,** 497-505.

BERRIMAN, M., GHEDIN, E., HERTZ-FOWLER, C., BLANDIN, G., RENAULD, H., BARTHOLOMEU, D. C., LENNARD, N. J., CALER, E., HAMLIN, N. E., HAAS, B., BOHME, U., HANNICK, L., ASLETT, M. A., SHALLOM, J., MARCELLO, L., HOU, L., WICKSTEAD, B., ALSMARK, U. C., ARROWSMITH, C., ATKIN, R. J., BARRON, A. J., BRINGAUD, F., BROOKS, K., CARRINGTON, M., CHEREVACH, I., CHILLINGWORTH, T. J., CHURCHER, C., CLARK, L. N., CORTON, C. H., CRONIN, A., DAVIES, R. M., DOGGETT, J., DJIKENG, A., FELDBLYUM, T., FIELD, M. C., FRASER, A., GOODHEAD, I., HANCE, Z., HARPER, D., HARRIS, B. R., HAUSER, H., HOSTETLER, J., IVENS, A., JAGELS, K., JOHNSON, D., JOHNSON, J., JONES, K., KERHORNOU, A. X., KOO, H., LARKE, N., LANDFEAR, S., LARKIN, C., LEECH, V., LINE, A., LORD, A., MACLEOD, A., MOONEY, P. J., MOULE, S., MARTIN, D. M., MORGAN, G. W., MUNGALL, K., NORBERTCZAK, H., ORMOND, D., PAI, G., PEACOCK, C. S., PETERSON, J., QUAIL, M. A., RABBINOWITSCH, E., RAJANDREAM, M. A., REITTER, C., SALZBERG, S. L., SANDERS, M., SCHOBEL, S., SHARP, S., SIMMONDS, M., SIMPSON, A. J., TALLON, L., TURNER, C. M., TAIT, A., TIVEY, A. R., VAN AKEN, S., WALKER, D., WANLESS, D., WANG, S., WHITE, B., WHITE, O., WHITEHEAD, S., WOODWARD, J., WORTMAN, J., ADAMS, M. D., EMBLEY, T. M., GULL, K., ULLU, E., BARRY, J. D., FAIRLAMB, A. H., OPPERDOES, F., BARRELL, B. G., DONELSON, J. E., HALL, N., FRASER, C. M., et al. 2005. The genome of the African trypanosome Trypanosoma brucei. *Science,* 309**,** 416-22.

BIEBINGER, S., RETTENMAIER, S., FLASPOHLER, J., HARTMANN, C., PENA-DIAZ, J., WIRTZ, L. E., HOTZ, H. R., BARRY, J. D. & CLAYTON, C. 1996. The PARP promoter of Trypanosoma brucei is developmentally regulated in a chromosomal context. *Nucleic Acids Res,* 24**,** 1202-11.

BILAUD, T., BRUN, C., ANCELIN, K., KOERING, C. E., LAROCHE, T. & GILSON, E. 1997. Telomeric localization of TRF2, a novel human telobox protein. *Nat Genet,* 17**,** 236-9.

BLACKBURN, E. 2009. Telomeres and Tetrahymena: an interview with Elizabeth Blackburn. *Dis Model Mech,* 2**,** 534-7.

BLACKBURN, E. H. 1991. Telomeres. *Trends Biochem Sci,* 16**,** 378-81.

BLACKBURN, E. H. & GALL, J. G. 1978. A tandemly repeated sequence at the termini of the extrachromosomal ribosomal RNA genes in Tetrahymena. *J Mol Biol,* 120**,** 33-53.

BLASCO, M. A. 2007. The epigenetic regulation of mammalian telomeres. *Nat Rev Genet,* 8**,** 299-309.

BOOTHROYD, C. E., DREESEN, O., LEONOVA, T., LY, K. I., FIGUEIREDO, L. M., CROSS, G. A. & PAPAVASILIOU, F. N. 2009. A yeast-endonuclease-generated DNA break induces antigenic switching in Trypanosoma brucei. *Nature,* 459**,** 278-81.

BORST, P. & SABATINI, R. 2008. Base J: discovery, biosynthesis, and possible functions. *Annu Rev Microbiol,* 62**,** 235-51.

BOTTIUS, E., BAKHSIS, N. & SCHERF, A. 1998. Plasmodium falciparum telomerase: de novo telomere addition to telomeric and nontelomeric sequences and role in chromosome healing. *Mol Cell Biol,* 18**,** 919-25.

BRANDENBURG, J., SCHIMANSKI, B., NOGOCEKE, E., NGUYEN, T. N., PADOVAN, J. C., CHAIT, B. T., CROSS, G. A. & GUNZL, A. 2007. Multifunctional class I transcription in Trypanosoma brucei depends on a novel protein complex. *EMBO J,* 26**,** 4856-66.

BREIDBACH, T., NGAZOA, E. & STEVERDING, D. 2002. Trypanosoma brucei: in vitro slender-to-stumpy differentiation of culture-adapted, monomorphic bloodstream forms. *Exp Parasitol,* 101**,** 223-30.

BROCCOLI, D., SMOGORZEWSKA, A., CHONG, L. & DE LANGE, T. 1997. Human telomeres contain two distinct Myb-related proteins, TRF1 and TRF2. *Nat Genet,* 17**,** 231-5.

BROCCOLI, D., YOUNG, J. W. & DE LANGE, T. 1995. Telomerase activity in normal and malignant hematopoietic cells. *Proc Natl Acad Sci U S A,* 92**,** 9082-6.

BRUN, R., BLUM, J., CHAPPUIS, F. & BURRI, C. 2010. Human African trypanosomiasis. *Lancet,* 375**,** 148-59.

BRUN, R. & SCHÖNENBERGER 1979. Cultivation and in vitro cloning or procyclic culture forms of Trypanosoma brucei in a semi-defined medium. Short communication. *Acta Trop,* 36**,** 289-92.

BRUN, R. & SCHÖNENBERGER, M. 1981. Stimulating effect of citrate and cis-Aconitate on the transformation of Trypanosoma brucei bloodstream forms to procyclic forms in vitro. *Z Parasitenkd,* 66**,** 17-24.

BURRI, M., SCHLIMME, W., BETSCHART, B. & HECKER, H. 1994. Characterization of the histones of Trypanosoma brucei brucei bloodstream forms. *Acta Trop,* 58**,** 291-305.

BUTTER, F., BUCERIUS, F., MICHEL, M., CICOVA, Z., MANN, M. & JANZEN, C. J. 2013. Comparative proteomics of two life cycle stages of stable isotope-labeled Trypanosoma brucei reveals novel components of the parasite's host adaptation machinery. *Mol Cell Proteomics,* 12**,** 172-9.

CANO, M. I., BLAKE, J. J., BLACKBURN, E. H. & AGABIAN, N. 2002. A Trypanosoma brucei protein complex that binds G-overhangs and co-purifies with telomerase activity. *J Biol Chem,* 277**,** 896-906.

CASAS-VILA, N., SCHEIBE, M., FREIWALD, A., KAPPEI, D. & BUTTER, F. 2015. Identification of TTAGGG-binding proteins in Neurospora crassa, a fungus with vertebrate-like telomere repeats. *BMC Genomics,* 16**,** 965.

CESTARI, I. & STUART, K. 2015. Inositol phosphate pathway controls transcription of telomeric expression sites in trypanosomes. *Proc Natl Acad Sci U S A,* 112**,** E2803-12.

CHONG, L., VAN STEENSEL, B., BROCCOLI, D., ERDJUMENT-BROMAGE, H., HANISH, J., TEMPST, P. & DE LANGE, T. 1995. A human telomeric protein. *Science,* 270**,** 1663-7.

CLAYTON, C. 2013. The regulation of trypanosome gene expression by RNA-binding proteins. *PLoS Pathog,* 9**,** e1003680.

CLAYTON, C. E. 2002. Life without transcriptional control? From fly to man and back again. *EMBO J,* 21**,** 1881-8.

CLAYTON, C. E. 2014. Networks of gene expression regulation in Trypanosoma brucei. *Mol Biochem Parasitol,* 195**,** 96-106.

COHN, M. & BLACKBURN, E. H. 1995. Telomerase in yeast. *Science,* 269**,** 396-400.

CONOMOS, D., PICKETT, H. A. & REDDEL, R. R. 2013. Alternative lengthening of telomeres: remodeling the telomere architecture. *Front Oncol,* 3**,** 27.

CONWAY, C., MCCULLOCH, R., GINGER, M. L., ROBINSON, N. P., BROWITT, A. & BARRY, J. D. 2002. Ku is important for telomere maintenance, but not for differential expression of telomeric VSG genes, in African trypanosomes. *J Biol Chem,* 277**,** 21269-77.

COREY, D. R. 2009. Telomeres and telomerase: from discovery to clinical trials. *Chem Biol,* 16**,** 1219-23.

CORONA, D. F., CLAPIER, C. R., BECKER, P. B. & TAMKUN, J. W. 2002. Modulation of ISWI function by site-specific histone acetylation. *EMBO Rep,* 3**,** 242-7.

COUNTER, C. M., HIRTE, H. W., BACCHETTI, S. & HARLEY, C. B. 1994. Telomerase activity in human ovarian carcinoma. *Proc Natl Acad Sci U S A,* 91**,** 2900-4.

COX, J., HEIN, M. Y., LUBER, C. A., PARON, I., NAGARAJ, N. & MANN, M. 2014. Accurate proteome-wide label-free quantification by delayed normalization and maximal peptide ratio extraction, termed MaxLFQ. *Mol Cell Proteomics,* 13**,** 2513-26.

COX, J. & MANN, M. 2008. MaxQuant enables high peptide identification rates, individualized p.p.b.-range mass accuracies and proteome-wide protein quantification. *Nat Biotechnol,* 26**,** 1367-72.

CRABBE, L., CESARE, A. J., KASUBOSKI, J. M., FITZPATRICK, J. A. & KARLSEDER, J. 2012. Human telomeres are tethered to the nuclear envelope during postmitotic nuclear assembly. *Cell Rep,* 2**,** 1521-9.

CROSS, G. A., KIM, H. S. & WICKSTEAD, B. 2014. Capturing the variant surface glycoprotein repertoire (the VSGnome) of Trypanosoma brucei Lister 427. *Mol Biochem Parasitol,* 195**,** 59-73.

CZICHOS, J., NONNENGAESSER, C. & OVERATH, P. 1986. Trypanosoma brucei: cis-aconitate and temperature reduction as triggers of synchronous transformation of bloodstream to procyclic trypomastigotes in vitro. *Exp Parasitol,* 62**,** 283-91.

DANIELS, J. P., GULL, K. & WICKSTEAD, B. 2010. Cell biology of the trypanosome genome. *Microbiol Mol Biol Rev,* 74**,** 552-69.

DAS, A., BELLOFATTO, V., ROSENFELD, J., CARRINGTON, M., ROMERO-ZALIZ, R., DEL VAL, C. & ESTEVEZ, A. M. 2015. High throughput sequencing analysis of Trypanosoma brucei DRBD3/PTB1-bound mRNAs. *Mol Biochem Parasitol,* 199**,** 1-4.

DE LANGE, T. 2005. Shelterin: the protein complex that shapes and safeguards human telomeres. *Genes Dev,* 19**,** 2100-10.

DE LANGE, T., KOOTER, J. M., MICHELS, P. A. & BORST, P. 1983. Telomere conversion in trypanosomes. *Nucleic Acids Res,* 11**,** 8149-65.

DE LANGE, T., SHIUE, L., MYERS, R. M., COX, D. R., NAYLOR, S. L., KILLERY, A. M. & VARMUS, H. E. 1990. Structure and variability of human chromosome ends. *Mol Cell Biol,* 10**,** 518-27.

DEAN, S., MARCHETTI, R., KIRK, K. & MATTHEWS, K. R. 2009. A surface transporter family conveys the trypanosome differentiation signal. *Nature,* 459**,** 213-7.

DEITSCH, K. W., LUKEHART, S. A. & STRINGER, J. R. 2009. Common strategies for antigenic variation by bacterial, fungal and protozoan pathogens. *Nat Rev Microbiol,* 7**,** 493-503.

DEJARDIN, J. & KINGSTON, R. E. 2009. Purification of proteins associated with specific genomic Loci. *Cell,* 136**,** 175-86.

DEJUNG, M., SUBOTA, I., BUCERIUS, F., DINDAR, G., FREIWALD, A., ENGSTLER, M., BOSHART, M., BUTTER, F. & JANZEN, C. J. 2016. Quantitative Proteomics Uncovers Novel Factors Involved in Developmental Differentiation of Trypanosoma brucei. *PLoS Pathog,* 12**,** e1005439.

DENNINGER, V., FULLBROOK, A., BESSAT, M., ERSFELD, K. & RUDENKO, G. 2010. The FACT subunit TbSpt16 is involved in cell cycle specific control of VSG expression sites in Trypanosoma brucei. *Mol Microbiol,* 78**,** 459-74.

DENNINGER, V. & RUDENKO, G. 2014. FACT plays a major role in histone dynamics affecting VSG expression site control in Trypanosoma brucei. *Mol Microbiol,* 94**,** 945-62.

DEVLIN, R., MARQUES, C. A. & MCCULLOCH, R. 2017. Does DNA replication direct locus-specific recombination during host immune evasion by antigenic variation in the African trypanosome? *Curr Genet,* 63**,** 441-449.

DING, X., XU, R., YU, J., XU, T., ZHUANG, Y. & HAN, M. 2007. SUN1 is required for telomere attachment to nuclear envelope and gametogenesis in mice. *Dev Cell,* 12**,** 863-72.

DREESEN, O., LI, B. & CROSS, G. A. 2007. Telomere structure and function in trypanosomes: a proposal. *Nat Rev Microbiol,* 5**,** 70-5.

DUBOIS, K. N., ALSFORD, S., HOLDEN, J. M., BUISSON, J., SWIDERSKI, M., BART, J. M., RATUSHNY, A. V., WAN, Y., BASTIN, P., BARRY, J. D., NAVARRO, M., HORN, D., AITCHISON, J. D., ROUT, M. P. & FIELD, M. C. 2012. NUP-1 Is a large coiled-coil nucleoskeletal protein in trypanosomes with lamin-like functions. *PLoS Biol,* 10**,** e1001287.

DURAISINGH, M. T. & HORN, D. 2016. Epigenetic Regulation of Virulence Gene Expression in Parasitic Protozoa. *Cell Host Microbe,* 19**,** 629-40.

EID, J. E. & SOLLNER-WEBB, B. 1995. ST-1, a 39-kilodalton protein in Trypanosoma brucei, exhibits a dual affinity for the duplex form of the 29-base-pair subtelomeric repeat and its C-rich strand. *Mol Cell Biol,* 15**,** 389-97.

EID, J. E. & SOLLNER-WEBB, B. 1997. ST-2, a telomere and subtelomere duplex and G-strand binding protein activity in Trypanosoma brucei. *J Biol Chem,* 272**,** 14927-36.

EIFLER, K. & VERTEGAAL, A. C. 2015. Mapping the SUMOylated landscape. *FEBS J,* 282**,** 3669-80.

ENGSTLER, M. & BOSHART, M. 2004. Cold shock and regulation of surface protein trafficking convey sensitization to inducers of stage differentiation in Trypanosoma brucei. *Genes Dev,* 18**,** 2798-811.

ERSFELD, K. 2011. Nuclear architecture, genome and chromatin organisation in Trypanosoma brucei. *Res Microbiol,* 162**,** 626-36.

ERSFELD, K. & GULL, K. 1997. Partitioning of large and minichromosomes in Trypanosoma brucei. *Science,* 276**,** 611-4.

FARIA, J. C., GLOVER, L., HUTCHINSON, S., BOEHM, C., FIELD, M. C. & HORN, D. 2017. Control of allelic exclusion by a trypanosome 'Vex Histone Chaperone' complex. *KMCBM Abstract 7C,* Presented at the 7th Kinetoplastid Molecular Cell Biology Meeting, April 22-26, 2017, Woodshole, MA, USA.

FENN, K. & MATTHEWS, K. R. 2007. The cell biology of Trypanosoma brucei differentiation. *Curr Opin Microbiol,* 10**,** 539-46.

FERGUSON, M. A., LOW, M. G. & CROSS, G. A. 1985. Glycosyl-sn-1,2-dimyristylphosphatidylinositol is covalently linked to Trypanosoma brucei variant surface glycoprotein. *J Biol Chem,* 260**,** 14547-55.

FIELD, H. & FIELD, M. C. 1996. Leptomonas seymouri, Trypanosoma brucei: a method for isolating trypanosomatid nuclear factors which bind T. brucei single-stranded g-rich telomere sequence. *Exp Parasitol,* 83**,** 155-8.

FIGUEIREDO, L. M. & CROSS, G. A. 2010. Nucleosomes are depleted at the VSG expression site transcribed by RNA polymerase I in African trypanosomes. *Eukaryot Cell,* 9**,** 148-54.

FIGUEIREDO, L. M., CROSS, G. A. & JANZEN, C. J. 2009. Epigenetic regulation in African trypanosomes: a new kid on the block. *Nat Rev Microbiol,* 7**,** 504-13.

FIGUEIREDO, L. M., JANZEN, C. J. & CROSS, G. A. 2008. A histone methyltransferase modulates antigenic variation in African trypanosomes. *PLoS Biol,* 6**,** e161.

FIGUEIREDO, L. M., ROCHA, E. P., MANCIO-SILVA, L., PREVOST, C., HERNANDEZ-VERDUN, D. & SCHERF, A. 2005. The unusually large Plasmodium telomerase reverse-transcriptase localizes in a discrete compartment associated with the nucleolus. *Nucleic Acids Res,* 33**,** 1111-22.

FOJTOVA, M. & FAJKUS, J. 2014. Epigenetic regulation of telomere maintenance. *Cytogenet Genome Res,* 143**,** 125-35.

FRANCO, J. R., CECCHI, G., PRIOTTO, G., PAONE, M., DIARRA, A., GROUT, L., MATTIOLI, R. C. & ARGAW, D. 2017. Monitoring the elimination of human African trypanosomiasis: Update to 2014. *PLoS Negl Trop Dis,* 11**,** e0005585.

FRANCO, J. R., SIMARRO, P. P., DIARRA, A. & JANNIN, J. G. 2014. Epidemiology of human African trypanosomiasis. *Clin Epidemiol,* 6**,** 257-75.

FREHLICK, L. J., EIRIN-LOPEZ, J. M. & AUSIO, J. 2007. New insights into the nucleophosmin/nucleoplasmin family of nuclear chaperones. *Bioessays,* 29**,** 49-59.

GALATI, A., MICHELI, E. & CACCHIONE, S. 2013. Chromatin structure in telomere dynamics. *Front Oncol,* 3**,** 46.

GARCIA-SALCEDO, J. A., PEREZ-MORGA, D., GIJON, P., DILBECK, V., PAYS, E. & NOLAN, D. P. 2004. A differential role for actin during the life cycle of Trypanosoma brucei. *EMBO J,* 23**,** 780-9.

GILINGER, G. & BELLOFATTO, V. 2001. Trypanosome spliced leader RNA genes contain the first identified RNA polymerase II gene promoter in these organisms. *Nucleic Acids Res,* 29**,** 1556-64.

GINGER, M. L., BLUNDELL, P. A., LEWIS, A. M., BROWITT, A., GUNZL, A. & BARRY, J. D. 2002. Ex vivo and in vitro identification of a consensus promoter for VSG genes expressed by metacyclic-stage trypanosomes in the tsetse fly. *Eukaryot Cell,* 1**,** 1000-9.

GLOVER, L., ALSFORD, S., BEATTIE, C. & HORN, D. 2007. Deletion of a trypanosome telomere leads to loss of silencing and progressive loss of terminal DNA in the absence of cell cycle arrest. *Nucleic Acids Res,* 35**,** 872-80.

GLOVER, L., ALSFORD, S. & HORN, D. 2013a. DNA break site at fragile subtelomeres determines probability and mechanism of antigenic variation in African trypanosomes. *PLoS Pathog,* 9**,** e1003260.

GLOVER, L. & HORN, D. 2006. Repression of polymerase I-mediated gene expression at Trypanosoma brucei telomeres. *EMBO Rep,* 7**,** 93-9.

GLOVER, L., HUTCHINSON, S., ALSFORD, S. & HORN, D. 2016. VEX1 controls the allelic exclusion required for antigenic variation in trypanosomes. *Proc Natl Acad Sci U S A,* 113**,** 7225-30.

GLOVER, L., HUTCHINSON, S., ALSFORD, S., MCCULLOCH, R., FIELD, M. C. & HORN, D. 2013b. Antigenic variation in African trypanosomes: the importance of chromosomal and nuclear context in VSG expression control. *Cell Microbiol,* 15**,** 1984-93.

GOMMERS-AMPT, J., LUTGERINK, J. & BORST, P. 1991. A novel DNA nucleotide in Trypanosoma brucei only present in the mammalian phase of the life-cycle. *Nucleic Acids Res,* 19**,** 1745-51.

GOMMERS-AMPT, J. H., VAN LEEUWEN, F., DE BEER, A. L., VLIEGENTHART, J. F., DIZDAROGLU, M., KOWALAK, J. A., CRAIN, P. F. & BORST, P. 1993. beta-D-glucosyl-hydroxymethyluracil: a novel modified base present in the DNA of the parasitic protozoan T. brucei. *Cell,* 75**,** 1129-36.

GOTTSCHLING, D. E., APARICIO, O. M., BILLINGTON, B. L. & ZAKIAN, V. A. 1990. Position effect at S. cerevisiae telomeres: reversible repression of Pol II transcription. *Cell,* 63**,** 751-62.

GRAHAM, S. V. & BARRY, J. D. 1995. Transcriptional regulation of metacyclic variant surface glycoprotein gene expression during the life cycle of Trypanosoma brucei. *Mol Cell Biol,* 15**,** 5945-56.

GREIDER, C. W. & BLACKBURN, E. H. 1985. Identification of a specific telomere terminal transferase activity in Tetrahymena extracts. *Cell,* 43**,** 405-13.

GREIDER, C. W. & BLACKBURN, E. H. 1987. The telomere terminal transferase of Tetrahymena is a ribonucleoprotein enzyme with two kinds of primer specificity. *Cell,* 51**,** 887-98.

GREIDER, C. W. & BLACKBURN, E. H. 1989. A telomeric sequence in the RNA of Tetrahymena telomerase required for telomere repeat synthesis. *Nature,* 337**,** 331-7.

GRIFFITH, J. D., COMEAU, L., ROSENFIELD, S., STANSEL, R. M., BIANCHI, A., MOSS, H. & DE LANGE, T. 1999. Mammalian telomeres end in a large duplex loop. *Cell,* 97**,** 503-14.

GRUSZYNSKI, A. E., VAN DEURSEN, F. J., ALBAREDA, M. C., BEST, A., CHAUDHARY, K., CLIFFE, L. J., DEL RIO, L., DUNN, J. D., ELLIS, L., EVANS, K. J., FIGUEIREDO, J. M., MALMQUIST, N. A., OMOSUN, Y., PALENCHAR, J. B., PRICKETT, S., PUNKOSDY, G. A., VAN DOOREN, G., WANG, Q., MENON, A. K., MATTHEWS, K. R. & BANGS, J. D. 2006. Regulation of surface coat exchange by differentiating African trypanosomes. *Mol Biochem Parasitol,* 147**,** 211-23.

GUNZL, A., KIRKHAM, J. K., NGUYEN, T. N., BADJATIA, N. & PARK, S. H. 2015. Mono-allelic VSG expression by RNA polymerase I in Trypanosoma brucei: expression site control from both ends? *Gene,* 556**,** 68-73.

HAYFLICK, L. & MOORHEAD, P. S. 1961. The serial cultivation of human diploid cell strains. *Exp Cell Res,* 25**,** 585-621.

HELLEMOND, J. J., BAKKER, B. M. & TIELENS, A. G. 2005. Energy metabolism and its compartmentation in Trypanosoma brucei. *Adv Microb Physiol,* 50**,** 199-226.

HERNANDEZ-RIVAS, R., HERRERA-SOLORIO, A. M., SIERRA-MIRANDA, M., DELGADILLO, D. M. & VARGAS, M. 2013. Impact of chromosome ends on the biology and virulence of Plasmodium falciparum. *Mol Biochem Parasitol,* 187**,** 121-8.

HERTZ-FOWLER, C., FIGUEIREDO, L. M., QUAIL, M. A., BECKER, M., JACKSON, A., BASON, N., BROOKS, K., CHURCHER, C., FAHKRO, S., GOODHEAD, I., HEATH, P., KARTVELISHVILI, M., MUNGALL, K., HARRIS, D., HAUSER, H., SANDERS, M., SAUNDERS, D., SEEGER, K., SHARP, S., TAYLOR, J. E., WALKER, D., WHITE, B., YOUNG, R., CROSS, G. A., RUDENKO, G., BARRY, J. D., LOUIS, E. J. & BERRIMAN, M. 2008. Telomeric expression sites are highly conserved in Trypanosoma brucei. *PLoS One,* 3**,** e3527.

HIRUMI, H. & HIRUMI, K. 1989. Continuous cultivation of Trypanosoma brucei blood stream forms in a medium containing a low concentration of serum protein without feeder cell layers. *J Parasitol,* 75**,** 985-9.

HOLOCH, D. & MOAZED, D. 2015. RNA-mediated epigenetic regulation of gene expression. *Nat Rev Genet,* 16**,** 71-84.

HORN, D. 2001. Nuclear gene transcription and chromatin in Trypanosoma brucei. *Int J Parasitol,* 31**,** 1157-65.

HORN, D. 2014. Antigenic variation in African trypanosomes. *Mol Biochem Parasitol,* 195**,** 123-9.

HORN, D. & BARRY, J. D. 2005. The central roles of telomeres and subtelomeres in antigenic variation in African trypanosomes. *Chromosome Res,* 13**,** 525-33.

HORN, D. & CROSS, G. A. 1995. A developmentally regulated position effect at a telomeric locus in Trypanosoma brucei. *Cell,* 83**,** 555-61.

HORN, D. & CROSS, G. A. 1997. Position-dependent and promoter-specific regulation of gene expression in Trypanosoma brucei. *EMBO J,* 16**,** 7422-31.

HORN, D. & MCCULLOCH, R. 2010. Molecular mechanisms underlying the control of antigenic variation in African trypanosomes. *Curr Opin Microbiol,* 13**,** 700-5.

HOTZ, H. R., HARTMANN, C., HUOBER, K., HUG, M. & CLAYTON, C. 1997. Mechanisms of developmental regulation in Trypanosoma brucei: a polypyrimidine tract in the 3'-untranslated region of a surface protein mRNA affects RNA abundance and translation. *Nucleic Acids Res,* 25**,** 3017-26.

HOUGHTALING, B. R., CUTTONARO, L., CHANG, W. & SMITH, S. 2004. A dynamic molecular link between the telomere length regulator TRF1 and the chromosome end protector TRF2. *Curr Biol,* 14**,** 1621-31.

HOVEL-MINER, G., MUGNIER, M. R., GOLDWATER, B., CROSS, G. A. & PAPAVASILIOU, F. N. 2016. A Conserved DNA Repeat Promotes Selection of a Diverse Repertoire of Trypanosoma brucei Surface Antigens from the Genomic Archive. *PLoS Genet,* 12**,** e1005994.

HOVEL-MINER, G. A., BOOTHROYD, C. E., MUGNIER, M., DREESEN, O., CROSS, G. A. & PAPAVASILIOU, F. N. 2012. Telomere length affects the frequency and mechanism of antigenic variation in Trypanosoma brucei. *PLoS Pathog,* 8**,** e1002900.

HUG, M., CARRUTHERS, V. B., HARTMANN, C., SHERMAN, D. S., CROSS, G. A. & CLAYTON, C. 1993. A possible role for the 3'-untranslated region in developmental regulation in Trypanosoma brucei. *Mol Biochem Parasitol,* 61**,** 87-95.

HUGHES, K., WAND, M., FOULSTON, L., YOUNG, R., HARLEY, K., TERRY, S., ERSFELD, K. & RUDENKO, G. 2007. A novel ISWI is involved in VSG expression site downregulation in African trypanosomes. *EMBO J,* 26**,** 2400-10.

IMBODEN, M. A., LAIRD, P. W., AFFOLTER, M. & SEEBECK, T. 1987. Transcription of the intergenic regions of the tubulin gene cluster of Trypanosoma brucei: evidence for a polycistronic transcription unit in a eukaryote. *Nucleic Acids Res,* 15**,** 7357-68.

JANZEN, C. J., LANDER, F., DREESEN, O. & CROSS, G. A. 2004. Telomere length regulation and transcriptional silencing in KU80-deficient Trypanosoma brucei. *Nucleic Acids Res,* 32**,** 6575-84.

JANZEN, C. J., VAN DEURSEN, F., SHI, H., CROSS, G. A., MATTHEWS, K. R. & ULLU, E. 2006. Expression site silencing and life-cycle progression appear normal in Argonaute1-deficient Trypanosoma brucei. *Mol Biochem Parasitol,* 149**,** 102-7.

JEHI, S. E., LI, X., SANDHU, R., YE, F., BENMERZOUGA, I., ZHANG, M., ZHAO, Y. & LI, B. 2014a. Suppression of subtelomeric VSG switching by Trypanosoma brucei TRF requires its TTAGGG repeat-binding activity. *Nucleic Acids Res,* 42**,** 12899-911.

JEHI, S. E., NANAVATY, V. & LI, B. 2016. Trypanosoma brucei TIF2 and TRF Suppress VSG Switching Using Overlapping and Independent Mechanisms. *PLoS One,* 11**,** e0156746.

JEHI, S. E., WU, F. & LI, B. 2014b. Trypanosoma brucei TIF2 suppresses VSG switching by maintaining subtelomere integrity. *Cell Res,* 24**,** 870-85.

JENSEN, B. C., SIVAM, D., KIFER, C. T., MYLER, P. J. & PARSONS, M. 2009. Widespread variation in transcript abundance within and across developmental stages of Trypanosoma brucei. *BMC Genomics,* 10**,** 482.

JONES, N. G., THOMAS, E. B., BROWN, E., DICKENS, N. J., HAMMARTON, T. C. & MOTTRAM, J. C. 2014. Regulators of Trypanosoma brucei cell cycle progression and differentiation identified using a kinome-wide RNAi screen. *PLoS Pathog,* 10**,** e1003886.

JOSLING, G. A., SELVARAJAH, S. A., PETTER, M. & DUFFY, M. F. 2012. The role of bromodomain proteins in regulating gene expression. *Genes (Basel),* 3**,** 320-43.

KALIDAS, S., LI, Q. & PHILLIPS, M. A. 2011. A Gateway(R) compatible vector for gene silencing in bloodstream form Trypanosoma brucei. *Mol Biochem Parasitol,* 178**,** 51-5.

KAMINKER, P. G., KIM, S. H., DESPREZ, P. Y. & CAMPISI, J. 2009. A novel form of the telomere-associated protein TIN2 localizes to the nuclear matrix. *Cell Cycle,* 8**,** 931-9.

KAPPEI, D., BUTTER, F., BENDA, C., SCHEIBE, M., DRASKOVIC, I., STEVENSE, M., NOVO, C. L., BASQUIN, C., ARAKI, M., ARAKI, K., KRASTEV, D. B., KITTLER, R., JESSBERGER, R., LONDONO-VALLEJO, J. A., MANN, M. & BUCHHOLZ, F. 2013. HOT1 is a mammalian direct telomere repeat-binding protein contributing to telomerase recruitment. *EMBO J,* 32**,** 1681-701.

KASSEM, A., PAYS, E. & VANHAMME, L. 2014. Transcription is initiated on silent variant surface glycoprotein expression sites despite monoallelic expression in Trypanosoma brucei. *Proc Natl Acad Sci U S A,* 111**,** 8943-8.

KAWAHARA, T., SIEGEL, T. N., INGRAM, A. K., ALSFORD, S., CROSS, G. A. & HORN, D. 2008. Two essential MYST-family proteins display distinct roles in histone H4K10 acetylation and telomeric silencing in trypanosomes. *Mol Microbiol,* 69**,** 1054-68.

KELLEY, L. A., MEZULIS, S., YATES, C. M., WASS, M. N. & STERNBERG, M. J. 2015. The Phyre2 web portal for protein modeling, prediction and analysis. *Nat Protoc,* 10**,** 845-58.

KILIAN, A., BOWTELL, D. D., ABUD, H. E., HIME, G. R., VENTER, D. J., KEESE, P. K., DUNCAN, E. L., REDDEL, R. R. & JEFFERSON, R. A. 1997. Isolation of a candidate human telomerase catalytic subunit gene, which reveals complex splicing patterns in different cell types. *Hum Mol Genet,* 6**,** 2011-9.

KIM, H. S., LI, Z., BOOTHROYD, C. & CROSS, G. A. 2013a. Strategies to construct null and conditional null Trypanosoma brucei mutants using Cre-recombinase and loxP. *Mol Biochem Parasitol,* 191**,** 16-9.

KIM, H. S., PARK, S. H., GUNZL, A. & CROSS, G. A. 2013b. MCM-BP is required for repression of life-cycle specific genes transcribed by RNA polymerase I in the mammalian infectious form of Trypanosoma brucei. *PLoS One,* 8**,** e57001.

KIM, N. W., PIATYSZEK, M. A., PROWSE, K. R., HARLEY, C. B., WEST, M. D., HO, P. L., COVIELLO, G. M., WRIGHT, W. E., WEINRICH, S. L. & SHAY, J. W. 1994. Specific association of human telomerase activity with immortal cells and cancer. *Science,* 266**,** 2011-5.

KIM, S. H., DAVALOS, A. R., HEO, S. J., RODIER, F., ZOU, Y., BEAUSEJOUR, C., KAMINKER, P., YANNONE, S. M. & CAMPISI, J. 2008. Telomere dysfunction and cell survival: roles for distinct TIN2-containing complexes. *J Cell Biol,* 181**,** 447-60.

KIM, S. H., KAMINKER, P. & CAMPISI, J. 1999. TIN2, a new regulator of telomere length in human cells. *Nat Genet,* 23**,** 405-12.

KOERING, C. E., POLLICE, A., ZIBELLA, M. P., BAUWENS, S., PUISIEUX, A., BRUNORI, M., BRUN, C., MARTINS, L., SABATIER, L., PULITZER, J. F. & GILSON, E. 2002. Human telomeric position effect is determined by chromosomal context and telomeric chromatin integrity. *EMBO Rep,* 3**,** 1055-61.

KOLEV, N. G., FRANKLIN, J. B., CARMI, S., SHI, H., MICHAELI, S. & TSCHUDI, C. 2010. The transcriptome of the human pathogen Trypanosoma brucei at single-nucleotide resolution. *PLoS Pathog,* 6**,** e1001090.

KOLEV, N. G., RAMEY-BUTLER, K., CROSS, G. A., ULLU, E. & TSCHUDI, C. 2012. Developmental progression to infectivity in Trypanosoma brucei triggered by an RNA-binding protein. *Science,* 338**,** 1352-3.

KORNBERG, R. D. 1974. Chromatin structure: a repeating unit of histones and DNA. *Science,* 184**,** 868-71.

KOSUGI, S., HASEBE, M., TOMITA, M. & YANAGAWA, H. 2009. Systematic identification of cell cycle-dependent yeast nucleocytoplasmic shuttling proteins by prediction of composite motifs. *Proc Natl Acad Sci U S A,* 106**,** 10171-6.

KOUZARIDES, T. 2007. Chromatin modifications and their function. *Cell,* 128**,** 693-705.

KRAMER, S. 2012. Developmental regulation of gene expression in the absence of transcriptional control: the case of kinetoplastids. *Mol Biochem Parasitol,* 181**,** 61-72.

KRAMER, S., BANNERMAN-CHUKUALIM, B., ELLIS, L., BOULDEN, E. A., KELLY, S., FIELD, M. C. & CARRINGTON, M. 2013. Differential localization of the two T. brucei poly(A) binding proteins to the nucleus and RNP granules suggests binding to distinct mRNA pools. *PLoS One,* 8**,** e54004.

KUPIEC, M. 2014. Biology of telomeres: lessons from budding yeast. *FEMS Microbiol Rev,* 38**,** 144-71.

KYRION, G., LIU, K., LIU, C. & LUSTIG, A. J. 1993. RAP1 and telomere structure regulate telomere position effects in Saccharomyces cerevisiae. *Genes Dev,* 7**,** 1146-59.

LAGES, C. S., ETIENNE, O., COMTE, J., GAUTHIER, L. R., GRANOTIER, C., PENNARUN, G. & BOUSSIN, F. D. 2004. Identification of alternative transcripts of the TRF1/Pin2 gene. *J Cell Biochem,* 93**,** 968-79.

LANDEIRA, D. & NAVARRO, M. 2007. Nuclear repositioning of the VSG promoter during developmental silencing in Trypanosoma brucei. *J Cell Biol,* 176**,** 133-9.

LANGOUSIS, G. & HILL, K. L. 2014. Motility and more: the flagellum of Trypanosoma brucei. *Nat Rev Microbiol,* 12**,** 505-18.

LATRICK, C. M. & CECH, T. R. 2010. POT1-TPP1 enhances telomerase processivity by slowing primer dissociation and aiding translocation. *EMBO J,* 29**,** 924-33.

LEVIS, R., HAZELRIGG, T. & RUBIN, G. M. 1985. Effects of genomic position on the expression of transduced copies of the white gene of Drosophila. *Science,* 229**,** 558-61.

LI, B. 2015. DNA double-strand breaks and telomeres play important roles in trypanosoma brucei antigenic variation. *Eukaryot Cell,* 14**,** 196-205.

LI, B., ESPINAL, A. & CROSS, G. A. 2005. Trypanosome telomeres are protected by a homologue of mammalian TRF2. *Mol Cell Biol,* 25**,** 5011-21.

LI, B., OESTREICH, S. & DE LANGE, T. 2000. Identification of human Rap1: implications for telomere evolution. *Cell,* 101**,** 471-83.

LI, C. H., IRMER, H., GUDJONSDOTTIR-PLANCK, D., FREESE, S., SALM, H., HAILE, S., ESTEVEZ, A. M. & CLAYTON, C. 2006. Roles of a Trypanosoma brucei 5'->3' exoribonuclease homolog in mRNA degradation. *RNA,* 12**,** 2171-86.

LINGER, B. R. & PRICE, C. M. 2009. Conservation of telomere protein complexes: shuffling through evolution. *Crit Rev Biochem Mol Biol,* 44**,** 434-46.

LIU, D., SAFARI, A., O'CONNOR, M. S., CHAN, D. W., LAEGELER, A., QIN, J. & SONGYANG, Z. 2004. PTOP interacts with POT1 and regulates its localization to telomeres. *Nat Cell Biol,* 6**,** 673-80.

LOAYZA, D. & DE LANGE, T. 2003. POT1 as a terminal transducer of TRF1 telomere length control. *Nature,* 423**,** 1013-8.

LOGAN-KLUMPLER, F. J., DE SILVA, N., BOEHME, U., ROGERS, M. B., VELARDE, G., MCQUILLAN, J. A., CARVER, T., ASLETT, M., OLSEN, C., SUBRAMANIAN, S., PHAN, I., FARRIS, C., MITRA, S., RAMASAMY, G., WANG, H., TIVEY, A., JACKSON, A., HOUSTON, R., PARKHILL, J., HOLDEN, M., HARB, O. S., BRUNK, B. P., MYLER, P. J., ROOS, D., CARRINGTON, M., SMITH, D. F., HERTZ-FOWLER, C. & BERRIMAN, M. 2012. GeneDB--an annotation database for pathogens. *Nucleic Acids Res,* 40**,** D98-108.

LOPEZ-FARFAN, D., BART, J. M., ROJAS-BARROS, D. I. & NAVARRO, M. 2014. SUMOylation by the E3 ligase TbSIZ1/PIAS1 positively regulates VSG expression in Trypanosoma brucei. *PLoS Pathog,* 10**,** e1004545.

LOWELL, J. E. & CROSS, G. A. 2004. A variant histone H3 is enriched at telomeres in Trypanosoma brucei. *J Cell Sci,* 117**,** 5937-47.

MAIR, G., SHI, H., LI, H., DJIKENG, A., AVILES, H. O., BISHOP, J. R., FALCONE, F. H., GAVRILESCU, C., MONTGOMERY, J. L., SANTORI, M. I., STERN, L. S., WANG, Z., ULLU, E. & TSCHUDI, C. 2000. A new twist in trypanosome RNA metabolism: cis-splicing of pre-mRNA. *RNA,* 6**,** 163-9.

MAKAROV, V. L., HIROSE, Y. & LANGMORE, J. P. 1997. Long G tails at both ends of human chromosomes suggest a C strand degradation mechanism for telomere shortening. *Cell,* 88**,** 657-66.

MANTELL, L. L. & GREIDER, C. W. 1994. Telomerase activity in germline and embryonic cells of Xenopus. *EMBO J,* 13**,** 3211-7.

MARCELLO, L. & BARRY, J. D. 2007. Analysis of the VSG gene silent archive in Trypanosoma brucei reveals that mosaic gene expression is prominent in antigenic variation and is favored by archive substructure. *Genome Res,* 17**,** 1344-52.

MAREE, J. P. & PATTERTON, H. G. 2014. The epigenome of Trypanosoma brucei: a regulatory interface to an unconventional transcriptional machine. *Biochim Biophys Acta,* 1839**,** 743-50.

MARTIN, V., DU, L. L., ROZENZHAK, S. & RUSSELL, P. 2007. Protection of telomeres by a conserved Stn1-Ten1 complex. *Proc Natl Acad Sci U S A,* 104**,** 14038-43.

MARTINEZ, P. & BLASCO, M. A. 2015. Replicating through telomeres: a means to an end. *Trends Biochem Sci,* 40**,** 504-15.

MARTINEZ, P., THANASOULA, M., CARLOS, A. R., GOMEZ-LOPEZ, G., TEJERA, A. M., SCHOEFTNER, S., DOMINGUEZ, O., PISANO, D. G., TARSOUNAS, M. & BLASCO, M. A. 2010. Mammalian Rap1 controls telomere function and gene expression through binding to telomeric and extratelomeric sites. *Nat Cell Biol,* 12**,** 768-80.

MATTHEWS, K. R. 1999. Developments in the differentiation of Trypanosoma brucei. *Parasitol Today,* 15**,** 76-80.

MATTHEWS, K. R. 2005. The developmental cell biology of Trypanosoma brucei. *J Cell Sci,* 118**,** 283-90.

MCCLINTOCK, B. 1941. The Stability of Broken Ends of Chromosomes in Zea Mays. *Genetics,* 26**,** 234-82.

MCCULLOCH, R., MORRISON, L. J. & HALL, J. P. 2015. DNA Recombination Strategies During Antigenic Variation in the African Trypanosome. *Microbiol Spectr,* 3**,** MDNA3-0016-2014.

MCELLIGOTT, R. & WELLINGER, R. J. 1997. The terminal DNA structure of mammalian chromosomes. *EMBO J,* 16**,** 3705-14.

MICHELS, P. A., VAN DER PLOEG, L. H., LIU, A. Y. & BORST, P. 1984. The inactivation and reactivation of an expression-linked gene copy for a variant surface glycoprotein in Trypanosoma brucei. *EMBO J,* 3**,** 1345-51.

MORIN, G. B. 1989. The human telomere terminal transferase enzyme is a ribonucleoprotein that synthesizes TTAGGG repeats. *Cell,* 59**,** 521-9.

MOYZIS, R. K., BUCKINGHAM, J. M., CRAM, L. S., DANI, M., DEAVEN, L. L., JONES, M. D., MEYNE, J., RATLIFF, R. L. & WU, J. R. 1988. A highly conserved repetitive DNA sequence, (TTAGGG)n, present at the telomeres of human chromosomes. *Proc Natl Acad Sci U S A,* 85**,** 6622-6.

MULLER, H. J. 1938. The remaking of chromosomes. *Collecting Net,* 13**,** 181-98.

NAKAMURA, T. M., MORIN, G. B., CHAPMAN, K. B., WEINRICH, S. L., ANDREWS, W. H., LINGNER, J., HARLEY, C. B. & CECH, T. R. 1997. Telomerase catalytic subunit homologs from fission yeast and human. *Science,* 277**,** 955-9.

NANAVATY, V., SANDHU, R., JEHI, S. E., PANDYA, U. M. & LI, B. 2017. Trypanosoma brucei RAP1 maintains telomere and subtelomere integrity by suppressing TERRA and telomeric RNA:DNA hybrids. *Nucleic Acids Res*.

NARAYANAN, M. S., KUSHWAHA, M., ERSFELD, K., FULLBROOK, A., STANNE, T. M. & RUDENKO, G. 2011. NLP is a novel transcription regulator involved in VSG expression site control in Trypanosoma brucei. *Nucleic Acids Res,* 39**,** 2018-31.

NARAYANAN, M. S. & RUDENKO, G. 2013. TDP1 is an HMG chromatin protein facilitating RNA polymerase I transcription in African trypanosomes. *Nucleic Acids Res,* 41**,** 2981-92.

NAVARRO, M., CROSS, G. A. & WIRTZ, E. 1999. Trypanosoma brucei variant surface glycoprotein regulation involves coupled activation/inactivation and chromatin remodeling of expression sites. *EMBO J,* 18**,** 2265-72.

NAVARRO, M. & GULL, K. 2001. A pol I transcriptional body associated with VSG mono-allelic expression in Trypanosoma brucei. *Nature,* 414**,** 759-63.

NAVARRO, M., PENATE, X. & LANDEIRA, D. 2007. Nuclear architecture underlying gene expression in Trypanosoma brucei. *Trends Microbiol,* 15**,** 263-70.

NGUYEN, T. N., MULLER, L. S., PARK, S. H., SIEGEL, T. N. & GUNZL, A. 2014. Promoter occupancy of the basal class I transcription factor A differs strongly between active and silent VSG expression sites in Trypanosoma brucei. *Nucleic Acids Res,* 42**,** 3164-76.

NILSSON, D., GUNASEKERA, K., MANI, J., OSTERAS, M., FARINELLI, L., BAERLOCHER, L., RODITI, I. & OCHSENREITER, T. 2010. Spliced leader trapping reveals widespread alternative splicing patterns in the highly dynamic transcriptome of Trypanosoma brucei. *PLoS Pathog,* 6**,** e1001037.

NUGENT, C. I., BOSCO, G., ROSS, L. O., EVANS, S. K., SALINGER, A. P., MOORE, J. K., HABER, J. E. & LUNDBLAD, V. 1998. Telomere maintenance is dependent on activities required for end repair of double-strand breaks. *Curr Biol,* 8**,** 657-60.

O'CONNOR, M. S., SAFARI, A., LIU, D., QIN, J. & SONGYANG, Z. 2004. The human Rap1 protein complex and modulation of telomere length. *J Biol Chem,* 279**,** 28585-91.

OBERHOLZER, M., MORAND, S., KUNZ, S. & SEEBECK, T. 2006. A vector series for rapid PCR-mediated C-terminal in situ tagging of Trypanosoma brucei genes. *Mol Biochem Parasitol,* 145**,** 117-20.

OGBADOYI, E., ERSFELD, K., ROBINSON, D., SHERWIN, T. & GULL, K. 2000. Architecture of the Trypanosoma brucei nucleus during interphase and mitosis. *Chromosoma,* 108**,** 501-13.

OLOVNIKOV, A. M. 1973. A theory of marginotomy. The incomplete copying of template margin in enzymic synthesis of polynucleotides and biological significance of the phenomenon. *J Theor Biol,* 41**,** 181-90.

OVERATH, P., CZICHOS, J. & HAAS, C. 1986. The effect of citrate/cis-aconitate on oxidative metabolism during transformation of Trypanosoma brucei. *Eur J Biochem,* 160**,** 175-82.

OVERATH, P. & ENGSTLER, M. 2004. Endocytosis, membrane recycling and sorting of GPI-anchored proteins: Trypanosoma brucei as a model system. *Mol Microbiol,* 53**,** 735-44.

PALM, W. & DE LANGE, T. 2008. How shelterin protects mammalian telomeres. *Annu Rev Genet,* 42**,** 301-34.

PANDYA, U. M., SANDHU, R. & LI, B. 2013. Silencing subtelomeric VSGs by Trypanosoma brucei RAP1 at the insect stage involves chromatin structure changes. *Nucleic Acids Res,* 41**,** 7673-82.

PARSONS, M., NELSON, R. G., WATKINS, K. P. & AGABIAN, N. 1984. Trypanosome mRNAs share a common 5' spliced leader sequence. *Cell,* 38**,** 309-16.

PASTERNAK, N. D. & DZIKOWSKI, R. 2009. PfEMP1: an antigen that plays a key role in the pathogenicity and immune evasion of the malaria parasite Plasmodium falciparum. *Int J Biochem Cell Biol,* 41**,** 1463-6.

PAYS, E. 2006. The variant surface glycoprotein as a tool for adaptation in African trypanosomes. *Microbes Infect,* 8**,** 930-7.

PAYS, E., GUYAUX, M., AERTS, D., VAN MEIRVENNE, N. & STEINERT, M. 1985. Telomeric reciprocal recombination as a possible mechanism for antigenic variation in trypanosomes. *Nature,* 316**,** 562-4.

PAYS, E., LAURENT, M., DELINTE, K., VAN MEIRVENNE, N. & STEINERT, M. 1983a. Differential size variations between transcriptionally active and inactive telomeres of Trypanosoma brucei. *Nucleic Acids Res,* 11**,** 8137-47.

PAYS, E., LIPS, S., NOLAN, D., VANHAMME, L. & PEREZ-MORGA, D. 2001. The VSG expression sites of Trypanosoma brucei: multipurpose tools for the adaptation of the parasite to mammalian hosts. *Mol Biochem Parasitol,* 114**,** 1-16.

PAYS, E., VAN ASSEL, S., LAURENT, M., DARVILLE, M., VERVOORT, T., VAN MEIRVENNE, N. & STEINERT, M. 1983b. Gene conversion as a mechanism for antigenic variation in trypanosomes. *Cell,* 34**,** 371-81.

PEDRAM, M. & DONELSON, J. E. 1999. The anatomy and transcription of a monocistronic expression site for a metacyclic variant surface glycoprotein gene in Trypanosoma brucei. *J Biol Chem,* 274**,** 16876-83.

PENA, A. C., PIMENTEL, M. R., MANSO, H., VAZ-DRAGO, R., PINTO-NEVES, D., ARESTA-BRANCO, F., RIJO-FERREIRA, F., GUEGAN, F., PEDRO COELHO, L., CARMO-FONSECA, M., BARBOSA-MORAIS, N. L. & FIGUEIREDO, L. M. 2014. Trypanosoma brucei histone H1 inhibits RNA polymerase I transcription and is important for parasite fitness in vivo. *Mol Microbiol,* 93**,** 645-63.

PERRY, K. L., WATKINS, K. P. & AGABIAN, N. 1987. Trypanosome mRNAs have unusual "cap 4" structures acquired by addition of a spliced leader. *Proc Natl Acad Sci U S A,* 84**,** 8190-4.

PFEIFFER, V. & LINGNER, J. 2013. Replication of telomeres and the regulation of telomerase. *Cold Spring Harb Perspect Biol,* 5**,** a010405.

PHAM, V., TROPEA, J., WONG, S., QUACH, J. & HENZEL, W. J. 2003. High-throughput protein sequencing. *Anal Chem,* 75**,** 875-82.

POVELONES, M. L., GLUENZ, E., DEMBEK, M., GULL, K. & RUDENKO, G. 2012. Histone H1 plays a role in heterochromatin formation and VSG expression site silencing in Trypanosoma brucei. *PLoS Pathog,* 8**,** e1003010.

RAMEY-BUTLER, K., ULLU, E., KOLEV, N. G. & TSCHUDI, C. 2015. Synchronous expression of individual metacyclic variant surface glycoprotein genes in Trypanosoma brucei. *Mol Biochem Parasitol,* 200**,** 1-4.

RAPPSILBER, J., MANN, M. & ISHIHAMA, Y. 2007. Protocol for micro-purification, enrichment, pre-fractionation and storage of peptides for proteomics using StageTips. *Nat Protoc,* 2**,** 1896-906.

REUNER, B., VASSELLA, E., YUTZY, B. & BOSHART, M. 1997. Cell density triggers slender to stumpy differentiation of Trypanosoma brucei bloodstream forms in culture. *Mol Biochem Parasitol,* 90**,** 269-80.

REYNOLDS, D., HOFMEISTER, B. T., CLIFFE, L., ALABADY, M., SIEGEL, T. N., SCHMITZ, R. J. & SABATINI, R. 2016. Histone H3 Variant Regulates RNA Polymerase II Transcription Termination and Dual Strand Transcription of siRNA Loci in Trypanosoma brucei. *PLoS Genet,* 12**,** e1005758.

RICE, C. & SKORDALAKES, E. 2016. Structure and function of the telomeric CST complex. *Comput Struct Biotechnol J,* 14**,** 161-7.

ROBINSON, N. P., MCCULLOCH, R., CONWAY, C., BROWITT, A. & BARRY, J. D. 2002. Inactivation of Mre11 does not affect VSG gene duplication mediated by homologous recombination in Trypanosoma brucei. *J Biol Chem,* 277**,** 26185-93.

RODITI, I. & LEHANE, M. J. 2008. Interactions between trypanosomes and tsetse flies. *Curr Opin Microbiol,* 11**,** 345-51.

RODITI, I. & LINIGER, M. 2002. Dressed for success: the surface coats of insect-borne protozoan parasites. *Trends Microbiol,* 10**,** 128-34.

RODITI, I., SCHWARZ, H., PEARSON, T. W., BEECROFT, R. P., LIU, M. K., RICHARDSON, J. P., BUHRING, H. J., PLEISS, J., BULOW, R., WILLIAMS, R. O. & ET AL. 1989. Procyclin gene expression and loss of the variant surface glycoprotein during differentiation of Trypanosoma brucei. *J Cell Biol,* 108**,** 737-46.

ROUT, M. P. & FIELD, M. C. 2001. Isolation and characterization of subnuclear compartments from Trypanosoma brucei. Identification of a major repetitive nuclear lamina component. *J Biol Chem,* 276**,** 38261-71.

RUDD, S. G., GLOVER, L., JOZWIAKOWSKI, S. K., HORN, D. & DOHERTY, A. J. 2013. PPL2 translesion polymerase is essential for the completion of chromosomal DNA replication in the African trypanosome. *Mol Cell,* 52**,** 554-65.

SAHA, A., WITTMEYER, J. & CAIRNS, B. R. 2006. Chromatin remodelling: the industrial revolution of DNA around histones. *Nat Rev Mol Cell Biol,* 7**,** 437-47.

SAMPATHI, S. & CHAI, W. 2011. Telomere replication: poised but puzzling. *J Cell Mol Med,* 15**,** 3-13.

SCHERF, A., FIGUEIREDO, L. M. & FREITAS-JUNIOR, L. H. 2001. Plasmodium telomeres: a pathogen's perspective. *Curr Opin Microbiol,* 4**,** 409-14.

SCHERF, A., HERNANDEZ-RIVAS, R., BUFFET, P., BOTTIUS, E., BENATAR, C., POUVELLE, B., GYSIN, J. & LANZER, M. 1998. Antigenic variation in malaria: in situ switching, relaxed and mutually exclusive transcription of var genes during intra-erythrocytic development in Plasmodium falciparum. *EMBO J,* 17**,** 5418-26.

SCHERTHAN, H., SFEIR, A. & DE LANGE, T. 2011. Rap1-independent telomere attachment and bouquet formation in mammalian meiosis. *Chromosoma,* 120**,** 151-7.

SCHLIMME, W., BURRI, M., BENDER, K., BETSCHART, B. & HECKER, H. 1993. Trypanosoma brucei brucei: differences in the nuclear chromatin of bloodstream forms and procyclic culture forms. *Parasitology,* 107 (Pt 3)**,** 237-47.

SCHOEFTNER, S. & BLASCO, M. A. 2009. A 'higher order' of telomere regulation: telomere heterochromatin and telomeric RNAs. *EMBO J,* 28**,** 2323-36.

SCHOLZ, J., BESIR, H., STRASSER, C. & SUPPMANN, S. 2013. A new method to customize protein expression vectors for fast, efficient and background free parallel cloning. *BMC Biotechnol,* 13**,** 12.

SCHULZ, D., MUGNIER, M. R., PAULSEN, E. M., KIM, H. S., CHUNG, C. W., TOUGH, D. F., RIOJA, I., PRINJHA, R. K., PAPAVASILIOU, F. N. & DEBLER, E. W. 2015. Bromodomain Proteins Contribute to Maintenance of Bloodstream Form Stage Identity in the African Trypanosome. *PLoS Biol,* 13**,** e1002316.

SCHULZ, D., ZARINGHALAM, M., PAPAVASILIOU, F. N. & KIM, H. S. 2016. Base J and H3.V Regulate Transcriptional Termination in Trypanosoma brucei. *PLoS Genet,* 12**,** e1005762.

SFEIR, A., KABIR, S., VAN OVERBEEK, M., CELLI, G. B. & DE LANGE, T. 2010. Loss of Rap1 induces telomere recombination in the absence of NHEJ or a DNA damage signal. *Science,* 327**,** 1657-61.

SHARMA, R., GLUENZ, E., PEACOCK, L., GIBSON, W., GULL, K. & CARRINGTON, M. 2009. The heart of darkness: growth and form of Trypanosoma brucei in the tsetse fly. *Trends Parasitol,* 25**,** 517-24.

SHEN, M., HAGGBLOM, C., VOGT, M., HUNTER, T. & LU, K. P. 1997. Characterization and cell cycle regulation of the related human telomeric proteins Pin2 and TRF1 suggest a role in mitosis. *Proc Natl Acad Sci U S A,* 94**,** 13618-23.

SHEVCHENKO, A., TOMAS, H., HAVLIS, J., OLSEN, J. V. & MANN, M. 2006. In-gel digestion for mass spectrometric characterization of proteins and proteomes. *Nat Protoc,* 1**,** 2856-60.

SHORE, D. 2001. Telomeric chromatin: replicating and wrapping up chromosome ends. *Curr Opin Genet Dev,* 11**,** 189-98.

SIEGEL, T. N., GUNASEKERA, K., CROSS, G. A. & OCHSENREITER, T. 2011. Gene expression in Trypanosoma brucei: lessons from high-throughput RNA sequencing. *Trends Parasitol,* 27**,** 434-41.

SIEGEL, T. N., HEKSTRA, D. R., KEMP, L. E., FIGUEIREDO, L. M., LOWELL, J. E., FENYO, D., WANG, X., DEWELL, S. & CROSS, G. A. 2009. Four histone variants mark the boundaries of polycistronic transcription units in Trypanosoma brucei. *Genes Dev,* 23**,** 1063-76.

SIEGEL, T. N., HEKSTRA, D. R., WANG, X., DEWELL, S. & CROSS, G. A. 2010. Genome-wide analysis of mRNA abundance in two life-cycle stages of Trypanosoma brucei and identification of splicing and polyadenylation sites. *Nucleic Acids Res,* 38**,** 4946-57.

SIERRA-MIRANDA, M., VEMBAR, S. S., DELGADILLO, D. M., AVILA-LOPEZ, P. A., HERRERA-SOLORIO, A. M., LOZANO AMADO, D., VARGAS, M. & HERNANDEZ-RIVAS, R. 2017. PfAP2Tel, harbouring a non-canonical DNA-binding AP2 domain, binds to Plasmodium falciparum telomeres. *Cell Microbiol*.

SMOGORZEWSKA, A., VAN STEENSEL, B., BIANCHI, A., OELMANN, S., SCHAEFER, M. R., SCHNAPP, G. & DE LANGE, T. 2000. Control of human telomere length by TRF1 and TRF2. *Mol Cell Biol,* 20**,** 1659-68.

STANNE, T. M., KUSHWAHA, M., WAND, M., TAYLOR, J. E. & RUDENKO, G. 2011. TbISWI regulates multiple polymerase I (Pol I)-transcribed loci and is present at Pol II transcription boundaries in Trypanosoma brucei. *Eukaryot Cell,* 10**,** 964-76.

STANNE, T. M., NARAYANAN, M. S., RIDEWOOD, S., LING, A., WITMER, K., KUSHWAHA, M., WIESLER, S., WICKSTEAD, B., WOOD, J. & RUDENKO, G. 2015. Identification of the ISWI chromatin remodeling complex of the early branching eukaryote Trypanosoma brucei. *J Biol Chem,* 290**,** 29760.

STEGER, D. J., HASWELL, E. S., MILLER, A. L., WENTE, S. R. & O'SHEA, E. K. 2003. Regulation of chromatin remodeling by inositol polyphosphates. *Science,* 299**,** 114-6.

STEVENS, J. R., NOYES, H. A., SCHOFIELD, C. J. & GIBSON, W. 2001. The molecular evolution of Trypanosomatidae. *Adv Parasitol,* 48**,** 1-56.

SZOSTAK, J. W. & BLACKBURN, E. H. 1982. Cloning yeast telomeres on linear plasmid vectors. *Cell,* 29**,** 245-55.

TAYLOR, J. E. & RUDENKO, G. 2006. Switching trypanosome coats: what's in the wardrobe? *Trends Genet,* 22**,** 614-20.

TENNEN, R. I., BUA, D. J., WRIGHT, W. E. & CHUA, K. F. 2011. SIRT6 is required for maintenance of telomere position effect in human cells. *Nat Commun,* 2**,** 433.

TETLEY, L., TURNER, C. M., BARRY, J. D., CROWE, J. S. & VICKERMAN, K. 1987. Onset of expression of the variant surface glycoproteins of Trypanosoma brucei in the tsetse fly studied using immunoelectron microscopy. *J Cell Sci,* 87 (Pt 2)**,** 363-72.

TONKIN, C. J., CARRET, C. K., DURAISINGH, M. T., VOSS, T. S., RALPH, S. A., HOMMEL, M., DUFFY, M. F., SILVA, L. M., SCHERF, A., IVENS, A., SPEED, T. P., BEESON, J. G. & COWMAN, A. F. 2009. Sir2 paralogues cooperate to regulate virulence genes and antigenic variation in Plasmodium falciparum. *PLoS Biol,* 7**,** e84.

TURNER, C. M., BARRY, J. D., MAUDLIN, I. & VICKERMAN, K. 1988. An estimate of the size of the metacyclic variable antigen repertoire of Trypanosoma brucei rhodesiense. *Parasitology,* 97 (Pt 2)**,** 269-76.

URBANIAK, M. D., GUTHER, M. L. & FERGUSON, M. A. 2012. Comparative SILAC proteomic analysis of Trypanosoma brucei bloodstream and procyclic lifecycle stages. *PLoS One,* 7**,** e36619.

URWYLER, S., STUDER, E., RENGGLI, C. K. & RODITI, I. 2007. A family of stage-specific alanine-rich proteins on the surface of epimastigote forms of Trypanosoma brucei. *Mol Microbiol,* 63**,** 218-28.

VAN DEN ABBEELE, J., CLAES, Y., VAN BOCKSTAELE, D., LE RAY, D. & COOSEMANS, M. 1999. Trypanosoma brucei spp. development in the tsetse fly: characterization of the post-mesocyclic stages in the foregut and proboscis. *Parasitology,* 118 (Pt 5)**,** 469-78.

VAN DEURSEN, F. J., SHAHI, S. K., TURNER, C. M., HARTMANN, C., GUERRA-GIRALDEZ, C., MATTHEWS, K. R. & CLAYTON, C. E. 2001. Characterisation of the growth and differentiation in vivo and in vitro-of bloodstream-form Trypanosoma brucei strain TREU 927. *Mol Biochem Parasitol,* 112**,** 163-71.

VAN LEEUWEN, F., WIJSMAN, E. R., KIEFT, R., VAN DER MAREL, G. A., VAN BOOM, J. H. & BORST, P. 1997. Localization of the modified base J in telomeric VSG gene expression sites of Trypanosoma brucei. *Genes Dev,* 11**,** 3232-41.

VAN LEEUWEN, F., WIJSMAN, E. R., KUYL-YEHESKIELY, E., VAN DER MAREL, G. A., VAN BOOM, J. H. & BORST, P. 1996. The telomeric GGGTTA repeats of Trypanosoma brucei contain the hypermodified base J in both strands. *Nucleic Acids Res,* 24**,** 2476-82.

VAN STEENSEL, B. & DE LANGE, T. 1997. Control of telomere length by the human telomeric protein TRF1. *Nature,* 385**,** 740-3.

VANHAMME, L., POELVOORDE, P., PAYS, A., TEBABI, P., VAN XONG, H. & PAYS, E. 2000. Differential RNA elongation controls the variant surface glycoprotein gene expression sites of Trypanosoma brucei. *Mol Microbiol,* 36**,** 328-40.

VASQUEZ, J. J., HON, C. C., VANSELOW, J. T., SCHLOSSER, A. & SIEGEL, T. N. 2014. Comparative ribosome profiling reveals extensive translational complexity in different Trypanosoma brucei life cycle stages. *Nucleic Acids Res,* 42**,** 3623-37.

VASSELLA, E. & BOSHART, M. 1996. High molecular mass agarose matrix supports growth of bloodstream forms of pleomorphic Trypanosoma brucei strains in axenic culture. *Mol Biochem Parasitol,* 82**,** 91-105.

VASSELLA, E., REUNER, B., YUTZY, B. & BOSHART, M. 1997. Differentiation of African trypanosomes is controlled by a density sensing mechanism which signals cell cycle arrest via the cAMP pathway. *J Cell Sci,* 110 (Pt 21)**,** 2661-71.

WANG, Q. P., KAWAHARA, T. & HORN, D. 2010. Histone deacetylases play distinct roles in telomeric VSG expression site silencing in African trypanosomes. *Mol Microbiol,* 77**,** 1237-45.

WATSON, J. D. 1972. Origin of concatemeric T7 DNA. *Nat New Biol,* 239**,** 197-201.

WHO 2017. Trypanosomiasis, human African (sleeping sickness). *World Health Organization*.

WIRTZ, E., LEAL, S., OCHATT, C. & CROSS, G. A. 1999. A tightly regulated inducible expression system for conditional gene knock-outs and dominant-negative genetics in Trypanosoma brucei. *Mol Biochem Parasitol,* 99**,** 89-101.

YANG, X., FIGUEIREDO, L. M., ESPINAL, A., OKUBO, E. & LI, B. 2009. RAP1 is essential for silencing telomeric variant surface glycoprotein genes in Trypanosoma brucei. *Cell,* 137**,** 99-109.

YE, J. Z., DONIGIAN, J. R., VAN OVERBEEK, M., LOAYZA, D., LUO, Y., KRUTCHINSKY, A. N., CHAIT, B. T. & DE LANGE, T. 2004a. TIN2 binds TRF1 and TRF2 simultaneously and stabilizes the TRF2 complex on telomeres. *J Biol Chem,* 279**,** 47264-71.

YE, J. Z., HOCKEMEYER, D., KRUTCHINSKY, A. N., LOAYZA, D., HOOPER, S. M., CHAIT, B. T. & DE LANGE, T. 2004b. POT1-interacting protein PIP1: a telomere length regulator that recruits POT1 to the TIN2/TRF1 complex. *Genes Dev,* 18**,** 1649-54.

YI, X., WHITE, D. M., AISNER, D. L., BAUR, J. A., WRIGHT, W. E. & SHAY, J. W. 2000. An alternate splicing variant of the human telomerase catalytic subunit inhibits telomerase activity. *Neoplasia,* 2**,** 433-40.

YILDIRIM, S., CASTANO, E., SOBOL, M., PHILIMONENKO, V. V., DZIJAK, R., VENIT, T. & HOZAK, P. 2013. Involvement of phosphatidylinositol 4,5-bisphosphate in RNA polymerase I transcription. *J Cell Sci,* 126**,** 2730-9.

YOUNG, A. C., CHAVEZ, M., GIAMBERNARDI, T. A., MATTERN, V., MCGILL, J. R., HARRIS, J. M., SAROSDY, M. F., PATEL, P. & SAKAGUCHI, A. Y. 1997. Organization and expression of human telomere repeat binding factor genes. *Somat Cell Mol Genet,* 23**,** 275-86.

ZHONG, Z., SHIUE, L., KAPLAN, S. & DE LANGE, T. 1992. A mammalian factor that binds telomeric TTAGGG repeats in vitro. *Mol Cell Biol,* 12**,** 4834-43.

ZIEGELBAUER, K., STAHL, B., KARAS, M., STIERHOF, Y. D. & OVERATH, P. 1993. Proteolytic release of cell surface proteins during differentiation of Trypanosoma brucei. *Biochemistry,* 32**,** 3737-42.

ZIMMERMANN, H., SUBOTA, I., BATRAM, C., KRAMER, S., JANZEN, C. J., JONES, N. G. & ENGSTLER, M. 2017. A quorum sensing-independent path to stumpy development in Trypanosoma brucei. *PLoS Pathog,* 13**,** e1006324.

6 APPENDIX

6.1 Supplementary figures

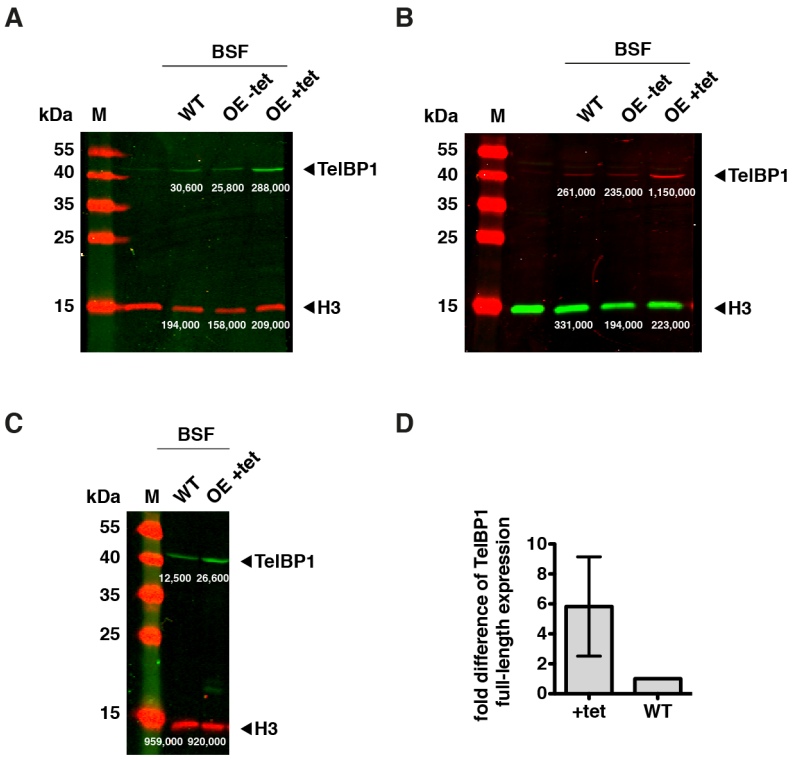

Figure 36. Quantification of TelBP1 upon induction of TelBP1 overexpression in BSF cells.
Quantitative western blot analyses of TelBP1 overexpression in BSF cells using the (A) (C) TelBP1-specific rat and (B) mouse antibodies. Three independent western blot analyses were conducted and the TelBP1 signal normalized against the Histone H3 signal intensity. The fold-difference of TelBP1 protein amount between WT and TelBP1 OE cells was determined for each experiment. (D) Graph showing the quantification of all three western blots. WT signal was set to 1. TelBP1 OE induction leads to a 5.83-fold upregulation (SD±3.31) of TelBP1 protein amount in BSF cells.

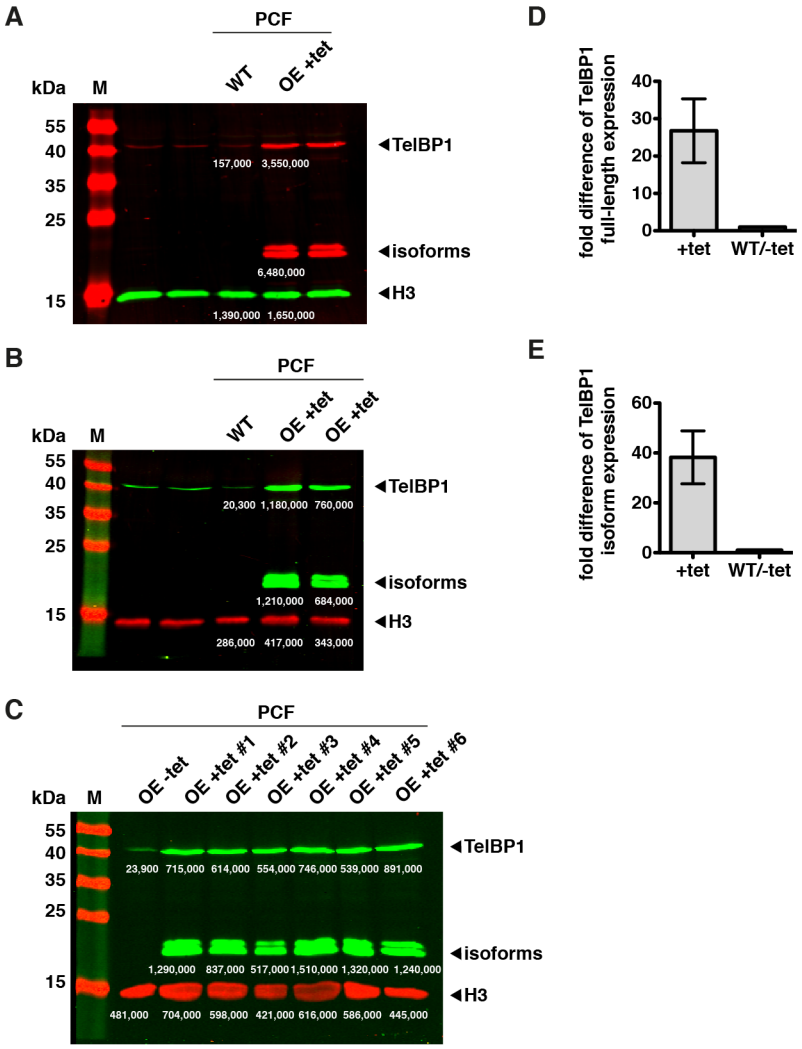

Figure 37. Quantification of TelBP1 full-length protein and isoforms upon induction of TelBP1 overexpression in PCF cells.

Quantitative western blot analyses of TelBP1 overexpression in PCF cells using the (**A**) TelBP1-specific mouse and (**B**) (**C**) rat specific antibodies. Three independent western blot analyses were conducted and the TelBP1 signal normalized against the Histone H3 signal intensity. The fold-difference of TelBP1 protein amount between WT or non–induced TelBP1 OE cells was determined for each experiment. (**C**) Here, TelBP1 OE was induced in two biological replicates and of each replicate cell lysates were prepared in triplicates. (**D**) Graph showing the quantification of all three western blots (n=9). WT signal was set to 1. TelBP1 OE induction leads to a 26.77-fold upregulation (SD±8.55) of TelBP1 full-length protein amount in BSF cells. (**E**) Graph showing the quantification of TelBP1 isoforms upon TelBP1 OE induction. WT signal of full-length TelBP1 protein was set to 1. 38.25-fold (SD±10.6) higher TelBP1 isoform expression compared to WT full-length TelBP1 expression levels was detected upon TelBP1 OE induction.

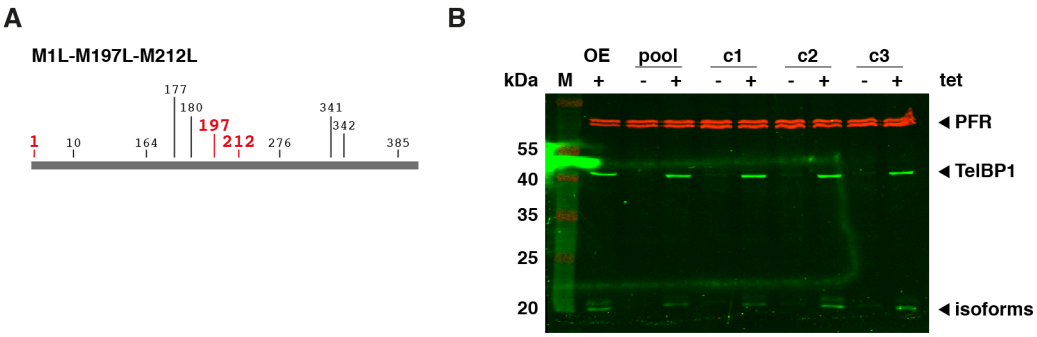

Figure 38. Mutation of methionines to leucines at position 1, 197 and 212 in the amino acid sequence of TelBP1.
(**A**) Schematic representation of mutated methionines in the TelBP1 coding sequence. (**B**) Western blot analysis of TelBP1 full-length and isoform expression upon induction of TelBP1 M1L-M197L-M212L overexpression. The TelBP1-specific rat antibody was used to detect TelBP1 and the isoforms. The PFR mouse antibody served as loading control. The pool and three different clones (c1-c3) were analyzed upon tet induction. Although three methionines were mutated the pool and all clones still expressed the full-length TelBP1 and the isoforms.

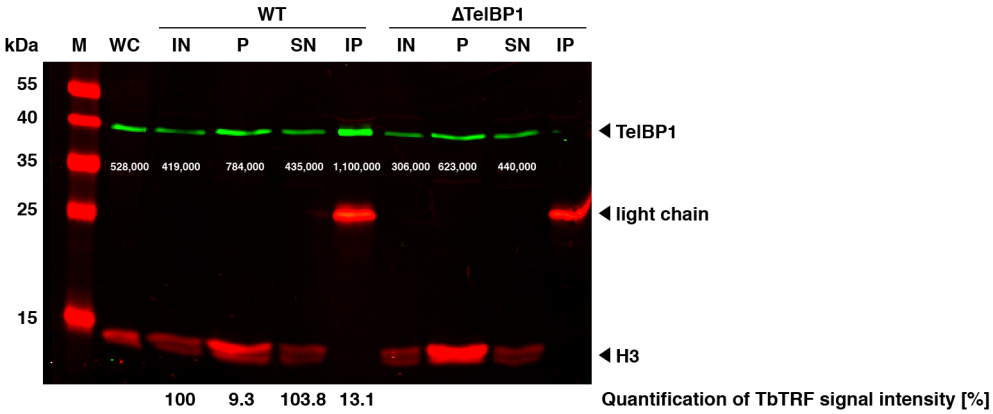

Figure 39. Quantification of co-purified TbTRF in the TelBP1 Co-IP.
Quantitative western blot analysis of TelBP1 Co-IP using the TbTRF-specific antibody. TbTRF signals were already shown in Figure 26B. 20-fold more of the pellet and IP sample was loaded compared to IN and SN samples. TbTRF signal intensity was quantified. 13% of the TbTRF input was co-precipitated with TelBP1. WC (whole cell lysate), IN (input), P (pellet), SN (supernatant), IP (immunoprecipitate).

6.2 Supplementary tables

Table 20. Absolute values of the luciferase assay conducted with wild-type and ΔTelBP1 dual luciferase reporter cells upon differentiation induction.

Fluc (tel) [RLU]	Replicate #	0 h	5 h	24 h	48 h	72 h
WT	1	1895	2194	2375	1512	551
	2	1968	2432	3140	1889	762
	3	1991	2078	2467	1709	657
	mean	1951.3	2234.7	2660.7	1703.3	656.7
ΔTelBP1	1	1995	1941	1866	1444	492
	2	1983	2406	1672	1243	425
	3	2073	2122	1700	1306	359
	mean	2017	2156.3	1746	1331	425.3

Rluc (pro) [RLU]	Replicate #	0 h	5 h	24 h	48 h	72 h
WT	1	405676	786334	747223	664686	190687
	2	431854	856047	980780	697961	226638
	3	428980	741638	821750	690976	193087
	mean	422170	794673	849917.7	684541	203470.7
ΔTelBP1	1	355291	571818	1516458	446236	127797
	2	359922	680119	481185	405107	102784
	3	371560	617556	520818	390850	85813
	mean	362257.7	623164.3	506153.7	414064.3	105464.7

Abbreviations: Firefly luciferase (Fluc), Renilla luciferase (Rluc), relative light units (RLU).

Table 21. Absolute values of the luciferase assay conducted with induced and non-induced ΔTelBP1R dual luciferase reporter cells upon differentiation induction.

Fluc (tel) [RLU]	Replicate #	0 h	5 h	24 h	48 h	72 h
ΔTelBP1R -tet	1	2294	2109	1673	1056	558
	2	2439	2229	1971	1000	577
	3	2029	2423	2007	1046	630
	mean	2254	2253.7	1883.7	1034	588.3
ΔTelBP1R +tet	1	1731	2331	2622	1481	652
	2	1879	2487	3152	1059	646
	3	1705	2270	3120	1811	665
	mean	1771.7	2362.7	2964.7	1450.3	654.3

Rluc (pro) [RLU]	Replicate #	0 h	5 h	24 h	48 h	72 h
ΔTelBP1R -tet	1	435575	500208	419234	255652	147114
	2	437623	525450	495187	227601	154283
	3	407167	604450	537954	265499	176234
	mean	426788.3	543369.3	484125	249584	159210.3
ΔTelBP1R +tet	1	391679	716337	812418	442072	182127
	2	419363	811421	940906	305194	186210
	3	435783	710966	1013165	566521	214116
	mean	415608.3	746241.3	922163	437929	194151

Abbreviations: Firefly luciferase (Fluc), Renilla luciferase (Rluc), relative light units (RLU).